From Time Transfer functions to a model for relativistic astrometry in the Gaia era

Stefano Bertone

OBSERVATOIRE DE PARIS
SYRTE

UNIVERSITÀ DI TORINO
INAF - OATo

Astronomy and Astrophysics Doctoral School of Paris Area
Torino Graduate School in Physics and Astrophysics

PHD THESIS

to obtain the title of

Ph.D. of Science

of the Observatoire de Paris - Università di Torino
Specialty : Astronomy and Astrophysics

Defended by

Stefano BERTONE

From Time Transfer Functions to a model for relativistic astrometry in the Gaia era

Advisors: Marie-Christine ANGONIN and Andrea MIGNONE

Co-Advisors: Christophe LE PONCIN-LAFITTE,
Mariateresa CROSTA and Alberto VECCHIATO

defended on September 18, 2013

JURY :

President :	Christophe SAUTY	- LUTH (Observatoire de Paris)
Reviewers :	Donato BINI	- Istituto "M. Picone" (CNR)
	Bertrand CHAUVINEAU	- Obs. de la Côte d'Azur
Examinators :	François MIGNARD	- Obs. de la Côte d'Azur
	Mario LATTANZI	- Oss. Astrofisico di Torino (INAF)
	Angelo TARTAGLIA	- Politecnico di Torino
Advisors :	Marie-Christine ANGONIN	- SYRTE (Observatoire de Paris)
	Andrea MIGNONE	- INFN (Università di Torino)
Invited :	Mariateresa CROSTA	- Oss. Astrofisico di Torino (INAF)
	Christophe LE PONCIN-LAFITTE	- SYRTE (Observatoire de Paris)
	Alberto VECCHIATO	- Oss. Astrofisico di Torino (INAF)

Abstract. Modern space projects currently under development, such as BepiColombo for the exploration of Mercury or Gaia for space astrometry, have the goal of getting high precision data about their main targets. It is then necessary to conceive several independent models in the framework of General Relativity to perform data analysis ensuring the appropriate treatment of all effects important at the required level of accuracy.
The first part of this thesis is dedicated to the study of light propagation. We use the Time Transfer Functions (TTF) formalism to characterize the influence of gravitational light deflection on the Ranging, Doppler and astrometric observables for applications to these future projects. In order to get an appropriate gravitational description of the Solar System, we consider the hypothesis of a weak gravitational field, adopting a metric tensor valid up to the second order of the post-Minkowskian (2PM) approximation. We obtain these observables as integrals depending on the metric tensor and its derivatives only. This very general form is particularly adapted to numerical computation and to the test of alternative theories of gravity. We also propose several analytical applications of our results up to the 2PM order.
In the second part of this thesis, we focus on high precision astrometry in the context of the Gaia mission, scheduled for launch in late 2013. We use an original procedure to get an analytical comparison of our light propagation model with the two approaches developed for Gaia, namely the Gaia Relativity Model (GREM) and the Relativistic Astrometric Model (RAMOD). Following this validation, we use the TTF and the Gaia tetrad developed for RAMOD to simulate a series of astrometric observations within the Global Sphere Reconstruction (GSR) software. We compare then our results with GREM and with a complete Schwarzschild model. The study is finally completed by the reconstruction of a celestial sphere using 5 years of observations simulated with our model.
These applications to astrometry are the result of the collaboration between the French group at SYRTE, responsible for the TTF and the Italian one at OATO, responsible for RAMOD and GSR.

Resumé. Actuellement, les projets spatiaux en cours de développement, tel que BepiColombo pour l'exploration de Mercure ou Gaia pour l'astrométrie spatiale, ont pour objectif d'obtenir des données de très haute précision sur leur objet d'étude. Il est donc maintenant indispensable de construire plusieurs modèles indépendantes d'analyse de données dans le cadre la Relativité Générale (RG) afin d'assurer une correcte prise en compte des effets qui se manifesteront très distinctement à ce niveau de précision.
La première partie de ce manuscrit est dédiée à l'étude de la propagation des signaux électromagnétiques, par le biais du formalisme des Fonctions de Transfert de Temps, afin de caractériser les effets de courbure des rayons lumineux sur les observables de Ranging, Doppler et astrométriques de ces futurs projets. Pour décrire correctement le Système Solaire, nous retenons l'hypothèse des champs gravitationnels faibles et nous considérons un tenseur métrique au premier et deuxième ordres d'approximation post-Minkowskienne (PM). Nous obtenons ainsi ces observables sous la forme d'intégrales, ne dépendant que du tenseur métrique et de ses dérivées. Cette forme très générale est particulièrement adaptée pour le calcul numérique et les test des théories alternatives à la RG. Des applications analytiques sont aussi données jusqu'au deuxième ordre PM.
Dans la seconde partie de ce travail, nous focalisons notre étude sur l'astrométrie de haute précision dans le contexte de la future mission Gaia qui sera lancée fin 2013. Nous confrontons donc notre modèle de propagation de la lumière avec les deux approches adoptées pour Gaia, à savoir les modèles GREM et RAMOD, par une procédure originale. Suite à cette validation analytique, nous utilisons la TTF avec la tétrade Gaia de RAMOD afin de simuler une série d'observations astrométriques dans le software GSR. Nos résultats sont comparés avec GREM et avec un modèle complet à symétrie sphérique. Le travail est complété par la reconstruction d'une sphère céleste à partir de 5 ans d'observations simulées avec notre modèle.
Ces applications à l'astrométrie sont issus de la collaboration entre le groupe parisien du SYRTE responsable de la TTF et celui turinois de OATO responsable pour RAMOD et GSR.

Sintesi. I progetti spaziali attualmente in sviluppo, come BepiColombo per l'esplorazione di Mercurio o Gaia per l'astrometria spaziale, hanno come obiettivo l'acquisizione di misure ad alta precisione sul loro oggetto di studio. È dunque indispensabile sviluppare più modelli indipendenti per l'analisi dati nell'ambito della Relatività Generale (RG), al fine di tener conto di effetti che risultano decisivi a questo livello di precisione.
La prima parte di questa tesi è dedicata allo studio della propagazione dei segnali elettro-magnetici per mezzo del formalismo delle "Funzioni di Trasferimento di Tempo" (TTF): il fine perseguito è la caratterizzazione degli effetti della curvatura dei raggi luminosi sulle osservabili Ranging, Doppler e astrometriche di questi futuri progetti. Per descrivere correttamente il Sistema Solare, ci si porrà dunque nell'ipotesi di campo gravitazionale debole e si considererà un tensore metrico al primo e secondo ordine dell'approssimazione post-Minkowskiana (PM). Le osservabili così ottenute saranno fornite sotto forma di integrali dipendenti dal solo tensore metrico e dalle sue derivate: questa forma molto generale è particolarmente adatta per il calcolo numerico ed i test delle teorie alternative alla RG. Delle applicazioni analitiche saranno inoltre fornite fino al secondo ordine PM.
Nella seconda parte di questo lavoro, concentriamo il nostro studio sull'astrometria di alta precisione nell'ambito della futura missione Gaia, il cui lancio è previsto per fine 2013. Ci proponiamo, per mezzo di una nuova procedura, di confrontare il nostro modello di propagazione della luce ai due approcci utilizzati per Gaia, chiamati GREM e RAMOD. Questa verifica analitica ci permette di combinare il nostro modello TTF con la tetrade Gaia di RAMOD con l'obiettivo per simulare così una serie di osservazioni astrometriche nel software GSR. Presentiamo i risultati del confronto di questo modello con GREM e PPN-RAMOD (una versione a simmetria sferica dell'omonimo modello). Questo studio è finalizzato con la ricostruzione di una sfera celeste a partire da 5 anni di osservazioni simulate con il nostro modello.
Queste applicazioni all'astrometria sono il risultato della collaborazione tra il gruppo parigino del SYRTE responsabile della TTF e quello torinese di OATO responsabile di RAMOD e GSR.

Partner institutions

SYRTE (Observatoire de Paris)

Oss. Astrofisico di Torino (INAF)

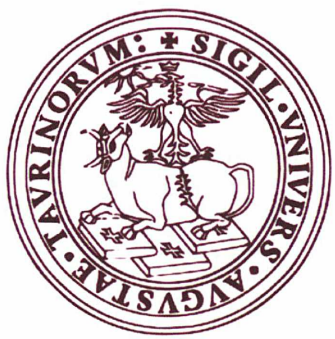

Università di Torino

Université franco-italienne - Università italo-francese

I dedicate this thesis to my grandparents,
to whom I owe so much of what I know and I am.
I hope they would be proud of the results of their teachings.

Ciò che conta è comunicare l'indispensabile lasciando perdere tutto il superfluo, ridurre noi stessi a comunicazione essenziale, a segnale luminoso che si muove in una data direzione, abolendo la complessità delle nostre persone e situazioni ed espressioni facciali, lasciandole nella scatola d'ambra che i fari si portano dietro e nascondono.

Il guidatore notturno, Italo Calvino

Insomma questo spazio non lo si vede mai e forse non esiste, è solo estensione delle cose e misura delle distanze.

L'inseguimento, Italo Calvino

There is a way out of every box, a solution to every puzzle; it's just a matter of finding it.

Attached, Star Trek TNG

Sokath! His eyes uncovered!

Darmok, Star Trek TNG

Acknowledgements. Thanks to my advisors for having been stubborn enough to pass me some of their knowledge, to my friends of 12h30 and of the "baby" for the daily mutual support and to my colleagues in Turin, Paris and around the world for the enlightening discussions. Thanks to my parents for standing my infinite complaints and sharing my happy moments, my friends in Turin for being there when I got back home and, last but not least, thanks to my "chapine" for always being at my side from far away and while exploring the world together during the three years of this arduous but finally enriching experience which is the Ph.D. thesis.

Contents

Notation and conventions

Throughout this work, c is the speed of light in vacuum and G is the Newtonian gravitational constant. The Lorentzian metric of space-time V_4 is denoted by g. We adopt the signature $(-+++)$. We suppose that space-time is covered by some global coordinate system $x^\alpha = (x^0, \boldsymbol{x})$, with $x^0 = ct$ and $\boldsymbol{x} = (x^i)$, centered on the Solar System barycenter. Greek indices run from 0 to 3 and Latin indices from 1 to 3. Any ordered triple is denoted by a bold letter. In order to distinguish the triples built with the space-like contravariant components of a vector from the ones built with covariant components, we systematically use the notation $\boldsymbol{a} = (a^1, a^2, a^3) = (a^i)$ and $\underline{\boldsymbol{b}} = (b_1, b_2, b_3) = (b_i)$. Considering two such quantities $\boldsymbol{a}$ and $\boldsymbol{b}$ we use $\boldsymbol{a} \cdot \boldsymbol{b}$ to denote $a^i b_i$ (Einstein convention on repeated indices is used). The quantity $|\boldsymbol{a}|$ stands for the ordinary Euclidean norm of $\boldsymbol{a}$. For any quantity $f(x^\lambda)$, $f_{,\alpha}$ denotes the partial derivative of f with respect to x^α. The indices in parentheses characterize the order of perturbation. They are set up or down, depending on the convenience.

CHAPTER 1

Introduction

Contents

1.1 High precision astronomy

Since the beginning of the so called space-era, the increasing accuracy of observations and the new observational techniques (like radar ranging) have made it no longer necessary to justify the importance of a consistent relativistic modeling in the field of fundamental astronomy.

Nowadays, applied relativity has become one of the basic ingredients of celestial mechanics, astrometry, time scales and time dissemination. Significant theoretical efforts have been necessary to follow the observational and engineering needs. The scientific community developed new theories for global and local reference systems [Damour *et al.* 1991] such as the Barycentric Celestial Reference System (BCRS) or the Geocentric Celestial Reference System (GCRS) as well as relativistic equations describing the translational and rotational motion of an N-body system of arbitrary composition and shape. A precise treatment of light propagation also became of central importance when dealing with high-accuracy observations [Brumberg 1987, Klioner & Kopeikin 1992].

Nevertheless, it is the whole astronomy which needs to be rethought from a classical Newtonian point of view to a relativistic one. Relativistic questions have been playing an important role in the work of several Commissions and Working Groups of the International Astronomical Union (IAU) for an extended period of time so that in 2006, it has been decided to establish IAU Commission 52 "Relativity in Fundamental Astronomy" (RIFA - http://www.iau.org/science/scientific_bodies/commissions/52/).

Today, there are a number of open issues of both theoretical and practical character that still need the attention of astronomers, experts in gravitation and relativists. Such issues particularly arise when dealing with modern space missions. In the following we give three examples of missions needing a systematic relativistic modeling of their observations

- Gaia [Bienayme & Turon 2002], a cornerstone mission of the European Space Agency (ESA), is meant to provide an high-accuracy 3D map of the Milky Way. Its launch will represent an epochal shift from classical to relativistic astrometry but the huge amount of data to be treated will also require massive computational capabilities;

- GAME [Gai *et al.* 2012], is a high-accuracy astrometry mission aiming at measuring the γ parameter of the parameterized post-Newtonian formalism (PPN, see section 1.2.1) from space. With respect to Gaia, a more accurate relativistic model of the astrometric observable will be needed in order to reach the required accuracy when observing near the limb of the Sun.

- BepiColombo [Benkhoff *et al.* 2010] will be launched in 2014 towards Mercury, where it will collect scientific data but also use its inboard instrumentation to test General Relativity (GR) [Iess *et al.* 2009] with a dedicated radio-science experiment. As other planetary missions, it requires a very precise knowledge of its orbital motion in order to attain its goals. This requires an accurate modeling of the Range and Doppler observables through the relativistic treatment of light propagation.

In the following, we present in more details these missions whose data need to be treated accurately and interpreted on the basis of reliable theoretical models as we shall outline in section 1.2.

1.1.1 GAIA

The launch of the HIgh Precision PARallax COllecting Satellite (HIPPARCOS [Perryman & ESA 1997]) space mission in 1989 provided the opportunity for Europe to establish its leadership in space astrometry, setting the state-of-the-art precision levels for astrometric measurements of nearby stars. For the first time, space astrometry allowed to determine the positions, parallaxes and proper motions of 10^5 stars with an accuracy of some milliarcseconds (mas). The HIPPARCOS

results have contributed immensely to a better understanding of a wide range of topics in astrophysics, such as galaxy kinematics and dynamics, and stellar physics.

Direct descendant of HIPPARCOS, Gaia [Bienayme & Turon 2002] has been accepted in 2000 as cornerstone mission of ESA space program and is now scheduled for launch for late 2013 on a Soyuz-Fregat launcher. Gaia will provide positions and velocities of a billion stars in our Galaxy and thousands of extragalactic sources of the local group, so around 1% of the stellar population of our Milky Way will be observed with the accuracy of some microarcseconds (μas) needed for answering today scientific questions. The satellite will operate in Lissajous orbits around the Earth-Sun Lagrangian point L2, scanning the sky continuously at a rate of 120 as/s (where as stands for arcseconds) over a 5 years mission, as illustrated in Fig. 1.1.

As for HIPPARCOS, Gaia results will be of capital importance in several areas of astronomy and fundamental physics. In particular, it is expected to provide :

- the physical characteristics, kinematics and distribution of a large fraction of stars in the Galaxy, thus allowing to determine its full history;
- distances of unprecedented accuracy for all kinds of stars, even those in rapid evolution, covering the whole Hertsprung-Russel diagram;
- a more precise determination of star luminosity and precise astrometric measures providing constraints for stellar population models;
- a complete study of the luminosity function, thanks to the observation of a large amount of all kinds of stars;
- the determination of a large number of stellar orbits, including those of the smallest stars (brown dwarf);
- a census of binary systems and extra-solar planets (all large planets to $200 - 500$ pc from Earth) thanks to very precise astrometric measures;
- the identification and characterization of a large number of asteroids and minor bodies in the Solar System;
- contributions to the structure, dynamics and stellar populations of local group galaxies;
- improvements in the orientation of the International Celestial Reference Frame (ICRF) thanks to better astrometric accuracy;
- the test of gravitational theories in the PPN approximation of GR, considering effects up to G/c^3 in light bending.

The payload consists of a single integrated instrument that comprises three major functions by using common telescopes and a shared focal plane:

1. the Astrometric instrument (ASTRO) is devoted to star angular position measurements, providing star positions, parallaxes and proper motions;

2. the Photometric instrument provides continuous star spectra for astrophysics in the band 320-1000 nm and the ASTRO chromaticity calibration;

3. the Radial Velocity Spectrometer (RVS) provides radial velocity and high resolution spectral data in the narrow band 847-874 nm.

Each function is achieved within a dedicated area on the focal plane, which allows it to take benefit from the two viewing directions separated by a fixed (and monitored) basic angle of 106°.

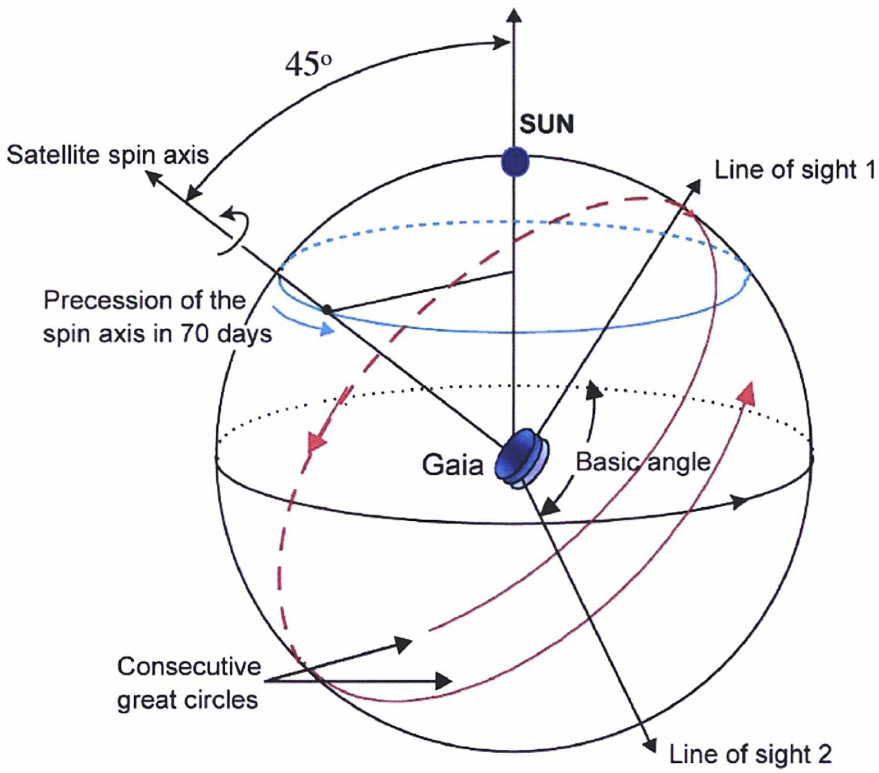

Figure 1.1: Scanning principle of Gaia: The constant spin rate of 60"/s corresponds to one revolution (great-circle scans) in six hours. The angle between the slowly precessing spin axis and the Sun is maintained at an aspect angle of 45°. The basic angle is between the two fields of view is constant at 106.5°. (Figure courtesy: Karen O'Flaherty, ESA)

Thanks to this apparatus, Gaia can aim for the following accuracies:

- systematic observation of all objects (more than a billion) brighter than magnitude V=20;

- better than 10 μas positional accuracy for stars up to magnitude V = 10, 12-25 μas at V = 15, and 100-200 μas at V = 20;
- parallax accuracy better than 1% for 20 millions of stars in our galaxy;
- constraints on relativistic parameters (see section 1.2.1) : γ to $\approx 5 \times 10^{-6}$, β to 10^{-3} and η to 2.4×10^{-3}; moreover, the quadrupole moment of the Sun J_2, describing its flattening, should be evaluated with $10^{-7} - 10^{-8}$ precision, the GM of Jupiter (where G is the universal constant of gravitation and M is Jupiter mass) to $2.9 \times 10^{-15} AU^3 d^{-2}$ and the gravitational "constant" variation $\dot{G}/G$ with a precision of 3×10^{-12} $years^{-1}$ [Hobbs *et al.* 2010, Mouret 2011].

1.1.2 GAME

GAME [Gai *et al.* 2012], for Gamma Astrometric Measurement Experiment, is a concept of a small mission proposed to ESA for the Cosmic Vision program whose main goal is to measure from space the γ parameter of the PPN formalism. A satellite, looking as close as possible to the Solar limb, measures the gravitational bending of light in a way similar to that followed by past experiments from the ground during solar eclipses. This is done in order to maximize the observed effect, since the Sun is the most massive body in the Solar System. The proposed mission lifetime of two years will allow a repetition of the basic experiment to validate and improve the final accuracy of the mission results. In addition to the test of the parameter γ, thanks to its flexible observation strategy, GAME is also able to target other interesting scientific goals (in the realm of General Relativity, extrasolar systems, etc.).

The basic idea of GAME is to measure the astrometric angle between the stars in two fields of view (FOVs) pointing symmetrically with respect to the ecliptic as illustrated in Fig. 1.2. The relativistic light deflection is estimated directly by

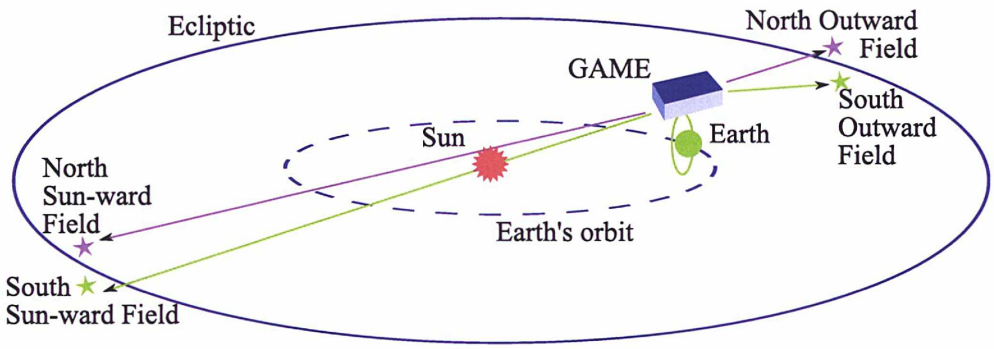

Figure 1.2: GAME will orbit around the Earth and will observe fields respectively in conjunction and opposition to the Sun [Gai *et al.* 2012]

measuring the same angles at two epochs: (a) with the Sun in conjunction and

(b) when, after some months, our parent star is in opposition. This experiment is implemented as a small mission, with a satellite in Earth polar orbit at an altitude of 1500 km. Its payload includes a telescope observing in the visible two fields of view with a few degrees of separation, simultaneously.

Preliminary simulations have shown that the expected final accuracy on γ can reach the 10^{-7} level, two orders of magnitude better than actual estimates (*i.e.* the recent radio links experiment with Cassini [Bertotti *et al.* 2003]).

1.1.3 BepiColombo

The European Space Agency (ESA) and the Japanese Aerospace Exploration Agency (JAXA) will jointly explore Mercury with BepiColombo mission [Benkhoff *et al.* 2010], due for launch by 2014 and comprising ESA's Mercury Planetary Orbiter (MPO) and JAXA's Mercury Magnetospheric Orbiter (MMO). From dedicated orbits, the two spacecrafts will observe the planet and its environment. Their scientific payload will provide the detailed information necessary to understand the origin and evolution of the planet itself and its surrounding environment. The scientific objectives focus on a global characterization of Mercury through the investigation of its interior, surface, exosphere and magnetosphere. In addition, testing relativistic gravity was recognized as a scientific objective of BepiColombo since the inception of the project.

Mercury is in fact the innermost and fastest orbiting planet of the Solar System so that relativistic effects on its motion are larger than for any other major Solar System body. Mercury is then a unique laboratory for probing gravity (the explanation of the anomalous periastron advance of Mercury's orbit was the first experimental success of GR), which pushed for the development of the Mercury Orbiter Radio Experiment (MORE) [Iess *et al.* 2009]. Based on the Cassini radio system which has been used to carry out the most accurate test of General Relativity in the Solar System to date [Bertotti *et al.* 2003], MORE will carry out a navigation experiment, aiming to a precise assessment of the orbit determination accuracies attainable with the use of the novel instrumentation and will repeat classical tests with much improved accuracy exploring new aspects of gravitational theories.

In particular, as shown in Table 1.1, MORE should test GR and alternative theories of gravity to a level better than 10^{-5} by measuring the time delay and Doppler shift of radio waves and the precession of Mercury's perihelion, test the strong equivalence principle to a level better than 4×10^{-5}, determine the gravitational oblateness of the Sun J_2 to better than 10^{-8} and finally set improved upper limits to the time variation of the gravitational "constant" G.

1.2 Relativistic framework for high-precision data

As seen in section 1.1, modern space astronomy relies on high precision observations whose data need to be reduced and interpreted in the framework of General Relativ-

Parameter	Present accuracy	Gaia	GAME	MORE
γ	2×10^{-5}	5×10^{-6}	$10^{-7} - 10^{-8}$	2×10^{-6}
β	1×10^{-4}	$10^{-3} - 10^{-5}$	10^{-6}	2×10^{-6}
η	5×10^{-4}	2×10^{-3}	-	8×10^{-6}
$J_2(Sun)$	4×10^{-8}	10^{-8}	5×10^{-9}	2×10^{-9}
$\frac{d(\ln G)}{dt}(years^{-1})$	9×10^{-13}	3×10^{-12}	-	3×10^{-13}

Table 1.1: Present and attainable accuracies with Gaia [Hobbs *et al.* 2010, Mouret 2011], GAME [Gai *et al.* 2012] and MORE [Iess *et al.* 2009] for the relativity parameters

ity (GR) [Soffel *et al.* 1991, Moyer 2000, Soffel *et al.* 2003]. To ensure the accuracy demanded by the missions presented in section 1.1, different issues need to be considered in the analysis of their observations: in particular, the definition of the observation in a proper reference frame, global reference systems allowing the comparison of observations made in each proper reference frame and a precise modeling for the propagation of the observed signal. Each of these issues has been deeply studied in the literature: the definition of global reference systems has been given by the IAU 2000 Resolution B1.3 in the post-Newtonian approximation of GR [Soffel *et al.* 2003] while several relativistic definitions of physically adequate local reference frames of a test observer have been proposed in [Bini *et al.* 2003, Klioner 2004]. As mentioned above, a precise modeling for the relativistic propagation of Electromagnetic Waves (EW) is also required. In fact, the behavior of the EW in the Solar System is intrinsically related to its space-time curvature [Misner *et al.* 1973, Weinberg 1972] and therefore one has to take it into account for modern astrometry.

In the following, we will briefly present these different aspects, illustrated in Fig. 1.3, with particular attention to the covariant definition of an observable and the most current approximations of GR used in the data analysis of space observations.

1.2.1 General Relativity and its approximations

Even if General Relativity is not the only theory of gravitation, it still seems to be the most simple among those successfully passing all the observational tests. A detailed review of the modern experimental foundations of gravitational physics can be found in [Will 2006]. Here, we shall just briefly recall the basic principle of the theory, the Einstein Equivalence Principle (EP). This principle states [Will 2006]

- that the inertial mass m_{iner} and the gravitational mass m_{grav} appearing on the two sides of the Newtonian gravitational law coincide. This has been tested with a precision of $|\delta m| / m < 5 \times 10^{-13}$;
- that light velocity in vacuum, c, is constant in any inertial reference frame. This has been tested at level $|\delta c^2| / c^2 < 10^{-21}$;

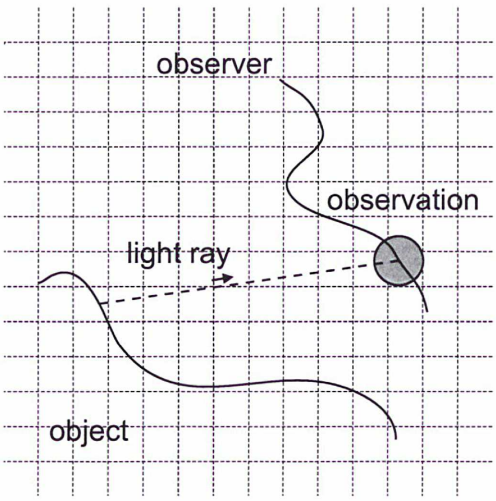

(a) From the point of view of Newtonian physics. The coordinate grid in the background symbolizes a global inertial reference system.

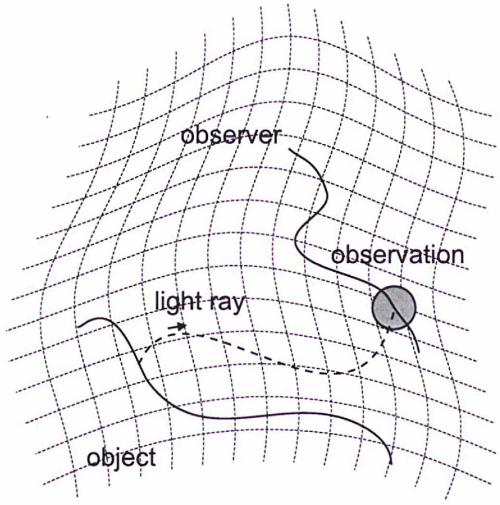

(b) From the point of view of relativistic physics. The grid of curved coordinates in the background symbolizes the chosen relativistic reference system.

Figure 1.3: Four parts of an astronomical event: motion of the observed object; motion of the observer; trajectory of an electromagnetic signal from the observed object to the observer; process of observation (from [Klioner 2005]).

- the local positional invariance, which can be tested by measuring the gravitational red-shift

$$\Delta\nu/\nu = (1+\alpha)c^{-2}\Delta U \ ,$$

where $\alpha = 0$ in GR. This too has been proven at level $|\alpha| < 2 \times 10^{-4}$.

Moreover, the theory of GR also states that

> *"The general laws of nature are to be expressed by equations which hold good for all systems of coordinates that is, are covariant with respect to any substitutions whatever (generally covariant)."* [Einstein 1916]

It is the so-called General Covariance Principle, stating that the laws of physics have to be the same for all observers. This principle is translated in mathematical terms by the use of tensorial identities and it has important consequences, such as the fact that space-time coordinates are no longer to be considered as intrinsic observables.

One of the consequences of the Equivalence Principle is that gravitation can be represented by a metric tensor $g_{\mu\nu}$. It is now question to explicit this metric tensor. In GR, its evolution is determined by solving Einstein's equations [Misner *et al.* 1973]

$$R_{\mu\nu} - \frac{1}{2}g_{\mu\nu}R + \Lambda g_{\mu\nu} = \frac{8\pi G}{c^4}T_{\mu\nu} \ , \tag{1.1}$$

where $R_{\mu\nu}$ is the Ricci tensor, R is the curvature scalar, G is the universal constant of gravitation, Λ the cosmological constant and $T_{\mu\nu}$ the stress-energy tensor. Eq. (1.1) tells us how space-time geometry is determined by its energy-matter content but its solution in a general case is a complex matter. Nevertheless, for most applications within the Solar System several hypothesis and simplifications can be assumed.

Indeed, since the Solar System can be considered as a gravitational weak field, the space-time metric can be expanded as

$$g_{\mu\nu} = \eta_{\mu\nu} + h_{\mu\nu} \,, \tag{1.2}$$

where η is the flat Minkowski metric and h is a small perturbation. Expansion (1.2) opens two main possibilities : the post-Minkowskian (PM) and the post-Newtonian (PN) approximations. The PM approximation of GR consists in supposing that the perturbation h can be expanded with respect to the universal gravitational constant G. This approximation only requires the weak field hypothesis (1.2), without limitations on the velocity of the sources of the gravitational field. We call it generalized PM approximation when the perturbation h is represented by an infinite series of powers of G; in this case, the covariant components of the metric tensor can be expanded as

$$g_{\mu\nu}(x, G) = \eta_{\mu\nu} + \sum_{n=1}^{\infty} G^n \, g^{(n)}_{\mu\nu}(x) \,, \tag{1.3}$$

while the contravariant components $g^{\mu\nu}_{(n)}$ are given by

$$g^{\mu\nu}_{(1)} = -\eta^{\mu\rho}\eta^{\nu\sigma} g^{(1)}_{\rho\sigma} \,, \tag{1.4a}$$

$$g^{\mu\nu}_{(n)} = -\eta^{\mu\rho}\eta^{\nu\sigma} g^{(n)}_{\rho\sigma} - \sum_{p=1}^{n-1} \eta^{\mu\rho} \, g^{(p)}_{\rho\sigma} \, g^{\nu\sigma}_{(n-p)} \,. \tag{1.4b}$$

In building the PN approximation of GR, we make additional assumptions. We suppose Solar System bodies to move slowly ($v^2 << c^2$) and that they are auto-gravitating, so that their orbits are gravitationally bounded. The equations of Newtonian dynamics show that the square velocity of an auto-gravitating body satisfies the following relation

$$v^2 \approx U \equiv \frac{GM}{r} \,, \tag{1.5}$$

where M is the mass of the body and r the distance from its center of mass, so that

$$\frac{v^2}{c^2} \approx \frac{GM}{c^2 r} \,. \tag{1.6}$$

Taking into account approximation (1.5), the perturbations $h_{\mu\nu}$ of the space-time metric (1.2) can be expanded in series of $1/c$ as follows

$$h_{00} = \frac{1}{c^2} h_{00}^{(2)} + \frac{1}{c^4} h_{00}^{(4)} + \mathcal{O}\left(\frac{1}{c^6}\right), \tag{1.7a}$$

$$h_{0i} = \frac{1}{c^3} h_{0i}^{(3)} + \mathcal{O}\left(\frac{1}{c^5}\right), \tag{1.7b}$$

$$h_{ij} = \frac{1}{c^2} h_{ij}^{(2)} + \mathcal{O}\left(\frac{1}{c^4}\right). \tag{1.7c}$$

Since GR is not the only possible theory of gravitation and other metric theories of gravitation exist, the so called post-Newtonian parameters have been introduced in order to distinguish and test these theories. The resulting formalism, the parametrized post-Newtonian (PPN) approximation [Will 1993], contains around ten parameters; in particular, we can write the metric tensor $g_{\mu\nu}$ in the global PPN reference system [Klioner & Soffel 2000] as

$$g_{00} = -1 + \frac{2}{c^2} w(t, \boldsymbol{x}) - \frac{2}{c^4} \beta w^2(t, \boldsymbol{x}) + \mathcal{O}(c^{-5}) \tag{1.8a}$$

$$g_{0i} = -\frac{2(1+\gamma)}{c^3} w^i(t, \boldsymbol{x}) + \mathcal{O}(c^{-5}) \tag{1.8b}$$

$$g_{ij} = \delta_{ij}\left(1 + \frac{2}{c^2}\gamma w(t, x)\right) + \mathcal{O}(c^{-4}) \tag{1.8c}$$

where w and w^i are the scalar and vector gravitational potentials while β and γ are the first two PPN parameters appearing in the metric. The parameter β is related to the non-linearity of the superposition of the gravity fields of different bodies while γ quantifies the effect of a mass unit on space-time curvature. Both parameters are unity in GR. Moreover, we can also define the Nordtvedt parameter $\eta = 4\beta - \gamma - 3$, used in the tests of the EP and equal to 0 in GR.

We shall point out that the PM approximation does not make any hypothesis about the internal physics and the motion of the sources of the gravitational field, thus keeping far more general than the PN/PPN approximation. In this thesis, we have chosen to define all needed quantities within the PM approximation while further expansions within the PPN approximation will be used for selected applications in the Solar System.

1.2.2 IAU relativistic reference systems

The IAU 2000 framework for relativistic modeling [Soffel *et al.* 2003] represents a self-consistent theoretical scheme enabling one to model any kind of astronomical observations in the PN approximation of GR. This paradigm is based on the assumption that the Solar System is the only source of weak gravitational field and that, at infinity, space-time is asymptotically flat. It deals with a number of local and one global reference frames which are connected to each other by PN coordinate transformations. The framework has three main theoretical ingredients. First,

a theory of local reference systems (mainly for application in the vicinity of the Earth) has been studied with the construction of the Geocentric Celestial Reference System (GCRS). Second, a PN theory of multipole expansions of a gravitational field has been performed and finally a careful investigation of the orders of magnitude of various effects has allowed to make the PN reduction formulas for time scales as simple as possible.

The local reference systems have two fundamental properties:

1. The gravitational field of external bodies (*i.e.* for the GCRS all Solar System bodies except the Earth) is represented only in the form of a relativistic tidal potential which is at least of second order in the local spatial coordinates and coincides with the usual Newtonian tidal potential in the Newtonian limit.

2. The internal gravitational field of the subsystem (e.g. the Earth for the GCRS) coincides with the gravitational field of a corresponding isolated source provided that the tidal influence of the external matter is neglected.

These two properties guarantee that the coordinate description of the local physical processes in the vicinity of the considered body (e.g. in the vicinity of the Earth in the case of GCRS) is as close as possible to the physical character of those processes. This means, for example, that if some relativistic effect is present in the coordinates (e.g., of a satellite of that body) the effect cannot be eliminated by selecting some other (more suitable) coordinates and therefore has physical character. It should be noted that although only one local reference system -GCRS- is explicitly defined by the IAU 2000 framework, it foresees GCRS-like local reference systems for each Solar System body for which the local physics (e.g. the structure of the gravitational field and the theory of rotational motion) should be precisely formulated. For example, the modeling of Lunar Laser Ranging (LLR) data requires a local Selenocentric Celestial Reference System [Kopeikin & Xie 2010]. Recent projects aimed at precise modeling of the rotational motions of Mercury and Mars will have to use the corresponding reference system for Mercury and Mars, respectively. All these local systems are defined by the same formulae as those given in the IAU 2000 framework for the GCRS, but with an index referring to the corresponding body. Moreover, a local reference system defined by the same IAU 2000 formulae, but constructed for a massless observer (with an index referring to a fictitious "body" of mass zero), is suitable to describe physical phenomena in the vicinity of that observer and, in particular, to define measurable quantities (observables) produced by that observer. The relation between this point of view and several standard ways to describe observables in GR is described by [Klioner 2004].

1.2.3 Relativistic equations of motion

The analysis of high precision observations also needs an accurate knowledge of the ephemerides of all Solar System bodies for both navigation and scientific purposes. For this reason, all modern planetary ephemerides such as the JPL

DE [Folkner *et al.* 2009], the IMCCE INPOP [Fienga *et al.* 2011] and the IAA RAS EPM [Pitjeva 2005] are built in a relativistic framework.

The principal relativistic effects on the dynamics of Solar System bodies can be divided in two categories [Klioner 2000] : translational and rotational motion.

The effects on the translational motion are mostly given by the so called Einstein-Infeld-Hoffmann (EIH) equations of motion of N gravitating bodies, whose gravitational field can be described by their masses $\mathcal{M}_A$ only. We get the acceleration

$$\ddot{\boldsymbol{x}}_A = -\sum_{B\neq A} G\mathcal{M}_B \frac{\boldsymbol{x}_A - \boldsymbol{x}_B}{|\boldsymbol{x}_A - \boldsymbol{x}_B|^3} + \frac{1}{c^2} F_{PN}(\mathcal{M}_B, \boldsymbol{x}_B, \dot{\boldsymbol{x}}_B, \boldsymbol{x}_A, \dot{\boldsymbol{x}}_A) + \mathcal{O}(c^{-4}) \ , \quad (1.9)$$

where we define $\boldsymbol{x}_{A/B}$ the coordinates of body A/B, F_{PN} representing the post-Newtonian perturbation to the Newtonian orbital motion and $\dot{\boldsymbol{x}}_B$ the coordinate velocity of body B. In order to derive F_{PN}, we need to know all terms contained in the metric tensor (1.2). The main detectable effects represented by F_{PN} are

- perihelion shifts ($\approx 43"/cty$ for Mercury, $\approx 10"/cty$ for Icarus, ...);
- geodetic precession ($\approx 2"/cty$ for the lunar orbit);
- various periodic relativistic effects (important mostly for LLR and binary pulsar timing observations).

Further relativistic effects due to the rotation of the bodies (Lense-Thirring or gravitomagnetic effects) and those due to the asphericity of the gravitating bodies are mostly neglected in the construction of planetary ephemerides.

Nevertheless, an adequate relativistic description of the rotational motion is also required for the definition of local reference systems (for example, the GCRS). In this case, the PN equations of motion

$$d^2S^i/dt^2 = L^i_N + c^{-2}L^i_{PN} + \mathcal{O}(c^{-4}) \ , \quad (1.10)$$

where S^i is the relativistic spin of the body, L^i_N and L^i_{PN} are the Newtonian and post-Newtonian torques, respectively [Klioner & Soffel 1998]. Again, a full post-Newtonian metric tensor is required to derive these equations. The most important effects on Earth rotation are [Klioner *et al.* 2008] the geodetic precession ($\approx 1.914"/cty$) and nutation ($\approx 153\ \mu as$).

Moreover, some recent ephemerides such as INPOP08 [Fienga *et al.* 2009], also include a relativistic time scale transformation. The idea is to provide positions and velocities of Solar System celestial objects, as well as time ephemerides relating the Terrestrial time-scale (TT) and the time argument of INPOP, the so-called barycentric dynamical time (TDB), based on the definition adopted by the International Astronomical Union in 2006. This makes INPOP08 a 4D ephemeris and fully suitable for building Gaia timescale [Le Poncin-Lafitte 2010].

1.2.4 Relativistic light propagation

Observations of all space missions presented in section 1.1 are based on time delay, frequency shift or angular measurements of an EW. In the approximation of optical geometry this EW is described from a theoretical point of view by a light ray propagating along a null-geodesic path, *i.e.* a curbe obeying the equations

$$\frac{dk^\mu}{d\lambda} + \Gamma^\mu_{\alpha\beta} k^\alpha k^\beta = 0 \quad , \quad k^\mu k_\mu = 0 \, , \tag{1.11}$$

where $k^\mu = dx^\mu/d\lambda$ is a vector tangent to the light ray, λ being an affine parameter and

$$\Gamma^\alpha_{\beta\gamma} = \frac{1}{2} g^{\alpha\mu} \left(\partial_\gamma g_{\mu\beta} + \partial_\beta g_{\mu\gamma} - \partial_\mu g_{\beta\gamma} \right) \tag{1.12}$$

are the Christoffel symbols. One should note that this approximation only applies when the amplitude and frequency of the signal can be considered constant over its period and when the wavelength of the observed signal is smaller than the typical dimension of space-time curvature [Misner *et al.* 1973], which is the case of the Solar System.

In Table 1.2 we present the angular deviation of a light ray grazing the main bodies of the Solar System. The column δ_{PN} represents the contribution of the

gravitational body	δ_{PN}	δ_{J_2}	δ_{J_4}	δ_{J_6}	δ_R	δ_{T^*}	δ_{2PN}
Sun	$1.75\ 10^6$	$\sim$1	—	—	0.7	0.1	11
Mercury	83	—	—	—	—	—	—
Venus	493	—	—	—	—	—	—
Earth	574	0.6	—	—	—	—	—
Moon	26	—	—	—	—	—	—
Mars	116	0.2	—	—	—	—	—
Jupiter	16270	240	10	$\sim$1	0.2	0.8	—
Saturn	5780	95	6	—	—	0.2	—
Uranus	2080	8	—	—	—	—	—
Neptune	2533	10	—	—	—	—	—

Table 1.2: Relativistic deflection of light grazing Solar System bodies [Klioner 2003] (unit : microarcsecond - μas).

spherical shape of the massive body to the direction of the light ray: this effect weakens in $1/b$ (see Fig. 1.4), where b is an impact parameter. The columns δ_{J_n} (with $n = 2, 4, 6$) show that one should also take into account the effects due to the asphericity of the planets: even if these effects are important at the μas precision,

at least for the largest bodies of the Solar System, their influence lowers as $1/b^{2n+1}$ so that they need to be taken into account only for light rays grazing the perturbing bodies. The δ_{T^*} and δ_R columns represent the influence of the translational and rotational motion of the bodies: one can note that even these effects have to be controlled when the μas accuracy is required. Finally, the δ_{2PN} column provides the deflection due to a spherical body at the second order of the post-Newtonian approximation : this effect is still important when focusing on observations towards the Sun (which is not the case for the Gaia mission but is relevant for the GAME mission). The combined result of all these effects on the celestial sphere is illustrated in Figure 1.4.

Figure 1.4: Magnitude of light deflection due to solar system planets at some fixed moment of time as distributed on the celestial sphere shown from three sides. The larger the deflection the darker is the area. Although the deflection from each planet monotonically falls off with the angular distance from the planet, vectorial character of the deflection leads to a complicated distribution of the magnitude when several planets come into play. The solid lines are lines of constant declination (from [Klioner 2012]).

During the last decades, many approaches have been developed to describe the trajectory of such light signals and to provide its coordinate direction, frequency shift and time of flight, defined as the coordinate time lapse between the emission and reception events. We shall briefly enumerate the methods existing in the literature:

1. a first method is the analytical derivation of the null-geodesic equation followed by the integration of the trajectory of the light ray. It is the method applied by [Blanchet *et al.* 2001] in the weak-field approximation to determine the time transfer in the Schwarzschild geometry up to the $1/c^3$ order. This method has also been used by [Chauvineau *et al.* 2005] for the mission LISA in the PPN framework and by [Minazzoli & Chauvineau 2011] in the case of scalar-tensor theories of gravity. [Kopeikin & Schäfer 1999] analytically computed the solution up to the 1PM order for a system of arbitrary moving bodies while [Klioner & Zschocke 2010] pushed the computation up to the 2PM order in the static case. In a non-perturbative approach, we shall note that some

solutions of the null-geodesic equation have been given for the Schwarzschild and Kerr metric [Hagihara 1931, Chandrasekhar 1983, Čadež & Kostić 2005, Fujita & Hikida 2009, Kostić 2012].

2. another method, developed by [de Felice *et al.* 2004], analytically solves a set of so called *master equations* representing a projection of the null-geodesic equation in the frame of a local barycentric observer, following the specifications of the relativistic theory of measurement [de Felice & Clarke 1992, de Felice & Bini 2010].

3. the third method consists in a purely numerical integration of the geodesic equations using the "shooting method" to solve the boundary problem. This method, developed by [San Miguel 2007] is general and can be applied to any metric.

4. a fourth method uses the eikonal theory in place of the integration of the null-geodesic equation. This method has been developed by [Ashby & Bertotti 2010] and used for the data analysis of the Cassini mission.

5. the last method uses the Synge World Function instead of an explicit computation of the null-geodesic. The World Function introduced by [Synge 1960] is used by [Linet & Teyssandier 2002] to compute the time transfer at the $1/c^4$ order in axisymmetric geometries. This approach has been then further generalized in the PM approximation by [Le Poncin-Lafitte *et al.* 2004]. Finally, a simpler version allowing for a direct computation of the time transfer has been developed by [Teyssandier & Le Poncin-Lafitte 2008]. Using this method, time transfer is computed as a PM expansion in which each of the perturbation terms is an integral of functions depending only on the metric and its derivatives taken along the Minkowskian trajectory of the photon (the straight line between the emission and reception of the photon).

In this thesis, we will apply this last approach to describe light propagation in a curved space-time.

1.2.5 Relativistic observables

As anticipated in section 1.2.1, in modern theories of gravitation the laws of physics are invariant under coordinate transformations. For this reason, we can choose in which reference system we want to write our equations (for example those describing light propagation). This freedom also implies that all coordinate quantities have generally speaking no physical sense and cannot be observed. A coordinate system is indeed only a mathematical tool that we choose to realize our computations and it is extremely important to focus on quantities which are invariant under a diffeomorphism.

In the end, the description of a physical system depends both on the observer and on the chosen frame of reference. If an observer u has operational control of the instrumentation used for the measurement we shall then define a reference frame adapted to him. This is a set of one unit time-like vector and three unit space-like vectors (defined up to an arbitrary spatial rotation) constituting a comoving tetrad. In most cases, the result of a measurement is affected by contributions from the background curvature and from the peculiarity of the reference frame. As long as we can neglect the influence of the curvature, we call a measurement "local"; conversely, if the curvature is strong enough with respect to the measurement's domain (the region of space-time in which a measurement takes place) , the measurement will be called "non-local". The aim of the relativistic theory of measurement [de Felice & Bini 2010] is to enable one to devise, out of the tensorial representation of a physical system and with respect to a given frame, those scalars which describe specific properties of the system and which can be called "observables".

1.3 Outline

This study sets the basis of an accurate model for data analysis within a relativistic framework based on the well assessed Time Transfer Functions formalism. It has been developed under the joint supervision of a French team at Paris Observatory and an Italian team in Turin and it can be ideally separated in two parts. In chapters 2, 3 and 4, we focus on the study of light propagation in a curved space-time and on the modeling of the observables currently used in radio-science and astrometry. In chapters 5 and 6, we apply our model to space astrometry focusing on the Gaia mission. In the following, we provide a detailed outline of our work.

In chapter 2, we study light propagation between two distinct events in space-time $x_A = (ct_A, \boldsymbol{x}_A)$ and $x_B = (ct_B, \boldsymbol{x}_B)$ relied by a null-geodesic curve Γ_{AB} parametrized by a parameter λ and located at finite distance from the origin of the coordinates. We use the Time Transfer Functions formalism, developed at Paris Observatory, to write two functions $\mathcal{T}_r(t_B, \boldsymbol{x}_A, \boldsymbol{x}_B)$ and $\mathcal{T}_e(t_A, \boldsymbol{x}_A, \boldsymbol{x}_B)$ describing the coordinate time of flight $t_B - t_A$ of a light signal between these events as a PM expansion; it has been shown that deriving these quantities gives the direction triple $\left(\widehat{k_i}\right)_{A/B} \equiv \left.\frac{k_i}{k_0}\right|_{A/B}$, ratio of the spatial and temporal components of the tangent vector $k_\alpha = g_{\alpha\beta}\frac{dx^\beta}{d\lambda}$ to the light ray at $\boldsymbol{x}_A$ and $\boldsymbol{x}_B$, respectively as well as the ratio of its time components at boundaries $\mathcal{K} \equiv \frac{(k_0)_B}{(k_0)_A}$.

Using the properties of the TTF, we compute a general closed-form formula for

the direction triple $\left(\widehat{k}_i\right)_B$ up to the 2PM order as

$$\left(\widehat{k}_i\right)_B = -N_{AB}{}^i + \int_0^1 F_i^{(1)}\left[\partial h_{\mu\nu}^{(1)}\right]_{z_-^\alpha(\lambda)} d\lambda + \int_0^1 F_i^{(2)}\left[h_{\mu\nu}^{(1)}, \partial h_{\mu\nu}^{(1,2)}\right]_{z_-^\alpha(\lambda)} d\lambda + \mathcal{O}(h^3)\,, \tag{1.13}$$

where the integrals are computed along z_-, the Minkowskian straight line between x_A and x_B and $F_i^{(n)}$ are explicit functions of the gravitational perturbation h and its partial derivatives. Similarly, we compute general closed form equations also for $\left(\widehat{k}_i\right)_A$ and $\mathcal{K}$. These formulae are valid for any material content in a weak-field and are particularly adapted for numerical integration.

Nevertheless, when dealing with a huge amount of data, numerical integration becomes very time consuming. For this reason, in chapter 3 we provide analytical solutions of these integrals in some simple, but widely used, cases. First, we apply our results to the Schwarzschild's geometry to provide an explicit solution for the time transfer, the direction triple and the ratio $\mathcal{K}$ up to the 2PM order. It allows us to check our result with [Teyssandier 2012] in order to validate the general formulae presented in chapter 2. Then, we place ourselves in the PPN framework, which is allowed when dealing with space missions within the Solar System. We use the PPN metric recommended by IAU2000 to write $\mathcal{T}_{e/r}$ and $\hat{k}_i$ as functions of the scalar and vector gravitational potentials w and $\boldsymbol{w}$ obeying to the Poisson equations [Linet & Teyssandier 2002]. First, we present the case of an isolated axisymmetric body treated in [Le Poncin-Lafitte & Teyssandier 2008] and then we focus on the solution for a system of point masses in linear uniform motion.

Chapter 4 focuses on the covariant general modeling of the observables needed in space navigation, namely the Ranging and Doppler for a moving emitter and receiver, and in astrometry, namely the angular distance between two light sources and the projection of the direction of an incident light ray on the $3-$*plane* of a given observer. Such an observer can be represented by a comoving tetrad that we also provide up to the 2PM order. We obtain exact relations for these observables within the TTF formalism. This means that these quantities can be explicitly determined without the knowledge of the null geodesic connecting the emission x_A and reception x_B events. Using the results of the previous chapters, we present our equations in a form well adapted to numerical integration for any weak field metric. We also present their analytical solution in a spherically symmetric gravitational field as well as estimates of the relativistic correction up to 2PM for BepiColombo and GAME-like missions [Hees *et al.* 2013].

In chapter 5 we apply the results of the first part of this thesis to astrometry, focusing on the Gaia mission. In this context, two well-assessed relativistic models already exist: the Gaia Relativity Model (GREM) [Klioner 2003] and the Relativistic Astrometric Model (RAMOD) [de Felice *et al.* 2006]. Thanks to the collaboration between the French group and the Italian group responsible for RAMOD, we de-

veloped an analytical comparison of the modeling for the astrometric observable between the three models. In particular, we show how the time of flight and direction triple of a light ray propagating between x_A and x_B can be computed within GREM and RAMOD giving results equivalent to those presented for the TTF in chapter 3, at least at the approximation needed for Gaia [Bertone *et al.* 2013a]. This comparison provides a further validation of our formulae and it completes a previous study about the different approaches used to model relativistic aberration in the Gaia context [Crosta & Vecchiato 2010].

In chapter 6, we apply our model to the analysis of a simulated astrometric observation. In collaboration with the italian group responsible for GSR (one of the two software in charge for the reduction of Gaia observations), we implement a "GSR-TTF" code, implementing our formulae and Gaia attitude to compute the astrometric observable. Thanks to the functionalities of GSR, we compare our results with those of GREM and of PPN-RAMOD (a non-perturbative model of the RAMOD family). Finally, we present its application to the reconstruction of a small celestial sphere.

CHAPTER 2

TTF formalism for light propagation

Contents

A large part of this work is based on the mathematical formalism of the Time Transfer Functions (TTF) [Linet & Teyssandier 2002, Le Poncin-Lafitte *et al.* 2004, Teyssandier & Le Poncin-Lafitte 2008]. In section 2.1, we define the emission and reception Time Transfer Functions $\mathcal{T}_{e/r}(x_A, x_B, t_{A/B})$, giving the coordinate time of flight of a photon between x_A and x_B and we present the relations to get the ratios of the covariant components of the tangent vectors $k^\alpha = dx^\alpha/d\lambda$ to the light ray at x_A and x_B. In section 2.2, we recall that in the weak field approximation it is possible to get explicit equations for $\mathcal{T}_{e/r}(x_A, x_B, t_{A/B})$ as a PM expansion without computing the whole trajectory of light. Once the TTF is known, it is then possible to derive explicitly the ratios giving the direction triples $(\hat{k}_i)_{A/B} \equiv (k_i/k_0)_{A/B}$ as well as $\mathcal{K} \equiv (k_0)_B/(k_0)_A$. Finally, in section 2.3 we present our procedure to directly compute these ratios within the PM approximation of GR and up to the second order as closed form integrals (*i.e.* function of a metric tensor and its derivatives only) taken along the straight Minkowskian line between x_A and x_B.

2.1 Synge World Function and direction of a light ray

We suppose the existence of a unique light ray Γ connecting two events $x_A = (ct_A, \boldsymbol{x}_A)$ and $x_B = (ct_B, \boldsymbol{x}_B)$ in a spacetime described by a given metric $g_{\mu\nu}$. We denote by λ the unique affine parameter along Γ parametrized by the curve x^α which fulfills the boundary conditions $\lambda(x_B) = 1$ and $\lambda(x_A) = 0$. The Synge World

Function [Synge 1960] of space-time is the two point function $\Omega(x_A, x_B)$ defined as

$$\Omega(x_A, x_B) = \frac{1}{2}\int_0^1 g_{\mu\nu}(x^\alpha(\lambda))\frac{dx^\mu}{d\lambda}\frac{dx^\nu}{d\lambda}d\lambda, \tag{2.1}$$

the integral being taken along the null-geodesic Γ connecting the two events. For our purpose, the World Function has some interesting properties,

i) two points x_A and x_B are linked by a light ray if and only if

$$\Omega(x_A, x_B) = 0\ , \tag{2.2}$$

so that $\Omega(x, x_B)$ is the equation of the light cone $\mathcal{C}(x_B)$ at x_B. If $\Omega(x_A, x_B)$ is explicitly known, it is then possible to determine the travel time $t_B - t_A$ of a photon connecting the two points as a function of their coordinates. It must be pointed out, however, that solving the equation $\Omega(t_A, \boldsymbol{x}_A, t_B, \boldsymbol{x}_B) = 0$ for t_A yields two distinct solutions t_A^+ and t_A^- since the time-like curve $\boldsymbol{x} = \boldsymbol{x}_B$ cuts the light cone $\mathcal{C}(x_B)$ at two points x_A^+ and x_A^-, x_A^+ being in the future of x_A^-. If we consider x_A to be the point of emission of the photon and if x_B is its point of reception, we are only concerned by the solution t_A^-. A similar reasoning can be stated for the solution with respect to t_B and for the light cone $\Omega(x_A, x)$. For the sake of compactness, we will from now on use the notations $t_A \equiv t_A^-$ and $t_B \equiv t_B^+$.

Indeed, it is possible to define two Time Transfer Functions [Linet & Teyssandier 2002]

$$t_B - t_A = \mathcal{T}_r(\boldsymbol{x}_A, t_B, \boldsymbol{x}_B) = \mathcal{T}_e(t_A, \boldsymbol{x}_A, \boldsymbol{x}_B), \tag{2.3}$$

depending on the instant of reception t_B or emission t_A of the signal and called the reception and the emission Time Transfer Function, respectively. Explicit expressions of these functions are different except in a stationary space-time in which the coordinate system is chosen so that the metric does not depend on $x^0 = ct$. In this case, we get $\mathcal{T}_r(\boldsymbol{x}_A, t_B, \boldsymbol{x}_B) = \mathcal{T}_e(t_A, \boldsymbol{x}_A, \boldsymbol{x}_B) = \mathcal{T}(\boldsymbol{x}_A, \boldsymbol{x}_B)$.

ii) the vectors $(k^\alpha)_A = \left(\frac{dx^\alpha}{d\lambda}\right)_A$ and $(k^\alpha)_B = \left(\frac{dx^\alpha}{d\lambda}\right)_B$ tangent to the geodesic Γ at x_A and x_B, respectively are given by

$$\left(g_{\alpha\beta}\frac{dx^\beta}{d\lambda}\right)_A = -\frac{\partial\Omega}{\partial x_A^\alpha} \qquad \text{and} \qquad \left(g_{\alpha\beta}\frac{dx^\beta}{d\lambda}\right)_B = \frac{\partial\Omega}{\partial x_B^\alpha}\ . \tag{2.4}$$

From property i) it follows straightforwardly that

$$\Omega(t_B - c\mathcal{T}_r(\boldsymbol{x}_A, t_B, \boldsymbol{x}_B), \boldsymbol{x}_A, t_B, \boldsymbol{x}_B) \equiv 0 \tag{2.5}$$

and differentiating this equation with respect to x_B^i, t_B and x_A^i, one obtains

$$-\frac{\partial\Omega(x_A,x_B)}{\partial t_A}\frac{\partial\mathcal{T}_r(\boldsymbol{x}_A,t_B,\boldsymbol{x}_B)}{\partial x_B^i}+\frac{\partial\Omega(x_A,x_B)}{\partial x_B^i}=0\,, \tag{2.6a}$$

$$\frac{\partial\Omega(x_A,x_B)}{\partial t_A}\left[1-\frac{\partial\mathcal{T}_r(\boldsymbol{x}_A,t_B,\boldsymbol{x}_B)}{\partial t_B}\right]+\frac{\partial\Omega(x_A,x_B)}{\partial t_B}=0\,, \tag{2.6b}$$

$$-\frac{\partial\Omega(x_A,x_B)}{\partial t_A}\frac{\partial\mathcal{T}_r(\boldsymbol{x}_A,t_B,\boldsymbol{x}_B)}{\partial x_A^i}+\frac{\partial\Omega(x_A,x_B)}{\partial x_A^i}=0\,. \tag{2.6c}$$

These relations hold for any couple of points (x_A,x_B) connected by a null geodesic. Substituting now Eq. (2.4) into Eq. (2.6), we get the following relations [Le Poncin-Lafitte *et al.* 2004] between the ratio of the covariant components of the tangent vectors to the geodesic and $\mathcal{T}_r$

$$\left(\widehat{k}_i\right)_B\equiv\left(\frac{k_i}{k_0}\right)_B=-c\frac{\partial\mathcal{T}_r}{\partial x_B^i}\left[1-\frac{\partial\mathcal{T}_r}{\partial t_B}\right]^{-1}\,, \tag{2.7a}$$

$$\left(\widehat{k}_i\right)_A\equiv\left(\frac{k_i}{k_0}\right)_A=c\frac{\partial\mathcal{T}_r}{\partial x_A^i}\,, \tag{2.7b}$$

$$\mathcal{K}\equiv\frac{(k_0)_B}{(k_0)_A}=1-\frac{\partial\mathcal{T}_r}{\partial t_B}\,. \tag{2.7c}$$

Also, noting that

$$\Omega(t_A,\boldsymbol{x}_A,t_A+c\mathcal{T}_e(t_A,\boldsymbol{x}_A,\boldsymbol{x}_B),\boldsymbol{x}_B)\equiv 0\,, \tag{2.8}$$

similar expressions for $\left(\widehat{k}_i\right)_{A/B}$ and $\mathcal{K}$ can be deduced for $\mathcal{T}_e(t_A,\boldsymbol{x}_A,\boldsymbol{x}_B)$. Once known explicitly, the quantities defined in Eq. (2.3) and Eq. (2.7) can be used to define Ranging and Doppler in space navigation and astrometric observables (which will be detailed in chapter 4). We will now focus on the determination of the function $\mathcal{T}_r(\boldsymbol{x}_A,t_B,\boldsymbol{x}_B)$ in its PM expansion.

2.2 Post-Minkowskian time transfer and delay functions

The covariant components of the tangent vector to the null geodesic Γ_{AB} at x_A must satisfy the isotropic conditions

$$(g^{\mu\nu}k_\mu k_\nu)_{x_A}=0\,. \tag{2.9}$$

Dividing this equation side by side by $[(k_0)_A]^2$, and then taking equation (2.7b) into account yields the following partial differential equation [Teyssandier & Le Poncin-Lafitte 2008]

$$g^{00}(x_B^0-c\mathcal{T}_r,\boldsymbol{x}_A)+2c\,g^{0i}(x_B^0-c\mathcal{T}_r,\boldsymbol{x}_A)\frac{\partial\mathcal{T}_r}{\partial x_A^i}$$
$$+c^2\,g^{ij}(x_B^0-c\mathcal{T}_r,\boldsymbol{x}_A)\frac{\partial\mathcal{T}_r}{\partial x_A^i}\frac{\partial\mathcal{T}_r}{\partial x_A^j}=0\,. \tag{2.10}$$

Obtaining a solution to this equation is as challenging as the determination of the null geodesic equations. However, this task is easier in the weak field approximation. Let us write the metric tensor as follows

$$g_{\mu\nu} = \eta_{\mu\nu} + h_{\mu\nu} \,, \tag{2.11}$$

with $\eta_{\mu\nu}$ =diag$(-1,+1,+1,+1)$ a Minkowskian background and $h_{\mu\nu}$ a perturbation admitting the following general PM expansion

$$h_{\mu\nu} = \sum_{n=1}^{\infty} G^n g^{(n)}_{\mu\nu} \,. \tag{2.12}$$

Considering Eq. (2.11), the reception Time Transfer Function can then be expanded as

$$\mathcal{T}_r(\boldsymbol{x}_A, t_B, \boldsymbol{x}_B) = \frac{R_{AB}}{c} + \frac{\Delta_r(\boldsymbol{x}_A, t_B, \boldsymbol{x}_B)}{c} \,, \tag{2.13}$$

where

$$R_{AB} = |\boldsymbol{x}_B - \boldsymbol{x}_A| \tag{2.14}$$

and $\Delta_r(\boldsymbol{x}_A, t_B, \boldsymbol{x}_B)/c$ is of the order of $h_{\mu\nu}$. We call it the *reception time delay* function. Our problem is then to determine $\Delta_r(\boldsymbol{x}_A, t_B, \boldsymbol{x}_B)$. Following [Teyssandier & Le Poncin-Lafitte 2008], we shall replace x_A by a variable x and consider t_B and $\boldsymbol{x}_B$ as fixed parameters. Inserting $\mathcal{T}_r(\boldsymbol{x}, t_B, \boldsymbol{x}_B) = \dfrac{|\boldsymbol{x}_B - \boldsymbol{x}|}{c} + \dfrac{\Delta_r(\boldsymbol{x}, t_B, \boldsymbol{x}_B)}{c}$ into equation (2.10), it yealds now

$$2N^i \frac{\partial \Delta_r(\boldsymbol{x}, t_B, \boldsymbol{x}_B)}{\partial x^i} = W(\boldsymbol{x}, t_B, \boldsymbol{x}_B), \tag{2.15}$$

where $\boldsymbol{N} = \dfrac{\boldsymbol{x}_B - \boldsymbol{x}}{|\boldsymbol{x}_B - \boldsymbol{x}|}$ and $W(\boldsymbol{x}, t_B, \boldsymbol{x}_B)$ is given by

$$\begin{aligned} W(\boldsymbol{x}, t_B, \boldsymbol{x}_B) = {} & h^{00}(x_-) - 2N^i h^{0i}(x_-) + N^i N^j h^{ij}(x_-) + 2\Big[h^{0i}(x_-) - N^j h^{ij}(x_-)\Big] \\ & \times \frac{\partial \Delta_r(\boldsymbol{x}, t_B, \boldsymbol{x}_B)}{\partial x^i} + \Big[\eta^{ij} + h^{ij}(x_-)\Big] \frac{\partial \Delta_r(\boldsymbol{x}, t_B, \boldsymbol{x}_B)}{\partial x^i} \frac{\partial \Delta_r(\boldsymbol{x}, t_B, \boldsymbol{x}_B)}{\partial x^j} \,, \end{aligned} \tag{2.16}$$

x_- being the point-event defined by

$$x_- = (x^0_B - |\boldsymbol{x}_B - \boldsymbol{x}| - \Delta_r(\boldsymbol{x}, t_B, \boldsymbol{x}_B), \boldsymbol{x}) \,. \tag{2.17}$$

Since x is a free variable, we consider the case where x is varying along the straight segment joining x_A and x_B . Then we get

$$\boldsymbol{N} = \boldsymbol{N}_{AB} \,, \tag{2.18}$$

where $\boldsymbol{N}_{AB} \equiv \dfrac{\boldsymbol{x}_B - \boldsymbol{x}_A}{R_{AB}}$ while we define $\boldsymbol{x} = \boldsymbol{z}_-(\lambda)$ and

$$\boldsymbol{z}_-(\lambda) = \boldsymbol{x}_B - \lambda R_{AB} \boldsymbol{N}_{AB} \qquad , \qquad 0 < \lambda < 1 \,. \tag{2.19}$$

Using Eq. (2.15) and Eq. (2.19), the reception delay function is then governed by the differential equation

$$\frac{d\Delta_r(\boldsymbol{z}_-(\lambda), t_B, \boldsymbol{x}_B)}{d\lambda} = -\frac{R_{AB}}{2} W(\boldsymbol{z}_-(\lambda), t_B, \boldsymbol{x}_B) \,, \tag{2.20}$$

with the boundary condition

$$\Delta_r(\boldsymbol{z}_-(0), t_B, \boldsymbol{x}_B) = 0 \,, \tag{2.21}$$

which follows from the boundary condition $\Delta_r(\boldsymbol{x}_B, t_B, \boldsymbol{x}_B) = 0$ and from Eq. (2.19). As a consequence, we have

$$\Delta_r(\boldsymbol{z}_-(\lambda), t_B, \boldsymbol{x}_B) = -\frac{R_{AB}}{2} \int_0^\lambda W(\boldsymbol{z}_-(\lambda'), t_B, \boldsymbol{x}_B) d\lambda' \,. \tag{2.22}$$

Using now Eq. (2.16) and noting that $\boldsymbol{z}_-(1) = \boldsymbol{x}_A$, we can get from Eq. (2.22) the integral-differential equation

$$\begin{aligned} \Delta_r(\boldsymbol{x}_A, t_B, \boldsymbol{x}_B) \;=\; & -\frac{R_{AB}}{2} \int_0^1 \Big[(h^{00} - 2N^i h^{0i} + N^i N^j h^{ij})_{\tilde{z}_-(\lambda)} + \\ & 2\left[h^{0i}(\tilde{z}_-(\lambda)) - N^j h^{ij}(\tilde{z}_-(\lambda))\right] \times \frac{\partial \Delta_r(\boldsymbol{z}_-(\lambda), t_B, \boldsymbol{x}_B)}{\partial x^i} + \\ & \left[\eta^{ij} + h^{ij}(\tilde{z}_-(\lambda))\right] \frac{\partial \Delta_r(\boldsymbol{z}_-(\lambda), t_B, \boldsymbol{x}_B)}{\partial x^i} \frac{\partial \Delta_r(\boldsymbol{z}_-(\lambda), t_B, \boldsymbol{x}_B)}{\partial x^j} \Big] d\lambda' \,, \end{aligned} \tag{2.23}$$

where $\tilde{z}_-(\lambda)$ is the point-event

$$\tilde{z}_-(\lambda) = \Big(x_B^0 - \lambda R_{AB} - \Delta_r\Big(\boldsymbol{z}_-(\lambda), t_B, \boldsymbol{x}_B\Big), \boldsymbol{z}_-(\lambda) \Big) \,. \tag{2.24}$$

This result is quite convenient to obtain the general PM expansion of the reception delay function.

We define the PM expansion of the contravariant components of the metric as

$$g^{\mu\nu} = \eta^{\mu\nu} + h^{\mu\nu} \,, \tag{2.25}$$

where

$$h^{\mu\nu} = \sum_{n=1}^{\infty} G^n g^{\mu\nu}_{(n)} \tag{2.26}$$

and the set of quantities $g^{\mu\nu}_{(n)}$ can be obtained using the relations

$$g^{\mu\nu}_{(1)} = -\eta^{\mu\rho}\eta^{\nu\sigma} g^{(1)}_{\rho\sigma} \,, \tag{2.27a}$$

and for $n \geq 2$

$$g^{\mu\nu}_{(n)} = -\eta^{\mu\rho}\eta^{\nu\sigma} g^{(n)}_{\rho\sigma} - \sum_{p=1}^{n-1} \eta^{\mu\rho} g^{(p)}_{\rho\sigma} g^{\nu\sigma}_{(p)} \,. \tag{2.27b}$$

It is then possible to expand the reception delay function as a series of ascending powers of the Newtonian gravitational constant G

$$\Delta_r(\boldsymbol{x}, t_B, \boldsymbol{x}_B, G) = \sum_{n=1}^{\infty} G^n \Delta_r^{(n)}(\boldsymbol{x}, t_B, \boldsymbol{x}_B) \ , \tag{2.28}$$

where it has been demonstrated by [Teyssandier & Le Poncin-Lafitte 2008] that each perturbation term $\Delta_r^{(n)}$ can be obtained as a line integral taken along the straight line (2.19). This result is particularly interesting and can be interpreted as an application of the Fermat principle [Perlick 1990] in the nth-post-Minkowskian approximation. It follows from Eq. (2.24) that each term of Eq. (2.26) can be written as

$$h^{\mu\nu}(\tilde{z}_-(\lambda), G) = \sum_{n=1}^{\infty} G^n g_{(n)}^{\mu\nu}(x_B^0 - \lambda R_{AB} - \Delta_r(\boldsymbol{z}_-(\lambda), t_B, \boldsymbol{x}_B), \boldsymbol{z}_-(\lambda)) \tag{2.29}$$

where we can substitute Δ_r from eq. (2.28) and then perform a Taylor expansion around the point $z_-(\lambda)$ defined by

$$z_-(\lambda) = (x_B^0 - \lambda R_{AB}, \boldsymbol{z}_-(\lambda)) \tag{2.30}$$

in order to obtain the PM expansion of $h^{\mu\nu}(\tilde{z}_-(\lambda), G)$. A straightforward calculation yields

$$h^{\mu\nu}(\widetilde{z}_-(\lambda), G) = \sum_{n=1}^{\infty} G^n \widehat{g}_{-(n)}^{\mu\nu}(z_-(\lambda), t_B, \boldsymbol{x}_B), \tag{2.31}$$

where the quantities $\widehat{g}_{-(n)}^{\mu\nu}(z_-(\lambda), t_B, \boldsymbol{x}_B)$ are given by

$$\widehat{g}_{-(1)}^{\mu\nu}(z_-(\lambda), t_B, \boldsymbol{x}_B) = g_{(1)}^{\mu\nu}(z_-(\lambda)) \tag{2.32}$$

and

$$\begin{aligned} \widehat{g}_{-(n)}^{\mu\nu}(z_-(\lambda), t_B, \boldsymbol{x}_B) \ &= \ g_{(n)}^{\mu\nu}(z_-(\lambda)) \\ &\quad + \sum_{m=1}^{n-1} \sum_{k=1}^{m} \Phi_r^{(m,k)}(\boldsymbol{z}_-(\lambda), t_B, \boldsymbol{x}_B) \left[\frac{\partial^k g_{(n-m)}^{\mu\nu}}{(\partial x^0)^k} \right]_{z_-(\lambda)} \end{aligned} \tag{2.33}$$

for $n \geq 2$ with

$$\Phi_r^{(m,k)}(\boldsymbol{x}, t_B, \boldsymbol{x}_B) = \frac{(-1)^k}{k!} \sum_{l_1 + \cdots + l_k = m-k} \left[\prod_{j=1}^{k} \Delta_r^{(l_j+1)}(\boldsymbol{x}, t_B, \boldsymbol{x}_B) \right] , \tag{2.34}$$

where $l_1, l_2, ..., l_k$ are either positive integers or zero ($m \geq 1$ and $1 \leq k \leq m$).

Substituting for $h^{\mu\nu}(\widetilde{z}_-(\lambda), G)$ from Eq. (2.31) into Eq. (2.23), we get the terms of the PM expansion (2.28) of the reception time delay function Δ_r as

$$\Delta_r^{(1)}(\boldsymbol{x}_A, t_B, \boldsymbol{x}_B) = \frac{1}{2} R_{AB} \int_0^1 \left[g^{00}_{(1)} - 2N^i_{AB} g^{0i}_{(1)} + N^i_{AB} N^j_{AB} g^{ij}_{(1)} \right]_{z_-(\lambda)} d\lambda \,, \tag{2.35a}$$

$$\begin{aligned} \Delta_r^{(2)}(\boldsymbol{x}_A, t_B, \boldsymbol{x}_B) = \frac{1}{2} R_{AB} \int_0^1 \Bigg\{ & \left[\widehat{g}^{00}_{-(2)} - 2N^i_{AB} \widehat{g}^{0i}_{-(2)} + N^i_{AB} N^j_{AB} \widehat{g}^{ij}_{-(2)} \right]_{(z_-(\lambda), t_B, \boldsymbol{x}_B)} \\ & + 2 \left[g^{0i}_{(1)} - N^j_{AB} g^{ij}_{(1)} \right]_{z_-(\lambda)} \frac{\partial \Delta_r^{(1)}}{\partial x^i}(\boldsymbol{z}_-(\lambda), t_B, \boldsymbol{x}_B) \\ & + \eta^{ij} \left[\frac{\partial \Delta_r^{(1)}}{\partial x^i} \frac{\partial \Delta_r^{(1)}}{\partial x^j} \right]_{(\boldsymbol{z}_-(\lambda), t_B, \boldsymbol{x}_B)} \Bigg\} d\lambda \end{aligned} \tag{2.35b}$$

and

$$\begin{aligned} \Delta_r^{(n)}(\boldsymbol{x}_A, t_B, \boldsymbol{x}_B) = \frac{1}{2} R_{AB} \int_0^1 \Bigg\{ & \left[\widehat{g}^{00}_{-(n)} - 2N^i_{AB} \widehat{g}^{0i}_{-(n)} + N^i_{AB} N^j_{AB} \widehat{g}^{ij}_{-(n)} \right]_{(z_-(\lambda), t_B, \boldsymbol{x}_B)} \\ & + 2 \sum_{p=1}^{n-1} \left[\widehat{g}^{0i}_{-(p)} - N^j_{AB} \widehat{g}^{ij}_{-(p)} \right]_{(z_-(\lambda), t_B, \boldsymbol{x}_B)} \frac{\partial \Delta_r^{(n-p)}}{\partial x^i}(\boldsymbol{z}_-(\lambda), t_B, \boldsymbol{x}_B) \\ & + \sum_{p=1}^{n-1} \eta^{ij} \left[\frac{\partial \Delta_r^{(p)}}{\partial x^i} \frac{\partial \Delta_r^{(n-p)}}{\partial x^j} \right]_{(\boldsymbol{z}_-(\lambda), t_B, \boldsymbol{x}_B)} + \sum_{p=1}^{n-2} \widehat{g}^{ij}_{-(p)}(z_-(\lambda), t_B, \boldsymbol{x}_B) \\ & \times \sum_{q=1}^{n-p-1} \left[\frac{\partial \Delta_r^{(q)}}{\partial x^i} \frac{\partial \Delta_r^{(n-p-q)}}{\partial x^j} \right]_{(\boldsymbol{z}_-(\lambda), t_B, \boldsymbol{x}_B)} \Bigg\} d\lambda \end{aligned} \tag{2.35c}$$

for $n \geq 3$, the quantities $\widehat{g}^{\mu\nu}_{-(n)}$ being defined by equations (2.32) and (2.33). It should be noted that the integral expressions occurring in Eq. (2.35) are line integrals taken along the zeroth-order null geodesic of parametric equation $x = z_-(\lambda)$, where $z_-(\lambda)$ is defined by equation (2.30). Following a similar reasoning is then possible to derive the *emission delay functions* Δ_e.

2.3 Post-Minkowskian expansion of $(\hat{k}_i)_{A/B}$ and $\mathcal{K}$

The PM expansion of the direction triple $(\hat{k}_i)_{A/B}$ and of the ratio $\mathcal{K}$ defined in Eq. (2.7) can in principle be obtained through an analytical derivation of Eq. (2.13) where the terms $\Delta_r^{(n)}$ are given by Eq. (2.35). This is done explicitly in [Teyssandier 2012] up to the 2PM approximation in the case of a Schwarzschild metric. In this section, we present a general way of computing Eq. (2.7) up to 2PM order and for any weak field metric. In particular, we develop a procedure close to the one used for the TTF in section 2.2, showing that these quantities can be also computed as integrals of the metric and its derivatives, the integral being performed over a straight line joining the emitter and the receiver. Using Eq. (2.13)

into Eq. (2.7), it yealds

$$\left(\widehat{k}_i\right)_B = -\left(N^i_{AB} + \frac{\partial \Delta_r}{\partial x^i_B}\right)\left[1 - \frac{1}{c}\frac{\partial \Delta_r}{\partial t_B}\right]^{-1} \tag{2.36a}$$

$$\left(\widehat{k}_i\right)_A = -N^i_{AB} + \frac{\partial \Delta_r}{\partial x^i_A} \tag{2.36b}$$

$$\mathcal{K} = 1 - \frac{1}{c}\frac{\partial \Delta_r}{\partial t_B} . \tag{2.36c}$$

The goal of this section is to present analytical formulae for the partial derivatives of the PM expansion of the reception delay function valid up to the 2PM approximation [Hees *et al.* 2013].

Notations and variables used

The results presented in the following sections depend on some variables that we will define here. First of all, the Minkowskian path between the emitter and the receiver (which is a straight line) is parametrized by λ (whose values are between 0 and 1) and is given by Eq. (2.19) and Eq. (2.30) which it can be useful to rewrite as

$$z^0(\lambda) = ct_B - \lambda R_{AB} \quad , \quad \boldsymbol{z}(\lambda) = \boldsymbol{x}_B(1-\lambda) + \lambda \boldsymbol{x}_A . \tag{2.37}$$

The first derivatives of these expressions with respect to the variables $\boldsymbol{x}_{A/B}$ are given by

$$z^0_{A,i}(\lambda) = \frac{\partial z^0(\lambda)}{\partial x^i_A} = \lambda N^i_{AB} = -\frac{\partial z^0(\lambda)}{\partial x^i_B} = -z^0_{B,i}(\lambda) , \tag{2.38a}$$

$$z^j_{A,i}(\lambda) = \frac{\partial z^j(\lambda)}{\partial x^i_A} = \lambda \delta^j_i , \tag{2.38b}$$

and

$$z^j_{B,i}(\lambda) = \frac{\partial z^j(\lambda)}{\partial x^i_B} = (1-\lambda)\delta^j_i , \tag{2.38c}$$

while the second derivatives write

$$z^0_{AA,kl}(\lambda) = \frac{\partial^2 z^0}{\partial x^l_A \partial x^k_A} = \frac{\lambda}{R_{AB}}(N^k_{AB}N^l_{AB} - \delta_{kl}) = -\frac{\partial^2 z^0}{\partial x^l_B \partial x^k_A} = -z^0_{AB,kl}(\lambda) . \tag{2.38d}$$

We will use the function m and its derivatives $m_{,\alpha}$ defined from the PM expansion of the space-time metric as follows

$$m_{(i)}(\lambda) = \frac{R_{AB}}{2}\left[g^{00}_{(i)} - 2N^k_{AB}g^{0k}_{(i)} + N^k_{AB}N^l_{AB}g^{kl}_{(i)}\right]_{z^\beta(\lambda)} \tag{2.39a}$$

and

$$m_{(i),\alpha}(\lambda) = \frac{R_{AB}}{2}\left[g^{00}_{(i),\alpha} - 2N^k_{AB}g^{0k}_{(i),\alpha} + N^k_{AB}N^l_{AB}g^{kl}_{(i),\alpha}\right]_{z^\beta(\lambda)} , \tag{2.39b}$$

$g^{\mu\nu}_{(n)}$ being defined by Eqs. (2.11)-(2.27). Finally, we shall also define the functions $\tilde{h}^i$ and $\bar{h}^{ik}$ as

$$\begin{aligned}\tilde{h}^i_{(n),j}(\lambda) &= \left.\frac{\partial m_{(n),j}}{\partial x^i_A}\right|_{z^\alpha=\text{cst}} = -\left.\frac{\partial m_{(n),j}}{\partial x^i_B}\right|_{z^\alpha=\text{cst}} \\ &= \frac{1}{2}\Big[-N^i_{AB}g^{00}_{(n),j} + 2g^{0i}_{(n),j} - 2g^{ik}_{(n),j}N^k + N^kN^lN^i_{AB}g^{kl}_{(n),j}\Big]_{z^\alpha(\lambda)} \qquad (2.40a)\end{aligned}$$

and

$$\begin{aligned}\bar{h}^{ik}_{(n)} &= \left.\frac{\partial \tilde{h}^i_{(n)}}{\partial x^k_A}\right|_{z^\alpha=\text{cst}} = -\left.\frac{\partial \tilde{h}^i_{(n)}}{\partial x^k_B}\right|_{z^\alpha=\text{cst}} \\ &= \frac{1}{2R_{AB}}\Big[g^{00}_{(i),j}(\delta^{kl} - N^k_{AB}N^l_{AB}) + 2g^{kl}_{(i),j} - 2N^m_{AB}(g^{km}_{(i),j}N^l_{AB} \\ &\qquad + g^{lm}_{(i),j}N^k_{AB}) + g^{nm}_{(i),j}N^n_{AB}N^m_{AB}(3N^k_{AB}N^l_{AB} - \delta^{kl})\Big]_{z^\alpha(\lambda)} . \qquad (2.40b)\end{aligned}$$

Expansion at first PM order

Using the notations introduced in the previous section, the expression of $\Delta_r^{(1)}$ given in Eq. (2.35a) writes

$$\Delta_r^{(1)}(\boldsymbol{x}_A, t_B, \boldsymbol{x}_B) = \frac{R_{AB}}{2}\int_0^1 \Big[g^{00}_{(1)} - 2N^i_{AB}g^{0i}_{(1)} + N^i_{AB}N^j g^{ij}_{(1)}\Big]_{z^\alpha(\lambda)} d\lambda = \int_0^1 m_{(1)}(\lambda)d\lambda . \qquad (2.41)$$

Then, the derivatives of $\Delta_r^{(1)}$ can be easily determined as

$$\frac{\partial \Delta_r^{(1)}}{\partial x^i_A}(\boldsymbol{x}_A, t_B, \boldsymbol{x}_B) = \int_0^1 \Big[m_{(1),\alpha}(\lambda)z^\alpha_{A,i}(\lambda) + \tilde{h}^i_{(1)}(\lambda)\Big]\, d\lambda , \qquad (2.42a)$$

$$\frac{\partial \Delta_r^{(1)}}{\partial x^i_B}(\boldsymbol{x}_A, t_B, \boldsymbol{x}_B) = \int_0^1 \Big[m_{(1),\alpha}(\lambda)z^\alpha_{B,i}(\lambda) - \tilde{h}^i_{(1)}(\lambda)\Big]\, d\lambda , \qquad (2.42b)$$

and

$$\frac{\partial \Delta_r^{(1)}}{\partial t_B}(\boldsymbol{x}_A, t_B, \boldsymbol{x}_B) = c\int_0^1 m_{(1),0}(\lambda)d\lambda . \qquad (2.42c)$$

These equations are equivalent to those derived in [Hees *et al.* 2012b]. Finally, the following relations deduced from Eq. (2.42) will be useful for the computation of the 2PM order

$$\Delta_r^{(1)}(\boldsymbol{z}(\lambda), t_B, \boldsymbol{x}_B) = \int_0^1 m_{(1)}(\lambda\mu)d\mu , \qquad (2.43a)$$

$$\frac{\partial \Delta_r^{(1)}}{\partial x^i}(\boldsymbol{z}(\lambda), t_B, \boldsymbol{x}_B) = \int_0^1 \Big[m_{(1),\alpha}(\lambda\mu)z^\alpha_{A,i}(\lambda\mu) + \tilde{h}^i_{(1)}(\lambda\mu)\Big]\, d\mu , \qquad (2.43b)$$

$$\frac{\partial \Delta_r^{(1)}}{\partial t_B}(\boldsymbol{z}(\lambda), t_B, \boldsymbol{x}_B) = \lambda\int_0^1 m_{(1),0}(\lambda\mu)d\mu . \qquad (2.43c)$$

Expansion at second PM order

The expression of $\Delta_r^{(2)}$ given in Eq. (2.35b) can also be rewritten with our notations as

$$\Delta_r^{(2)}(\boldsymbol{x}_A, t_B, \boldsymbol{x}_B) = \int_0^1 \left[\mathcal{I}_1(\lambda) + \mathcal{I}_2(\lambda) + \mathcal{I}_3(\lambda)\right] d\lambda \,, \tag{2.44}$$

with

$$\begin{aligned}
\mathcal{I}_1(\lambda) &= m_{(2)}(\lambda) - \Delta_r^{(1)}(\boldsymbol{z}(\lambda), t_B, \boldsymbol{x}_B)\; m_{(1),0}(\lambda) \\
&= m_{(2)}(\lambda) - m_{(1),0}(\lambda) \int_0^1 m_{(1)}(\lambda\mu) d\mu \,, && (2.45a) \\
\mathcal{I}_2(\lambda) &= \left[R_{AB}\; g_{(1)}^{0i} - R_{AB}^k\; g_{(1)}^{ik}\right]_{z^\alpha(\lambda)} \frac{\partial \Delta_r^{(1)}}{\partial x^i}(\boldsymbol{z}(\lambda)) && (2.45b) \\
&= \left[R_{AB}\; g_{(1)}^{0i} - R_{AB}^k\; g_{(1)}^{ik}\right]_{z^\alpha(\lambda)} \int_0^1 \left[m_{(1),\alpha}(\lambda\mu) z_{A,i}^\alpha(\lambda\mu) + \tilde{h}_{(1)}^i(\lambda\mu)\right] d\mu && (2.45c)
\end{aligned}$$

and

$$\begin{aligned}
\mathcal{I}_3(\lambda) &= -\frac{R_{AB}}{2} \sum_{j=1}^3 \left[\frac{\partial \Delta_r^{(1)}}{\partial x^j}(\boldsymbol{z}(\lambda))\right]^2 \\
&= -\frac{R_{AB}}{2} \sum_{j=1}^3 \left\{\int_0^1 \left[m_{(1),\alpha}(\lambda\mu) z_{A,j}^\alpha(\lambda\mu) + \tilde{h}_{(1)}^j(\lambda\mu)\right] d\mu\right\}^2 \,, && (2.45d)
\end{aligned}$$

where we have used the relations (2.43). We can now derive the expression of the partial derivatives of Eq. (2.44) as

$$\frac{\partial \Delta_r^{(2)}}{\partial x_{A/B}^i}(\boldsymbol{x}_A, t_B, \boldsymbol{x}_B) = \int_0^1 \left[\frac{\partial \mathcal{I}_1}{\partial x_{A/B}^i}(\lambda) + \frac{\partial \mathcal{I}_2}{\partial x_{A/B}^i}(\lambda) + \frac{\partial \mathcal{I}_3}{\partial x_{A/B}^i}(\lambda)\right] d\lambda \,, \tag{2.46a}$$

and

$$\frac{\partial \Delta_r^{(2)}}{\partial t_B}(\boldsymbol{x}_A, t_B, \boldsymbol{x}_B) = \int_0^1 \left[\frac{\partial \mathcal{I}_1}{\partial t_B}(\lambda) + \frac{\partial \mathcal{I}_2}{\partial t_B}(\lambda) + \frac{\partial \mathcal{I}_3}{\partial t_B}(\lambda)\right] d\lambda \,, \tag{2.46b}$$

where the derivatives with respect to the emission coordinates $\boldsymbol{x}_A$ and reception coordinates $\boldsymbol{x}_B$ can be written as follows

$$\frac{\partial \mathcal{I}_1}{\partial x^i_{A/B}} = m_{(2),\alpha} z^\alpha_{A/B,i} \pm \tilde{h}^i_{(2)} - \Delta^{(1)}_r(\boldsymbol{z}(\lambda), t_b, \boldsymbol{x}_B)\left[m_{(1),0\alpha} z^\alpha_{A/B,i} \pm \tilde{h}^i_{(1),0}\right] - m_{(1),0}\frac{\partial \Delta^{(1)}_r}{\partial x^i_{A/B}}(\boldsymbol{z}(\lambda)), \tag{2.47a}$$

$$\frac{\partial \mathcal{I}_2}{\partial x^i_{A/B}} = \left[\mp N^i_{AB} g^{0j}_{(1)} \pm g^{ij}_{(1)} + (R_{AB} g^{0j}_{(1),\alpha} - g^{jk}_{(1),\alpha} R^k_{AB}) z^\alpha_{A/B,i}\right]_{z^\beta(\lambda)} \frac{\partial \Delta^{(1)}_r}{\partial x^j}(\boldsymbol{z}(\lambda)) + \left[R_{AB} g^{0j}_{(1)} - R^k_{AB} g^{jk}_{(1)}\right]_{z^\beta(\lambda)} \frac{\partial^2 \Delta^{(1)}_r}{\partial x^i_{A/B} \partial x^j}(\boldsymbol{z}(\lambda)), \tag{2.47b}$$

and

$$\frac{\partial \mathcal{I}_3}{\partial x^i_{A/B}} = \pm \frac{N^i_{AB}}{2} \sum_{j=1}^{3} \left(\frac{\partial \Delta^{(1)}_r}{\partial x^j}(\boldsymbol{z}(\lambda))\right)^2 - R_{AB} \sum_{j=1}^{3} \left[\frac{\partial \Delta^{(1)}_r}{\partial x^j}(\boldsymbol{z}(\lambda)) \cdot \frac{\partial^2 \Delta^{(1)}_r}{\partial x^i_{A/B} \partial x^j}(\boldsymbol{z}(\lambda))\right] \tag{2.47c}$$

and those with respect to the coordinate time of reception t_B give

$$\frac{\partial \mathcal{I}_1}{\partial t_B} = c\, m_{(2),0} - c\, m_{(1),00} \Delta^{(1)}_r(z(\lambda)) - m_{(1),0} \frac{\partial \Delta^{(1)}_r}{\partial t_B}(\boldsymbol{z}(\lambda)), \tag{2.47d}$$

$$\frac{\partial \mathcal{I}_2}{\partial t_B} = c\left[R_{AB} g^{0i}_{(1),0} - R^k_{AB} g^{ik}_{(1),0}\right]_{z^\beta(\lambda)} \cdot \frac{\partial \Delta^{(1)}_r}{\partial x^i}(\boldsymbol{z}(\lambda)) + \left[R_{AB} g^{0i}_{(1)} - R^k_{AB} g^{ik}_{(1)}\right]_{z^\beta(\lambda)} \cdot \frac{\partial^2 \Delta^{(1)}_r}{\partial t_B \partial x^i}(\boldsymbol{z}(\lambda)) \tag{2.47e}$$

and

$$\frac{\partial \mathcal{I}_3}{\partial t_B} = -R_{AB} \sum_{j=1}^{3} \frac{\partial \Delta^{(1)}_r}{\partial x^j}(\boldsymbol{z}(\lambda)) \cdot \frac{\partial^2 \Delta^{(1)}_r}{\partial t_B \partial x^j}(\boldsymbol{z}(\lambda)) d\lambda, \tag{2.47f}$$

with all quantities being evaluated at λ, the notation given above and where we obtain

$$\frac{\partial^2 \Delta^{(1)}_r}{\partial x^i_{A/B} \partial x^j}(\boldsymbol{z}(\lambda)) = \int_0^1 \left[m_{(1),\alpha\beta} z^\alpha_{A,j} z^\beta_{A/B,i} \pm \tilde{h}^i_{(1),\alpha} z^\alpha_{A,j} + m_{(1),\alpha} z^\alpha_{AA/AB,ji} + \tilde{h}^j_{(1),\alpha} z^\alpha_{A/B,i} \pm \bar{h}^{ji}_{(1)}\right]_{\lambda\mu} d\mu \tag{2.48a}$$

and

$$\frac{\partial^2 \Delta^{(1)}_r}{\partial t_B \partial x^j}(\boldsymbol{z}(\lambda)) = c \int_0^1 \left[m_{(1),\alpha 0}(\lambda\mu) z^\alpha_{A,j}(\lambda\mu) + \tilde{h}^j_{(1),0}(\lambda\mu)\right] d\mu. \tag{2.48b}$$

The relations given above can be used to compute the direction triple $\hat{k}_i$ and $\mathcal{K}$ up to the 2PM order in an integral form particularly adapted for a numerical evaluation with any metric.

2.4 Conclusions

In this chapter we presented the TTF formalism [Linet & Teyssandier 2002], a powerful tool giving direct access to the coordinate time of flight and frequency shift of a photon between two points and to the tangent vectors to its null-geodesic at point-events x_A and x_B. We showed how these quantities have been derived by [Teyssandier & Le Poncin-Lafitte 2008] within the PM approximation using the properties of the time transfer function $\mathcal{T}_{e/r}(t_{A/B}, \boldsymbol{x}_A, \boldsymbol{x}_B)$. Finally, we presented a very general way of deriving the direction triple $(\hat{k}_i)_{A/B}$ and the ratio $\mathcal{K}$ up to the 2PM order as integrals of the metric and its derivatives along the Minkowskian straight line between x_A and x_B. This closed form expansion is valid for any weak field space-time metric and is particularly adapted for a numerical integration. These results have been presented in [Hees *et al.* 2012a] and will be summarized in [Hees *et al.* 2013].

In the next chapter, we will apply our results to the case of a static, spherically symmetric space time to retrieve analytical solution up to the 2PM order, which is known for this particular geometry. Moreover, we will provide the PPN expansion of our formulae as well as their solution in the gravitational field of a system of bodies in translational motion. These results will be then used in chapter 4 to define and compute the Doppler and astrometric observables.

CHAPTER 3

Applications at 1PN/2PM approximation

Contents

In chapter 2, we presented general equations in closed form up to the 2PM order for the coordinate time of flight of a light ray between two events x_A and x_B, for the direction triples $\left(\widehat{k}_i\right)_{A/B}$ at x_A and x_B and for the ratio $\mathcal{K}$. In this chapter, we present an application of these results to a static, spherically symmetric space-time where an analytical solution of Eqs. (2.35a)-(2.35b), (2.42) and (2.46) can be obtained at the 2PM order. Using the simplifications proposed in section 3.1, we compute Eq. (3.20) and Eq. (3.25) which are the main results of this section. By comparing these results with [Teyssandier 2012] we validate our formulation. For practical applications, we then use the metric tensor adopted in the IAU2000 (presented in section 1.2.2). In section 3.2.1, we provide a closed form PPN expansion of the TTF in Eq. (3.29) and of its derivatives in Eq. (3.30). These equations allow us to choose appropriate gravitational potentials for each application. An appropriate choice of w and $\boldsymbol{w}$, representing the scalar and vector gravitational potential respectively, allowed [Le Poncin-Lafitte & Teyssandier 2008] to provide the time transfer and tangent vectors in the field of an extended body (using Eq. (3.31)). We present here a further application of our equations to the gravitational field of a system of point bodies in motion (using Eqs. (3.38)-(3.40)). This work on the TTF formalism shall be useful to describe light propagation in the Solar System at (and in some cases beyond) the precision needed by most space missions at present times (see Table 1.2).

3.1 Static, spherically symmetric space-time

In this section, we consider the case of a static, spherically symmetric space-time. With these assumptions, we use isotropic coordinates, so that the space-time metric can be written as [Stephani *et al.* 2009]

$$ds^2 = -A(r)c^2dt^2 + B(r)\delta_{ij}dx^i dx^j. \tag{3.1}$$

As mentioned in [Linet & Teyssandier 2013], the light rays of metric (3.1) are the same as the light rays of any metric $d\tilde{s}^2$ conformal to Eq. (3.1). We can thus simplify the calculations by choosing $d\tilde{s}^2 = A^{-1}(r)ds^2$ and consider the following metric

$$d\tilde{s}^2 = -c^2dt^2 + \frac{B(r)}{A(r)}\delta_{ij}dx^i dx^j = -c^2dt^2 + U(r)\delta_{ij}dx^i dx^j. \tag{3.2}$$

We can now perform a PM expansion of the function $U(r)$ as

$$U(r) = 1 + U^{(1)}(r) + U^{(2)}(r) + \dots . \tag{3.3}$$

This procedure simplifies the results found in chapter 2, allowing for an explicit analytical solution of the delay function and its derivatives up to the 2PM order. Using Eq. (2.41), the reception delay function at the 1PM order is defined by

$$\Delta_r^{(1)}(\boldsymbol{x}_A, \boldsymbol{x}_B) = \frac{R_{AB}}{2}\int_0^1 U^{(1)}(z(\lambda))d\lambda\,. \tag{3.4a}$$

Then, using Eq. (2.42) its first derivatives can be written as

$$\begin{aligned}\frac{\partial\Delta_r^{(1)}}{\partial x_A^i}(\boldsymbol{x}_A, \boldsymbol{x}_B) &= -\frac{U^{(1)}(r_A)}{2}N_{AB}^i + \left[\frac{R_{AB}}{2}x_B^i + \frac{N_{AB}^i}{4}(r_A^2 - R_{AB}^2 - r_B^2)\right] \\ &\quad \times \int_0^1 \frac{\lambda}{z(\lambda)}\frac{\partial U^{(1)}}{\partial r}(z(\lambda))d\lambda\end{aligned} \tag{3.4b}$$

and

$$\begin{aligned}\frac{\partial\Delta_r^{(1)}}{\partial x_B^i}(\boldsymbol{x}_A, \boldsymbol{x}_B) &= \frac{U^{(1)}(r_A)}{2}N_{AB}^i + \frac{R_{AB}x_B^i}{2}\int_0^1 \frac{1}{z(\lambda)}\frac{\partial U^{(1)}}{\partial r}(z(\lambda))d\lambda \\ &\quad - \left[\frac{R_{AB}}{2}x_B^i + \frac{N_{AB}^i}{4}(r_A^2 + R_{AB}^2 - r_B^2)\right] \times \int_0^1 \frac{\lambda}{z(\lambda)}\frac{\partial U^{(1)}}{\partial r}(z(\lambda))d\lambda\,,\end{aligned} \tag{3.4c}$$

where $z(\lambda) = |\boldsymbol{z}(\lambda)|$, $\boldsymbol{z}(\lambda)$ is given by Eq. (2.37) and where, for the sake of simplicity, we put

$$r_A = |\boldsymbol{x}_A|\,, \quad r_B = |\boldsymbol{x}_B|.$$

Also, one can show that

$$\begin{aligned}\frac{\partial\Delta_r^{(1)}}{\partial x^i}(\boldsymbol{z}(\lambda), \boldsymbol{x}_B) &= -U^{(1)}(\boldsymbol{z}(\lambda))\frac{N_{AB}^i}{2} \\ &\quad + \lambda\left[\frac{R_{AB}}{2}x_B^i + \frac{N_{AB}^i}{4}(r_A^2 - R_{AB}^2 - r_B^2)\right]\int_0^1 \frac{\mu}{z(\lambda\mu)}\frac{\partial U^{(1)}}{\partial r}d\mu\,.\end{aligned} \tag{3.5}$$

Substituting for the metric tensor from Eq. (3.2) into Eq. (2.44), the 2PM order of the reception delay function is given by

$$\Delta_r^{(2)}(\boldsymbol{x}_A, \boldsymbol{x}_B) = \frac{R_{AB}}{2}\int_0^1 \Big[U^{(2)}(z(\lambda)) + \bar{\mathcal{I}}_3(\lambda)\Big]d\lambda\,, \tag{3.6}$$

where we defined $\bar{\mathcal{I}}_3(\lambda) \equiv 2\mathcal{I}_3(\lambda)/R_{AB}$. Using Eq. (3.5), one then gets

$$\begin{aligned}\bar{\mathcal{I}}_3(\lambda) &= -\sum_{j=1}^{3}\left[\frac{\partial\Delta_r^{(1)}(\boldsymbol{z}(\lambda))}{\partial x^j}\right]^2 \\ &= -\frac{1}{4}\left\{U_{(1)}^2(z(\lambda)) + \frac{V^2(z(\lambda))}{4}\Big[4r_B^2R_{zB}^2 - (z^2(\lambda) - R_{zB}^2 - r_B^2)^2\Big]\right\}\end{aligned} \tag{3.7}$$

where it can be useful to note the following relations

$$z^2 - R_{zB}^2 - r_B^2 = \lambda\Big(r_A^2 - R_{AB}^2 - r_B^2\Big) \tag{3.8a}$$

$$4R_{zB}^2r_B^2 - (z^2 - R_{zB}^2 - r_B^2)^2 = -\lambda^2\Big[(r_A + r_B)^2 - R_{AB}^2\Big]\Big[(r_A - r_B)^2 - R_{AB}^2\Big] \tag{3.8b}$$

and where we pose

$$V(z(\lambda)) \equiv \int_0^1 \frac{\mu}{z(\lambda\mu)}\frac{\partial U^{(1)}}{\partial r}(z(\lambda\mu))d\mu \quad \text{and} \quad R_{zB} \equiv |\boldsymbol{x}_B - \boldsymbol{z}(\lambda)|\,. \tag{3.9}$$

From Eq. (2.46), the derivatives of $\Delta_r^{(2)}$ are then given by

$$\frac{\partial\Delta_r^{(2)}}{\partial x_A^i} = -\frac{N_{AB}^i}{R_{AB}}\Delta_r^{(2)} + \frac{R_{AB}}{2}\int_0^1\left[\frac{\lambda z^i(\lambda)}{z(\lambda)}\frac{\partial U^{(2)}}{\partial r}(z(\lambda)) + \frac{\partial\bar{\mathcal{I}}_3}{\partial x_A^i}(\lambda)\right]d\lambda \tag{3.10a}$$

and

$$\frac{\partial\Delta_r^{(2)}}{\partial x_B^i} = \frac{N_{AB}^i}{R_{AB}}\Delta_r^{(2)} + \frac{R_{AB}}{2}\int_0^1\left[\frac{(1-\lambda)z^i(\lambda)}{z(\lambda)}\frac{\partial U^{(2)}}{\partial r}(z(\lambda)) + \frac{\partial\bar{\mathcal{I}}_3}{\partial x_B^i}(\lambda)\right]d\lambda\,, \tag{3.10b}$$

with

$$\begin{aligned}\frac{\partial\bar{\mathcal{I}}_3}{\partial x_A^i}(\lambda) &= -\frac{1}{4}\Big\{2\lambda\frac{z^i(\lambda)}{z(\lambda)}U^{(1)}(z(\lambda))\frac{\partial U^{(1)}}{\partial r}(z(\lambda)) \\ &\quad -\lambda^2\frac{V(z(\lambda))}{2}\frac{\partial V}{\partial x_A^i}(z(\lambda))\Big[(r_A + r_B)^2 - R_{AB}^2\Big]\times\Big[(r_A - r_B)^2 - R_{AB}^2\Big] \\ &\quad -\lambda^2V^2(z(\lambda))\left[2r_B^2R_{AB}^i + (r_A^2 - R_{AB}^2 - r_B^2)x_B^i\right]\Big\}\end{aligned} \tag{3.11a}$$

and

$$\begin{aligned}\frac{\partial\bar{\mathcal{I}}_3}{\partial x_B^i}(\lambda) &= -\frac{1}{4}\Big\{2(1-\lambda)\frac{z^i(\lambda)}{z(\lambda)}U^{(1)}(z(\lambda))\frac{\partial U^{(1)}}{\partial r}(z(\lambda)) - \lambda^2\frac{V(z(\lambda))}{2}\frac{\partial V}{\partial x_B^i}(z(\lambda)) \\ &\quad\times\Big[(r_A + r_B)^2 - R_{AB}^2\Big]\Big[(r_A - r_B)^2 - R_{AB}^2\Big] + \lambda^2V^2(z(\lambda)) \\ &\quad\times\Big[(r_A^2 + r_B^2 - R_{AB}^2)R_{AB}^i + (r_A^2 - R_{AB}^2 - r_B^2)x_B^i\Big]\Big\}\end{aligned} \tag{3.11b}$$

and where the derivatives of $V(z(\lambda))$ can be computed by

$$\frac{\partial V}{\partial x_A^i}(z(\lambda)) = \int_0^1 \left[\frac{\partial^2 U^{(1)}}{\partial r^2}(z(\lambda\mu))\frac{\lambda\mu^2 z^i(\lambda\mu)}{z^2(\lambda\mu)} - \lambda\mu^2\frac{\partial U^{(1)}}{\partial r}(z(\lambda))\frac{z^i(\lambda\mu)}{z^3(\lambda\mu)}\right] d\mu \quad (3.12a)$$

and

$$\frac{\partial V}{\partial x_B^i}(z(\lambda)) = \int_0^1 \left[\frac{\partial^2 U^{(1)}}{\partial r^2}(z(\lambda\mu))\frac{(1-\lambda\mu)\mu z^i(\lambda\mu)}{z^2(\lambda\mu)} - (1-\lambda\mu)\mu\frac{\partial U^{(1)}}{\partial r}(z(\lambda))\frac{z^i(\lambda\mu)}{z^3(\lambda\mu)}\right] d\mu\,. \quad (3.12b)$$

3.1.1 Application to Schwarzschild geometry

To illustrate the previous results, let us consider the Schwarzschild-like metric whose PM expansion in isotropic coordinates is

$$ds^2 = \left(-1 + 2\frac{m}{r} - 2\beta\frac{m^2}{r^2} + ...\right)c^2dt^2 + \left(1 + 2\gamma\frac{m}{r} + \frac{3}{2}\varepsilon\frac{m^2}{r^2} + ...\right)\delta_{ij}dx^i dx^j\,, \quad (3.13)$$

where $m \equiv GM/c^2$, β and γ are the usual PPN parameters, ε is a post-post-Newtonian parameter and $+\ldots$ means that terms of order $\mathcal{O}(G^3)$ are neglected ($\beta = \gamma = \varepsilon = 1$ in GR). The function $U(r)$ appearing in (3.2) can be written as

$$U(r) = 1 + 2(1+\gamma)\frac{m}{r} + 2\kappa\frac{m^2}{r^2} + \ldots\,, \quad (3.14)$$

where $\kappa = 2(1+\gamma) - \beta + \frac{3}{4}\varepsilon$. Introducing $U(r)$ from Eq. (3.14) into Eq. (3.4) leads to

$$\Delta_r^{(1)} = R_{AB}(1+\gamma)m\int_0^1 \frac{d\lambda}{z(\lambda)} = (\gamma+1)m\ln\left(\frac{r_A + r_B + R_{AB}}{r_A + r_B - R_{AB}}\right)\,, \quad (3.15a)$$

$$\begin{aligned}\frac{\partial\Delta_r^{(1)}}{\partial x_A^i} &= -(1+\gamma)\frac{m}{r_A}N_{AB}^i + \left[\frac{R_{AB}}{2}x_B^i + \frac{N_{AB}^i}{4}(r_A^2 - R_{AB}^2 - r_B^2)\right] \\ &\quad\times\frac{-4(1+\gamma)m}{r_A\left[(r_A+r_B)^2 - R_{AB}^2\right]} \\ &= -\frac{2(1+\gamma)m}{(r_A+r_B)^2 - R_{AB}^2}\left[\frac{R_{AB}}{r_A}x_A^i + N_{AB}^i(r_A+r_B)\right]\,, \quad (3.15b)\end{aligned}$$

$$\begin{aligned}\frac{\partial\Delta_r^{(1)}}{\partial x_B^i} &= (1+\gamma)\frac{m}{r_A}N_{AB}^i - \frac{R_{AB}x_B^i}{2}\left[\frac{4(1+\gamma)m\left(\frac{1}{r_A}+\frac{1}{r_B}\right)}{(r_A+r_B)^2 - R_{AB}^2}\right] \\ &\quad - \left[\frac{R_{AB}}{2}x_B^i + \frac{N_{AB}^i}{4}(r_A^2 + R_{AB}^2 - r_B^2)\right]\times\frac{-4(1+\gamma)m}{r_A\left[(r_A+r_B)^2 - R_{AB}^2\right]} \\ &= -\frac{2(1+\gamma)m}{(r_A+r_B)^2 - R_{AB}^2}\left[\frac{R_{AB}}{r_B}x_B^i - N_{AB}^i(r_A+r_B)\right] \quad (3.15c)\end{aligned}$$

The first result is equivalent to the expression of the Shapiro time delay [Shapiro 1964] while the two derivatives are in agreement with the results found in [Blanchet *et al.* 2001] at the first PM approximation. The computation at the 2PM order is more cumbersome. Substituting for $U(r)$ from Eq. (3.14) into Eq. (3.6), one gets

$$\Delta_r^{(2)} = R_{AB}\kappa\, m^2 \int_0^2 \frac{d\lambda}{z^2(\lambda)} + \frac{R_{AB}}{2}\int_0^1 \bar{\mathcal{I}}_3(\lambda)d\lambda \tag{3.16}$$

where $\bar{\mathcal{I}}_3(\lambda)$ is given by Eq. (3.7) as

$$\begin{aligned}\bar{\mathcal{I}}_3(\lambda) &= -\frac{4(1+\gamma)^2 m^2 r_B}{z(\lambda)\left[(z(\lambda)+r_B)^2-\lambda^2 R_{AB}^2\right]} \\ &= -4(1+\gamma)^2 m^2 \frac{d}{d\lambda}\left[\frac{\lambda}{(z(\lambda)+r_B)^2-\lambda^2 R_{AB}^2}\right]\end{aligned} \tag{3.17}$$

once $V(\lambda)$ is determined from Eq. (3.9) as

$$V(\lambda) = -2(1+\gamma)m\int_0^1 \frac{\mu}{z^3(\lambda\mu)}d\mu = -\frac{4(1+\gamma)m}{z(\lambda)\left[(z(\lambda)+r_B)^2-\lambda^2 R_{AB}^2\right]}\,. \tag{3.18}$$

Replacing this expression in Eq. (3.16) and integrating, one gets

$$\Delta_r^{(2)}(\boldsymbol{x}_A,\boldsymbol{x}_B) = m^2\frac{R_{AB}}{r_A r_B}\left[\frac{\kappa\arccos\mu}{\sqrt{1-\mu^2}} - \frac{(1+\gamma)^2}{1+\mu}\right], \tag{3.19}$$

with $\mu \equiv (\boldsymbol{n}_A.\boldsymbol{n}_B)$ and $\boldsymbol{n}_{A/B} = \boldsymbol{x}_{A/B}/r_{A/B}$. The TTF is obtained up to 2PM when one substitutes for Δ_r from Eqs. (3.15) and (3.19) into Eq. (2.13). We get

$$\begin{aligned}\mathcal{T}_r(\boldsymbol{x}_A,t_B,\boldsymbol{x}_B) = t_B - t_A &= \frac{R_{AB}}{c} + \frac{(\gamma+1)m}{c}\ln\left(\frac{r_A+r_B+R_{AB}}{r_A+r_B-R_{AB}}\right) \\ &+\frac{m^2 R_{AB}}{c\, r_A r_B}\left[\frac{\kappa\arccos\mu}{\sqrt{1-\mu^2}} - \frac{(1+\gamma)^2}{1+\mu}\right].\end{aligned} \tag{3.20}$$

We recover a result previously derived by different approaches in [Richter & Matzner 1983, Le Poncin-Lafitte *et al.* 2004, Ashby & Bertotti 2010] (see also [Brumberg 1987] in the case where $\beta=\gamma=\delta=1$).

We can now compute the derivatives of $\Delta_r^{(2)}$. As an example, we will only focus on the derivative with respect to x_A^i, the other derivative (with respect to x_B^i) can be computed similarly. Using Eq. (3.13)-(3.14) into Eq. (3.12), one gets

straightforwardly

$$\frac{\partial V}{\partial x_A^i}(z(\lambda)) = \frac{8(1+\gamma)m\lambda}{z^3(\lambda)\Big[(z(\lambda)+r_B)^2-\lambda^2 R_{AB}^2\Big]^2}\Bigg\{\Big[(z^2(\lambda)+2z(\lambda)r_B+\boldsymbol{z}(\lambda)\cdot\boldsymbol{x}_B\Big]x_B^i$$
$$-\lambda R_{AB}^i\Big[2z(\lambda)r_B+\boldsymbol{z}(\lambda)\cdot\boldsymbol{x}_B\Big]\Bigg\}. \tag{3.21}$$

Then, replacing this result in Eq. (3.11a) leads to

$$\frac{\partial\bar{I}_3}{\partial x_A^i} = \frac{4(1+\gamma)^2m^2r_B\lambda}{z^3(\lambda)\Big[(z(\lambda)+r_B)^2-\lambda^2R_{AB}^2\Big]^2}\Bigg\{x_B^i\Big[r_B^2+4r_Bz(\lambda)+3z^2(\lambda)-\lambda^2R_{AB}^2\Big]$$
$$-\lambda R_{AB}^i\Big[r_B^2+4r_Bz(\lambda)+z^2(\lambda)-\lambda^2R_{AB}^2\Big]\Bigg\}, \tag{3.22}$$

which, after some lengthy but straightforward calculations, can be written as

$$\frac{\partial\bar{I}_3}{\partial x_A^i} = 8(1+\gamma)^2m^2\frac{d}{d\lambda}\left[\lambda^2\frac{(z(\lambda)+r_B)z^i(\lambda)+z(\lambda)R_{AB}^i}{z(\lambda)\left[(z(\lambda)+r_B)^2-\lambda^2R_{AB}^2\right]^2}\right]. \tag{3.23}$$

Finally, one needs to compute the integral corresponding to the second term of the right hand side (r.h.s.) of Eq. (3.10a), namely

$$\frac{R_{AB}}{2}\int_0^1\left[\frac{\lambda z^i(\lambda)}{z(\lambda)}\frac{\partial U^{(2)}}{\partial r}(z(\lambda))\right]d\lambda = -2\kappa\,R_{AB}m^2\int_0^1\frac{\lambda z^i(\lambda)}{z^4(\lambda)}d\lambda \tag{3.24}$$
$$= \frac{\kappa\,m^2\arccos\mu}{r_Ar_B\sqrt{1-\mu^2}}\left(-\frac{R_{AB}n_A^i}{r_A(1-\mu^2)}+\mu\frac{R_{AB}n_B^i}{r_B(1-\mu^2)}\right)-\frac{\kappa\,m^2R_{AB}}{r_A^2r_B(1-\mu^2)}(n_B^i-\mu n_A^i).$$

Substituting from Eq. (3.19), Eq. (3.23) and Eq. (3.24) into Eq. (3.10a), one gets

$$\frac{\partial\Delta_r^{(2)}}{\partial x_A^i} = \frac{\kappa\,m^2}{r_Ar_B}\Bigg\{\frac{\arccos\mu}{\sqrt{1-\mu^2}}\left(-N_{AB}^i-\frac{R_{AB}n_A^i}{r_A(1-\mu^2)}+\mu\frac{R_{AB}n_B^i}{r_B(1-\mu^2)}\right) \tag{3.25a}$$
$$-\frac{R_{AB}}{r_A(1-\mu^2)}(n_B^i-\mu n_A^i)\Bigg\}+\frac{(1+\gamma)^2m^2}{r_Ar_B(1+\mu)}\left\{N_{AB}^i+\frac{R_{AB}}{r_A(1+\mu)}(n_A^i+n_B^i)\right\}.$$

A similar reasoning for $\frac{\partial\Delta_r^{(2)}}{\partial x_B^i}$ leads to

$$\frac{\partial\Delta_r^{(2)}}{\partial x_B^i} = \frac{\kappa\,m^2}{r_Ar_B}\Bigg\{\frac{\arccos\mu}{\sqrt{1-\mu^2}}\left[N_{AB}^i-\frac{R_{AB}n_B^i}{r_B(1-\mu^2)}+\mu\frac{R_{AB}n_A^i}{r_A(1-\mu^2)}\right] \tag{3.25b}$$
$$-\frac{R_{AB}}{r_B(1-\mu^2)}(n_A^i-\mu n_B^i)\Bigg\}+\frac{(1+\gamma)^2m^2}{r_Ar_B(1+\mu)}\left\{-N_{AB}^i+\frac{R_{AB}}{r_B(1+\mu)}(n_A^i+n_B^i)\right\}.$$

Some algebra allows to put the last two results in the same form as the one found by [Teyssandier 2012], which is an evidence that our formalism is correct. Of course, in the case of the Schwarzschild metric the analytical derivation of Eq. (3.19) is much more direct to get Eq. (3.25), which can also be used to check our calculation. Nevertheless the method presented here is very efficient for numerical evaluations of the derivatives of the TTF, necessary when using more complex metrics and for the test of alternative theories of gravity, when the integrals are no longer analytic.

3.2 Systems of moving or extended bodies

3.2.1 PPN expansion of the TTF and its derivatives

The metric recommended by the IAU2000 resolutions [Soffel *et al.* 2003] is expressed in the PPN framework and at 1PM order by [Klioner & Soffel 2000]

$$g_{00} = -1 - 2\frac{w}{c^2} \quad , \quad g_{0i} = 2(1+\gamma)\frac{w^i}{c^3} \quad \text{and} \quad g_{ij} = \delta_{ij}\left(1 + 2\gamma\frac{w}{c^2}\right) , \tag{3.26}$$

where w and w^i are the scalar and vector potentials, respectively. Computing the inverse of the previous metric, one gets

$$g^{00} = -1 + 2\frac{w}{c^2} \quad , \quad g^{0i}_{(1)} = 2(1+\gamma)\frac{w^i}{c^3} \quad \text{and} \quad g^{ij}_{(1)} = \delta^{ij}\left(1 - 2\gamma\frac{w}{c^2}\right) . \tag{3.27}$$

Since the PM expansion of our equations naturally includes the PN approximation, it is then straightforward to compute $m(\lambda)$, $m_{(1),\alpha}(\lambda)$ and $\tilde{h}(\lambda)$ from Eqs. (2.39-2.40) as

$$m_{(1)}(\lambda) = \frac{R_{AB}}{c^2}\left[(1+\gamma)w - 2(1+\gamma)\frac{\boldsymbol{N}_{AB}\cdot\boldsymbol{w}}{c}\right]_{z^\beta(\lambda)} , \tag{3.28a}$$

$$m_{(1),\alpha}(\lambda) = \frac{R_{AB}}{c^2}\left[(1+\gamma)w_{,\alpha} - 2(1+\gamma)\frac{\boldsymbol{N}_{AB}\cdot\boldsymbol{w}_{,\alpha}}{c}\right]_{z^\beta(\lambda)} \tag{3.28b}$$

and

$$\tilde{h}^k_{(1)}(\lambda) = \left[-(1+\gamma)\frac{w}{c^2}N^k_{AB} + 2(1+\gamma)\frac{w^k}{c^3}\right]_{z^\beta(\lambda)} . \tag{3.28c}$$

We can now use relations (2.13) and (2.41) to compute the TTF within the PPN framework as

$$\mathcal{T}_r(\boldsymbol{x}_A, t_B, \boldsymbol{x}_B) = t_B - t_A$$

$$= \frac{R_{AB}}{c} + \frac{R_{AB}}{c^3}\int_0^1 \left[(1+\gamma)w - 2(1+\gamma)\frac{\boldsymbol{N}_{AB}\cdot\boldsymbol{w}}{c}\right]_{z^\beta(\lambda)} d\lambda + \mathcal{O}(G^2) . \tag{3.29}$$

This relation can be used whatever the forms of the scalar and vector potentials are. The result of this integral is well-known in the case of a static point mass (see section 3.1) or in the case of an axis-symmetric static mass (see section 3.2.2). In the case of an ensemble of moving point-masses, this integral can be computed numerically or through a PN expansion of the potentials (see section 3.2.3).

Similarly, we can compute the derivatives of the Time Transfer Functions. Inserting (3.28) in (2.42) and using (2.38), it yields straightforwardly

$$\frac{\partial \Delta_r^{(1)}}{\partial x_A^i} = \frac{(1+\gamma)}{c^2}\int_0^1 \left[R_{AB}\lambda w_{,i} - wN_{AB}^i\right]_{z^\beta(\lambda)} d\lambda + \frac{1}{c^3}\int_0^1 \left[(1+\gamma)w_{,t}R_{AB}^i\lambda - 4\lambda \boldsymbol{R}_{AB}\cdot\boldsymbol{w}_{,i} + 2(1+\gamma)w^i\right]_{z^\beta(\lambda)} d\lambda\,, \tag{3.30a}$$

$$\frac{\partial \Delta_r^{(1)}}{\partial x_B^i} = \frac{(1+\gamma)}{c^2}\int_0^1 \left[R_{AB}(1-\lambda)w_{,i} + wN_{AB}^i\right]_{z^\beta(\lambda)} d\lambda - \frac{1}{c^3}\int_0^1 \left[(1+\gamma)w_{,t}R_{AB}^i\lambda + 4(1-\lambda)\boldsymbol{R}_{AB}\cdot\boldsymbol{w}_{,i} + 2(1+\gamma)w^i\right]_{z^\beta(\lambda)} d\lambda \tag{3.30b}$$

and

$$\frac{\partial \Delta_r^{(1)}}{\partial t_B} = \frac{R_{AB}}{c^2}\int_0^1 [(1+\gamma)w_{,t} - 2(1+\gamma)\frac{\boldsymbol{N}_{AB}\cdot\boldsymbol{w}_{,t}}{c}]_{z^\beta(\lambda)} d\lambda\,. \tag{3.30c}$$

These formulae are valid for any scalar and vector potentials, particularly adapted for a numerical integration and the modeling of observables for space science. If needed, the results of this section can be easily broadened by considering an extension of the IAU metric valid at the 2PM order [Minazzoli & Chauvineau 2009].

In the following, we shall recall the equations describing light propagation in the field of axisymmetric bodies and provide explicit formulae in the case of a system of bodies in translational motion.

3.2.2 Solution in the field of an extended body

The description of light propagation in the field of an isolated axisymmetric body has been developed within the TTF formalism as a PN expansion at the order $1/c^2$ by [Le Poncin-Lafitte & Teyssandier 2008]. Space-time is then stationary [Stephani *et al.* 2009], so that $\Delta_r(\boldsymbol{x}_A, \boldsymbol{x}_B) = \Delta_e(\boldsymbol{x}_A, \boldsymbol{x}_B) = \Delta(\boldsymbol{x}_A, \boldsymbol{x}_B)$, the center of mass O of the perturbing body is taken as the origin of the quasi-Cartesian coordinates x^i and the axis of symmetry is chosen as the x^3-axis. Let us also assume that the smallest sphere centered on O and containing the body has a radius equal to the equatorial radius r_e of the body and that the segment joining $\boldsymbol{x}_A$ and $\boldsymbol{x}_B$ is outside this sphere. At any point $\boldsymbol{x}$ such that $r \geq r_e$, the gravitational potentials w and $\boldsymbol{w}$ are then given by the multipole expan-

sion [Thorne 1980, Kopeikin 1997, Linet & Teyssandier 2002]

$$w = \frac{GM}{r}\left[1 - \sum_{n=2}^{\infty} J_n \left(\frac{r_e}{r}\right)^n P_n\left(\frac{\boldsymbol{k}.\boldsymbol{x}}{r}\right)\right] \qquad \text{and} \qquad \boldsymbol{w} = 0\ , \tag{3.31}$$

where $\boldsymbol{k}$ denotes the unit vector along the x^3-axis, the P_n are the Legendre polynomials, M is the mass of the body and the coefficients J_n are the mass multipole moments. Putting

$$\boldsymbol{n}_A = \frac{\boldsymbol{x}_A}{r_A} \qquad \text{and} \qquad \boldsymbol{n}_B = \frac{\boldsymbol{x}_B}{r_B}\ , \tag{3.32}$$

one can expand Eq. (3.29) as a series of J_n and write

$$\mathcal{T}(\boldsymbol{x}_A, \boldsymbol{x}_B) = \frac{1}{c} R_{AB} + \Delta_M(\boldsymbol{x}_A, \boldsymbol{x}_B) + \sum_{n=2}^{\infty} \Delta_{J_n}(\boldsymbol{x}_A, \boldsymbol{x}_B)\ , \tag{3.33}$$

where Δ_M is the coordinate time delay due to the monopolar part of the gravitational potential (3.31) and Δ_{J_n} are its multipolars components. Using Eq. (3.29) with Eq. (3.31) and integrating along the curve (2.30) gives the well-known Shapiro time delay [Shapiro 1964]

$$\Delta_M(\boldsymbol{x}_A, \boldsymbol{x}_B) = (\gamma + 1)\frac{GM}{c^3} \ln\left(\frac{r_A + r_B + R_{AB}}{r_A + r_B - R_{AB}}\right)\ , \tag{3.34a}$$

the quadrupole term Δ_{J_2} as in [Linet & Teyssandier 2002]

$$\begin{aligned}\Delta_{J_2}(\boldsymbol{x}_A, \boldsymbol{x}_B) = \frac{\gamma + 1}{2}\frac{GM}{c^3}\frac{J_2 r_e^2}{r_A r_B}\frac{R_{AB}}{1 + \boldsymbol{n}_A.\boldsymbol{n}_B}\Bigg[&\frac{1 - (\boldsymbol{k}.\boldsymbol{n}_A)^2}{r_A} + \frac{1 - (\boldsymbol{k}.\boldsymbol{n}_B)^2}{r_B} \\ &- \left(\frac{1}{r_A} + \frac{1}{r_B}\right)\frac{[\boldsymbol{k}.(\boldsymbol{n}_A + \boldsymbol{n}_B)]^2}{1 + \boldsymbol{n}_A.\boldsymbol{n}_B}\Bigg]\end{aligned} \tag{3.34b}$$

and the Δ_{J_n} terms presented explicitly in [Le Poncin-Lafitte & Teyssandier 2008].

The multipolar expansion of the direction triples at x_A and x_B is given by the analytical derivation of Eq. (3.33) with the delay functions (3.34). On these basis, one can rewrite Eq. (2.7a) as

$$\left(\hat{k}_i\right)_B = -\boldsymbol{N}_{AB} + \kappa_i^B(\boldsymbol{x}_A, \boldsymbol{x}_B), \tag{3.35}$$

where $\kappa_i^B(\boldsymbol{x}_A, \boldsymbol{x}_B)$ is given by the multipole expansion

$$\kappa_i^B(\boldsymbol{x}_A, \boldsymbol{x}_B) = (\kappa_i^B)_M(\boldsymbol{x}_A, \boldsymbol{x}_B) + \sum_{n=2}^{\infty}(\kappa_i^B)_{J_n}(\boldsymbol{x}_A, \boldsymbol{x}_B). \tag{3.36}$$

Then, one can derive the monopolar and quadrupolar terms of the direction triple from Eq. (3.34)

$$(\kappa_i^B)_M(\boldsymbol{x}_A,\boldsymbol{x}_B) = (\gamma+1)\frac{GM}{c^2 r_B}\frac{1}{1+\boldsymbol{n}_A\cdot\boldsymbol{n}_B}\left[\frac{R_{AB}}{r_A}\boldsymbol{n}_B - \left(1+\frac{r_B}{r_A}\right)\boldsymbol{N}_{AB}\right] , \quad (3.37a)$$

$$\begin{aligned}(\kappa_i^B)_{J_2}(\boldsymbol{x}_A,\boldsymbol{x}_B) = (\gamma+1)\frac{GM}{c^2}J_2 r_e^2\Bigg\{ &-\Big[\boldsymbol{k}\cdot(\boldsymbol{n}_A+\boldsymbol{n}_B)\Big]^2\\ &\left[\frac{\boldsymbol{n}_B-\boldsymbol{N}_{AB}}{(r_A+r_B-R_{AB})^3}-\frac{\boldsymbol{n}_B+\boldsymbol{N}_{AB}}{(r_A+r_B+R_{AB})^3}\right]+\frac{1}{2}\left[\frac{1-(\boldsymbol{k}\cdot\boldsymbol{n}_A)^2}{r_A}+\frac{1-(\boldsymbol{k}\cdot\boldsymbol{n}_B)^2}{r_B}\right]\\ &\left[\frac{\boldsymbol{n}_B-\boldsymbol{N}_{AB}}{(r_A+r_B-R_{AB})^2}-\frac{\boldsymbol{n}_B+\boldsymbol{N}_{AB}}{(r_A+r_B+R_{AB})^2}\right]+\frac{1}{r_B^3}\frac{(r_A+r_B)R_{AB}}{r_A^2}\frac{\boldsymbol{k}.(\boldsymbol{n}_A+\boldsymbol{n}_B)}{(1+\boldsymbol{n}_A\cdot\boldsymbol{n}_B)^2}\\ &\Big[\boldsymbol{k}-(\boldsymbol{k}\cdot\boldsymbol{n}_B)\boldsymbol{n}_B\Big]+\frac{1}{2r_B^3}\frac{R_{AB}}{r_A}\frac{2(\boldsymbol{k}\cdot\boldsymbol{n}_B)\boldsymbol{k}+[1-3(\boldsymbol{k}\cdot\boldsymbol{n}_B)^2]\,\boldsymbol{n}_B}{1+\boldsymbol{n}_A\cdot\boldsymbol{n}_B}\Bigg\} , \end{aligned} \quad (3.37b)$$

while an expression for the multipolar terms of higher order is given in [Le Poncin-Lafitte & Teyssandier 2008].

The contribution of the mass multipole moments to the deflection of light has to be taken into account in astrometric missions of high precision such as Gaia for light rays grazing the deflecting body (see Fig. 1.2 and discussion in [Klioner 2003, Le Poncin-Lafitte & Teyssandier 2008]). It shall then be included in an astrometric model aiming at interpreting Gaia's observations. In this sense, Eqs. (3.34)-(3.37) show that there would be no theoretical limitation to include the quadrupole light deflection term in an astrometric model based on the TTF formalism (see chapter 6).

3.2.3 Solution in the field of a system of moving point bodies

We provide now explicit formulae within the TTF formalism for the case of a system point-like, slowly moving and non-rotating bodies [Bertone *et al.* 2013a]. This system can be represented by the metric (3.26) where we consider for the scalar and vector gravitational potentials

$$w_P(\boldsymbol{x},t) = \sum_P \frac{G\mathcal{M}_P}{R_P(t,\boldsymbol{x})} \qquad \text{and} \qquad \boldsymbol{w}_P(\boldsymbol{x},t) = \sum_P \frac{G\mathcal{M}_P}{R_P(t,\boldsymbol{x})}\boldsymbol{v}_P , \quad (3.38)$$

with $\mathcal{M}_P$ the mass of the perturbing body P and $R_P \equiv |\boldsymbol{R}_P|$, with $\boldsymbol{R}_P(t,\boldsymbol{x})$ being defined as

$$\boldsymbol{R}_P(t,\boldsymbol{x}) = \boldsymbol{x} - \boldsymbol{x}_P(t) , \quad (3.39)$$

where $\boldsymbol{x}_P(t)$ is the coordinate position of the perturbing body P. We shall consider in the following a PN expansion of the trajectory of the perturbing bodies $\boldsymbol{x}_P$, namely

$$\boldsymbol{x}_P(t) = \boldsymbol{x}_P(t_C) + c(t-t_C)\frac{\boldsymbol{v}_P}{c} + \frac{c^2(t-t_C)^2}{2}\frac{\boldsymbol{a}_P}{c^2} + \dots , \quad (3.40)$$

where $\boldsymbol{v}_P(t_C)$ and $\boldsymbol{a}_P(t_C)$ are the velocity and acceleration of the body P, respectively and t_C is some fixed moment of time [Klioner & Kopeikin 1992] that we could use to optimize our approximation. Let us study the amplitude of the two first terms of the expansion. For quasi-circular orbits, one has

$$\left|\frac{\boldsymbol{v}_P}{c}\right| \lesssim \sqrt{\varepsilon_P}\sqrt{\frac{GM_S}{c^2\ R_{PS}}} \qquad \text{and} \qquad \left|\frac{\boldsymbol{a}_P}{c^2}\right| \lesssim \varepsilon_P \frac{GM_S}{c^2\ R_{PS}^2}\ , \tag{3.41}$$

where M_S is the mass of the Sun, R_{PS} the distance between the perturbing body and the Sun and $\varepsilon_P \equiv \dfrac{1+e_P}{1-e_P}$, e_P the orbital eccentricity of body P. Let us consider the circular case $\varepsilon_P = 1$. We know that $\dfrac{GM_S}{c^2} \sim 1.5\ km$, let us then consider the case where $R_{PS} = 10^8\ km$. Then one has

$$\left|\frac{\boldsymbol{v}_P}{c}\right| \sim 10^{-4} \qquad \text{and} \qquad \left|\frac{\boldsymbol{a}_P}{c^2}\right| \sim 1.5\ 10^{-16} km^{-1}\ , \tag{3.42}$$

so that one can reasonably neglect the acceleration terms.

Regarding the choice of t_C the simplest choice would seem to set $t_C \equiv t_B$ since in classical astrometric applications we only have direct access to the reception time t_B. Unfortunately, this choice would lead to unnecessarily big errors in some practical cases, as we show in the following. Let us imagine that the reception is done on a remote satellite at 10^9 km from the perturbing body.

If t_C is defined such that $t_C \equiv t_B$, one has $c(t_m - t_C) \sim 10^9$ km, where t_m is the time when the photon is at its closest distance to the perturbing body. Therefore, taking into account Eq. (3.42), one has

$$c(t_m - t_C)\left|\frac{\boldsymbol{v}_P}{c}\right| \sim 10^5 km \qquad \text{and} \qquad \frac{c^2(t_m - t_C)^2}{2}\left|\frac{\boldsymbol{a}_P}{c^2}\right| \sim 70km\ ,$$

meaning that by neglecting the acceleration term in the expansion one would have an error of 70 km on the impact parameter b of the trajectory of the light beam. For the deviation angle α, one has $\alpha \propto 1/b$. Therefore, the relative error on the deviation angle will be of the order of 70 km/b (since $1/(b \pm 70) \sim (1 \mp 70/b)\ 1/b$). If $b \sim 3.10^3$km (a photon grazing Mercury for instance), then the error on the deviation angle will be around 2% – which is unnecessarily big.

Indeed, one can compute the angular error introduced by the assumption $t_C \equiv t_B$ on the modeling of a light signal grazing Jupiter as

$$\Delta\alpha = -\frac{4GM_J}{c^2 b^2}\Delta b\ , \tag{3.43}$$

where M_J is Jupiter mass, Jupiter Schwarzschild radius is approximately 2.8 meters, b is Jupiter equatorial radius for a grazing photon and $\Delta b = 70km$ is the error on the impact parameter. Then $\Delta\alpha \sim 16\ \mu as$, well above the desired precision for the model. The same computation for Saturn and Mars gives respectively 15 μas and 0.2 μas.

On the contrary, if $t_C \approx t_m$, then $c(t_m - t_C) \sim 0$ and the error introduced by the approximation on the trajectory is small. This means that t_C is chosen as the maximum approach time of the photon to the perturbing body, such that $|\boldsymbol{x}_\gamma(t_C) - \boldsymbol{x}_P(t_C)| \sim b$, where $\boldsymbol{x}_\gamma(t)$ is the trajectory of the photon.

In that case, the additional $\boldsymbol{v}_P/cc^{-2}$ terms in the time transfer or deviation angle coming from the development of the trajectories of the bodies in the application of the TTF will be at the same numerical level that the terms coming from the c^{-3} part of the metric (also due to the motion of the perturbing bodies: $c^{-3} \approx \boldsymbol{v}_P/cc^{-2}$).

The last statement works for the most general case and therefore one should define t_C as being such that $|\boldsymbol{x}_\gamma(t_C) - \boldsymbol{x}_P(t_C)| \sim b$, similarly to what stated in [Klioner 2003, Klioner & Peip 2003].

In the following, we shall then consider a rectilinear uniform trajectory such as

$$\boldsymbol{x}_P(t) = \boldsymbol{x}_P(t_C) + c(t - t_C)\boldsymbol{\beta}_P + \Delta_{x_P}, \tag{3.44}$$

where $\boldsymbol{\beta_P} = \boldsymbol{v}_P(t_C)/c$ and Δ_{x_P} is some typical error made on the position of the perturbing body due to the linear approximation chosen for its trajectory and below the desired accuracy of our model.

In the next sections, we present the development of the TTF and direction triple with the gravitational potential (3.38). A similar reasoning would allow to compute $\mathcal{K}$.

Coordinate time of flight

Taking into account the metric (3.26) with the potential (3.38), Eq. (3.29) writes

$$\mathcal{T}_r(\boldsymbol{x}_A, t_B, \boldsymbol{x}_B; \boldsymbol{v}_P) = \frac{1}{c} R_{AB} + \Delta_r^{(1)}(\boldsymbol{x}_A, t_B, \boldsymbol{x}_B; \boldsymbol{v}_P)\ . \tag{3.45}$$

At the chosen approximation, we get

$$\Delta_r^{(1)}(\boldsymbol{x}_A, t_B, \boldsymbol{x}_B; \boldsymbol{v}_P) = (\gamma+1) R_{AB} \frac{G}{c^2} \sum_P \mathcal{M}_P\, g_P^2 \int_0^1 \left[\frac{1}{R_P(t, \boldsymbol{x})}\right]_{z_-^\alpha(\lambda)} d\lambda\ , \tag{3.46}$$

where the integration path $z_-^\alpha(\lambda)$ is given by Eq. (2.37) and where we define

$$\boldsymbol{g}_P \equiv \boldsymbol{N}_{AB} - \boldsymbol{\beta_P}\ . \tag{3.47}$$

Using Eq. (3.44), we then expand Eq. (3.39) as follows

$$\boldsymbol{R_P}\Big(z_-^0(\lambda), \boldsymbol{z}_-(\lambda)\Big) \;=\; \boldsymbol{R_{PB}} - \lambda R_{AB} \boldsymbol{g}_P + \mathcal{O}(R_P\, \Delta_{x_P})\ , \tag{3.48}$$

where for practical reasons we set the notation

$$\boldsymbol{R}_{PX} = \boldsymbol{x}_X - \boldsymbol{x}_P(t_C) - c(t_X - t_C)\boldsymbol{\beta}_P\ , \tag{3.49}$$

with $R_{PX} \equiv |\boldsymbol{R}_{PX}|$ and $\boldsymbol{N}_{PX} \equiv \dfrac{\boldsymbol{R}_{PX}}{R_{PX}}$. Noting the boundary conditions

$$\begin{aligned} \boldsymbol{R}_P(0) &= \boldsymbol{R}_{PB} \,, & (3.50a)\\ \boldsymbol{R}_P(1) &= \boldsymbol{R}_{PB} - R_{AB}\boldsymbol{g}_P \equiv \boldsymbol{R}_{PA} \,, & (3.50b)\\ \boldsymbol{R}_{PB} - \boldsymbol{R}_{PA} &= \boldsymbol{g}_P R_{AB} \,, & (3.50c) \end{aligned}$$

and substituting for R_P from Eqs. (3.48)-(3.49) into Eq.(3.46), one can compute the reception delay function $\Delta_r^{(1)}(\boldsymbol{x}_A, t_B, \boldsymbol{x}_B; \boldsymbol{v}_P)$ as functions of x_A, x_B and of the coordinate velocity $\boldsymbol{v}_P$ of the perturbing body. One gets

$$\Delta_r^{(1)}(\boldsymbol{x}_A, t_B, \boldsymbol{x}_B; \boldsymbol{v}_P) = (\gamma+1)\frac{G}{c^2}\sum_P \mathcal{M}_P g_P \ln\left[\frac{g_P R_{PA} - \boldsymbol{R_{PA}}\cdot\boldsymbol{g}_P}{g_P R_{PB} - \boldsymbol{R_{PB}}\cdot\boldsymbol{g}_P}\right] . \qquad (3.51)$$

Expanding $\boldsymbol{g_P}$ in Eq. (3.51) it is possible to show explicitely the terms depending on $\boldsymbol{\beta_P}$ as

$$\begin{aligned} \Delta_r^{(1)}(\boldsymbol{x}_A, t_B, \boldsymbol{x}_B; \boldsymbol{v}_P) &= (\gamma+1)\frac{G}{c^2}\sum_P \mathcal{M}_P \Bigg\{ \ln\left(\frac{R_{PA} - \boldsymbol{R_{PA}}\cdot\boldsymbol{N}_{AB}}{R_{PB} - \boldsymbol{R_{PB}}\cdot\boldsymbol{N}_{AB}}\right) \qquad (3.52)\\ &\quad + \boldsymbol{\beta_P}(t_C)\cdot\Bigg[\boldsymbol{N}_{AB}\ln\left(\frac{R_{PA} - \boldsymbol{R_{PA}}\cdot\boldsymbol{N}_{AB}}{R_{PB} - \boldsymbol{R_{PB}}\cdot\boldsymbol{N}_{AB}}\right) + \\ &\quad \frac{\boldsymbol{R_{PB}} - \boldsymbol{N}_{AB}R_{PB}}{R_{PB} - \boldsymbol{R_{PB}}\cdot\boldsymbol{N}_{AB}} - \frac{\boldsymbol{R_{PA}} - \boldsymbol{N}_{AB}R_{PA}}{R_{PA} - \boldsymbol{R_{PA}}\cdot\boldsymbol{N}_{AB}}\Bigg]\Bigg\} . \end{aligned}$$

By setting $\boldsymbol{\beta_P} = 0$ and then $\boldsymbol{g}_P = \boldsymbol{N}_{AB}$ in Eq. (3.51), we retrieve the static case given in [Le Poncin-Lafitte *et al.* 2004] in the case of a single gravitational source. We also applied Eq. (3.51) to the simple configuration of a signal propagating from the outer Solar System to the Earth and grazing Jupiter. Our evaluation of the impact of the orbital motion of Jupiter on the coordinate time of flight of the photon is of the order of 10 *ps*, in accordance to previous results [Linet & Teyssandier 2002]. A similar reasoning allows to compute the emission delay function $\Delta_e(t_A, \boldsymbol{x}_A, \boldsymbol{x}_B)$ as

$$\Delta_e^{(1)}(t_A, \boldsymbol{x}_A, \boldsymbol{x}_B; \boldsymbol{v}_P) = (\gamma+1)\frac{G}{c^2}\sum_P \mathcal{M}_P g_P \ln\left[\frac{g_P R_{PB} + \boldsymbol{R_{PB}}\cdot\boldsymbol{g}_P}{g_P R_{PA} + \boldsymbol{R_{PA}}\cdot\boldsymbol{g}_P}\right] . \qquad (3.53)$$

Finally, we check the formal equivalence $\Delta_r^{(1)}(\boldsymbol{x}_A, t_B, \boldsymbol{x}_B; \boldsymbol{v}_P) = \Delta_e^{(1)}(t_A, \boldsymbol{x}_A, \boldsymbol{x}_B; \boldsymbol{v}_P)$ stated in Eq. (2.3) when we consider Eq. (2.13). Using Eq. (3.50) and the relation

$$\begin{aligned} R_{AB}^2\left[g_P^2 R_X^2 - (\boldsymbol{g}_P\cdot\boldsymbol{R}_X)^2\right] &= R_{AB}^2 g_P^2 R_X^2 - (R_{AB}\,\boldsymbol{g}_P\cdot\boldsymbol{R}_X)^2\\ &= R_{PA}^2 R_{PB}^2 - (\boldsymbol{R}_{PA}\cdot\boldsymbol{R}_{PB})^2 \,, \qquad (3.54) \end{aligned}$$

with X taking the values "PB" or "PA", into Eq. (3.51) and after some algebra, it is straightforward to show its equivalence with Eq. (3.53).

Light direction triples

We provide here the steps to compute the tangent vector at reception event $\left(\widehat{k}_i\right)_B(\boldsymbol{x}_A, t_B, \boldsymbol{x}_B, \boldsymbol{x}_P, \boldsymbol{\beta}_P, \gamma)$. First, we need to compute the partial derivatives of $w(\boldsymbol{x},t)$ and $\boldsymbol{w}(\boldsymbol{x},t)$ as

$$w(\boldsymbol{x},t)_{,0} = \frac{2G}{c^2}\sum_P \mathcal{M}_P \frac{\boldsymbol{R}_P\cdot\boldsymbol{\beta_P}(t_C)}{R_P^3} \quad , \quad w(\boldsymbol{x},t)_{,i} = -G\sum_P \mathcal{M}_P \frac{R_P^i}{R_P^3} \tag{3.55a}$$

and

$$\boldsymbol{w}_{,0} = \frac{2G}{c^2}\sum_P \mathcal{M}_P \frac{\boldsymbol{R}_P\cdot\boldsymbol{\beta_P}(t_C)}{R_P^3}\boldsymbol{v}_P \quad , \quad \boldsymbol{w}_{,i} = -G\sum_P \mathcal{M}_P \frac{R_P^i}{R_P^3}\boldsymbol{v}_P \, . \tag{3.55b}$$

Then, using Eq. (2.7a) and Eq. (3.30) with the metric (3.26) and the gravitational potential (3.38) and (3.55), we compute the light direction triple

$$\begin{aligned}\left(\widehat{k}_i\right)_B = -N_{AB}^i + (\gamma+1)\frac{G}{c^2}\sum_P \mathcal{M}_P \int_0^1 \Bigg\{ R_{AB} g_P^2 \Bigg[\Big(R_{AB}\beta_P^i(t_C) - R_{AB}^i g_P\Big)\frac{\lambda-\lambda^2}{R_P^3(\lambda)} \\ + \Big(R_{PB}^i - N_{AB}^i \boldsymbol{R}_{PB}\cdot\boldsymbol{\beta}_P(t_C)\Big)\frac{1-\lambda}{R_P^3(\lambda)}\Bigg] + \frac{2\beta_P^i(t_C) - N_{AB}^i}{R_P(\lambda)}\Bigg\} d\lambda \, ,\end{aligned} \tag{3.56}$$

where the terms $\boldsymbol{\beta}$ and $\boldsymbol{g}_P$ describe the deflection due to the dynamics of the system.

The explicit computation of the integrals appearing in the r.h.s. of Eq. (3.56) may be obtained by taking into account the boundary conditions set in Eq. (3.50). After some algebra, we get an explicit expression for the light direction triple in the case of multiple deflecting bodies in uniform motion as

$$\begin{aligned}\left(\widehat{k}_i\right)_B = -N_{AB}{}^i + (\gamma+1)\frac{G}{c^2}\sum_P \frac{\mathcal{M}_P}{R_{AB}R_{PB}\Big[R_{PB}^2 g_P^2 - (\boldsymbol{R}_{PB}\cdot\boldsymbol{g}_P)^2\Big]} \\ \times\Bigg\{ g_P N_{AB}{}^i\Big[\Big(\boldsymbol{R}_{PB}\cdot\boldsymbol{N}_{AB}\Big)\Big(R_{PB}^2 - R_{PA}R_{PB} - R_{AB}\boldsymbol{R}_{PB}\cdot\boldsymbol{\beta}_P(t_C)\Big) \\ - R_{PB}^2 R_{AB} g_P^2\Big] \\ + R_{PB}^i g_P^2\Big[R_{PB}R_{PA} - R_{PB}^2 + R_{AB}\boldsymbol{R}_{PB}\cdot\boldsymbol{g}_P\Big] \\ + \beta_P^i(t_C) R_{PB}\Big[(R_{PA}-R_{PB})(\boldsymbol{R}_{PB}\cdot\boldsymbol{N}_{AB}) + R_{PB}R_{AB}\Big]\Bigg\} \\ + (\gamma+1)\frac{G}{c^2}\sum_P \mathcal{M}_P \frac{\beta_P^i(t_C) - N_{AB}{}^i\boldsymbol{\beta}_P(t_C)\cdot\boldsymbol{N}_{AB}}{R_{AB}g_P}\ln\frac{R_{PB}+\boldsymbol{R}_{PB}\cdot\boldsymbol{N}_{AB}}{R_{PA}+\boldsymbol{R}_{PA}\cdot\boldsymbol{N}_{AB}} \\ + \mathcal{O}(c^{-4}) \, .\end{aligned} \tag{3.57}$$

As far as we know, this result is new within the TTF approach. In chapter 6, we check our formulation with some previous results obtained in [Klioner & Kopeikin 1992] through the analytical solution of the null-geodesic equations. We shall note that, from the point of view of the astrometric data analysis, the last equation is obtained as a function of all known quantities (*i.e.* the coordinates of the observing satellite and the mass distribution in the Solar System) and of the astrometric unknown (*i.e.* the source coordinates). Again, by setting $\boldsymbol{\beta_P} = 0$ and $\boldsymbol{g}_P = \boldsymbol{N}_{AB}$, the perturbing bodies are fixed at their position at time t_C and we easily retrieve the static case proposed by [Teyssandier & Le Poncin-Lafitte 2008] in the case of an isolated deflecting body. It is also interesting to evaluate the contribution of the translational motion to light deflection using the definition given in [Teyssandier 2012]

$$\Delta\chi \approx |\boldsymbol{N}_{AB} \times \hat{\boldsymbol{k}}_B| \,, \tag{3.58}$$

where the light ray is considered as coming from infinity. The expression of $\left(\hat{k}_i\right)_B$ is then deduced from Eq. (3.57) where $\boldsymbol{N} \equiv \boldsymbol{N}_{AB}$ and $\boldsymbol{R_{PA}} \approx -\boldsymbol{R_{AB}}$ in this case. Introducing the impact parameter b_P and the angle α between $\boldsymbol{R}_{PB}$ and $\boldsymbol{N}$ we get $b_P = R_{PB}\sin\alpha$, so that

$$\Delta\chi = (\gamma+1)\frac{G}{c^2}\sum_P \frac{\mathcal{M}_P}{R_{PB}^2\left[g_P^2 - (\boldsymbol{N}_{PB}\cdot\boldsymbol{g}_P)^2\right]}\Bigg\{ b_P g_P^2\Big[1 + \boldsymbol{N}_{PB}\cdot\boldsymbol{g}_P\Big] + |\boldsymbol{N}\times\boldsymbol{\beta_P}|\, R_{PB}\big(1 - \boldsymbol{N}_{PB}\cdot\boldsymbol{N}\big)\Bigg\} + \mathcal{O}(c^{-4}, R_{AB}^{-1}) \,. \tag{3.59}$$

The logarithmic term disappears in Eq. (3.59) and can thus be neglected for sources at quasi-infinity. Moreover, numerical estimates of Eq. (3.59) for various deflecting Solar System bodies are in agreement with [Klioner 2003].

3.3 Conclusions

In this chapter, we illustrated the application of the general formulae presented in chapter 2 to a space-time metric well adapted to describe the impact of Solar System gravitational field according to the accuracy required for the data analysis of present and future space experiments. The application to spherical geometry at 2PM will be summarized in [Hees *et al.* 2013] while the PPN application of our formulae has been first presented in [Bertone & Le Poncin-Lafitte 2012] in a general case and then specialized for bodies in translational motion in [Bertone *et al.* 2013a]. In chapter 4, we shall use the developments presented here to define the relativistic observables used in radio-science and astrometry while in chapters 5 and 6 our formalism will be applied in the context of the Gaia mission.

Chapter 4

Doppler and astrometric observables up to the 2PM order

Contents

In this chapter, we will present the application of our formalism to the modeling of relativistic observables for radio-science and astrometry. First, we note that in a general case the emitter and receiver of an EM signal are in relative motion. In section 4.1, we provide an analytical and an iterative way of dealing with this problem and we retrieve the so-called Sagnac terms in Eq. (4.4). Then, we focus on the Doppler observable commonly used in radio-science, writing explicit formulae for the one-way (in Eq. (4.9)) and the multi-ways (in Eq. (4.11)) frequency shift. Concerning astrometry, we provide a formulation for two kinds of relativistic observables: the incident direction of an incoming light ray in the reference frame of an observer (at Eq. (4.15)) and the angular separation between two light sources (at Eq. (4.17)). All these quantities are expressed as functions of the metric tensor, its derivatives and the functions $\mathcal{T}$, $(\hat{k}_i)_{A/B}$ and $\mathcal{K}$ defined in the previous chapters as closed form integrals. Finally, in section 4.3 we apply our formulae to provide estimates of the 1PM and 2PM relativistic corrections to the observables of BepiColombo and of GAME-like missions in the Schwarzschild gravitational field of the Sun.

4.1 Moving emitter and receiver

Let us consider two observers $\mathcal{O}_\mathcal{A}$ and $\mathcal{O}_\mathcal{B}$ located at points $\mathcal{A}$ and $\mathcal{B}$. The second observer $\mathcal{O}_\mathcal{B}$ receives an electromagnetic signal from $\mathcal{O}_\mathcal{A}$. This signal is received at the coordinate time t_B and at the position $\boldsymbol{x}_B$ and it was emitted at time t_A and at the position $\boldsymbol{x}_A$.

The coordinate time of flight of a photon between $\mathcal{O}_\mathcal{A}$ and $\mathcal{O}_\mathcal{B}$ in the case of a fix emitter and receiver has been computed in Eq. (2.13) and Eq. (2.35). It can then be used to compute two physical quantities (see [Bertone *et al.* 2012b] and references therein) used in radio-science:

- the *Ranging*, describing the distance between probe and ground station, is defined by adding to the coordinate time of flight (times c, the speed of light) the corrections accounting for the tropospheric and ionospheric delay, the processing time of the signal, etc... Since the study of the atmospheric or electronic delay on an EW is far from the goals of this thesis, in the following we shall only focus on the definition of the TTF (2.3) in the general case of a moving emitter/receiver.

- the *Doppler*, related to the radial velocity of the probe with respect to the Earth, represents the frequency shift of the signal between $\mathcal{O}_\mathcal{A}$ and $\mathcal{O}_\mathcal{B}$ and, for practical applications, it is obtained by differentiating two successive measurements of the time of flight of the signal. We shall detail the Doppler observable in section 4.2.1.

In realistic cases, neither the emitter nor the receiver of the electromagnetic signal are static in space-time. Instead, they are following the trajectories $\boldsymbol{x}_A(t)$ and $\boldsymbol{x}_B(t)$, parametrized by the coordinate time t. In this case, relation (2.3) becomes implicit since $\boldsymbol{x}_A$ depends on t_A

$$t_B - t_A = \mathcal{T}_r(\boldsymbol{x}_A(t_A), t_B, \boldsymbol{x}_B(t_B)) = \frac{|\boldsymbol{x}_B(t_B) - \boldsymbol{x}_A(t_A)|}{c} + \frac{1}{c}\Delta_r(\boldsymbol{x}_A(t_A), t_B, \boldsymbol{x}_B(t_B)). \tag{4.1}$$

This causes difficulties in the computation of the TTF since t_A is not known a priori. We present two solutions : an analytical expansion of the emission time t_A or a numerical iterative method.

4.1.1 Sagnac terms

The analytical procedure follows the same method as the one presented in [Petit & Wolf 2005]. The idea is to expand the position of the emitter

$$\boldsymbol{x}_A(t_A) = \tilde{\boldsymbol{x}}_A + (t_A - t_B)\tilde{\boldsymbol{v}}_A + \frac{1}{2}(t_A - t_B)^2\tilde{\boldsymbol{a}}_A + \frac{1}{6}(t_A - t_B)^3\tilde{\boldsymbol{b}}_A + \dots \tag{4.2}$$

where the tilde refers to quantities evaluated at $t = t_B$, so that $\tilde{\boldsymbol{x}}_A = \boldsymbol{x}_A(t_B)$, $\tilde{\boldsymbol{v}}_A = \boldsymbol{v}_A(t_B) = \left.\frac{d\boldsymbol{x}_A}{dt}\right|_{t_B}$, $\tilde{\boldsymbol{a}}_A = \boldsymbol{a}_A(t_B) = \left.\frac{d^2\boldsymbol{x}_A}{dt^2}\right|_{t_B}$ and $\tilde{\boldsymbol{b}}_A = \boldsymbol{b}_A(t_B) = \left.\frac{d^3\boldsymbol{x}_A}{dt^3}\right|_{t_B}$.

Introducing expansion (4.2) in Eq.(4.1) leads to

$$\begin{aligned}\delta t &= \frac{D_{AB}}{c} + \delta t\frac{\tilde{\boldsymbol{v}}_A\cdot\boldsymbol{D}_{AB}}{cD_{AB}} + \frac{\delta t^2}{2cD_{AB}}\left[\tilde{v}_A^2 - \tilde{\boldsymbol{a}}_A\cdot\boldsymbol{D}_{AB} - \left(\frac{\tilde{\boldsymbol{v}}_A\cdot\boldsymbol{D}_{AB}}{D_{AB}}\right)^2\right]\\ &+\frac{\delta t^3}{2cD_{AB}}\left[\frac{1}{3}\tilde{\boldsymbol{b}}_A\cdot\boldsymbol{D}_{AB} - \tilde{\boldsymbol{v}}_A\cdot\boldsymbol{a}_A - \frac{\tilde{v}_A^2\tilde{\boldsymbol{v}}_A\cdot\boldsymbol{D}_{AB}}{D_{AB}^2} + \frac{(\tilde{\boldsymbol{v}}_A\cdot\boldsymbol{D}_{AB})(\tilde{\boldsymbol{a}}_A\cdot\boldsymbol{D}_{AB})}{D_{AB}^2}\right.\\ &\left.+\frac{(\boldsymbol{v}_A\cdot\boldsymbol{D}_{AB})^3}{D_{AB}^4}\right] + \frac{1}{c}\Delta_r(\tilde{\boldsymbol{x}}_A,t_B,\boldsymbol{x}_B) - \frac{\delta t}{c}\frac{\partial\Delta_r(\tilde{\boldsymbol{x}}_A,t_B,\boldsymbol{x}_B)}{\partial x_A^i}\tilde{v}_A^i\\ &+\frac{\delta t^2}{c}\left[\frac{1}{2}\frac{\partial\Delta_r(\tilde{\boldsymbol{x}}_A,t_B,\boldsymbol{x}_B)}{\partial x_A^i}\tilde{a}_A^i + \frac{\partial^2\Delta_r(\tilde{\boldsymbol{x}}_A,t_B,\boldsymbol{x}_B)}{\partial x_A^i\partial x_A^j}\tilde{v}_A^i\tilde{v}_A^j\right] + \dots\,, \end{aligned} \tag{4.3}$$

where $\delta t = t_B - t_A = \mathcal{T}_r(\boldsymbol{x}_A(t_A),t_B,\boldsymbol{x}_B(t_B))$, $\boldsymbol{D}_{AB} = \boldsymbol{x}_B(t_B) - \boldsymbol{x}_A(t_B)$ and $D_{AB} = |\boldsymbol{D}_{AB}|$. An iterative solution of the last equation gives

$$\begin{aligned}\mathcal{T}_r(\boldsymbol{x}_A(t_A),t_B,\boldsymbol{x}_B(t_B)) &= \frac{D_{AB}}{c} + \frac{\tilde{\boldsymbol{v}}_A\cdot\boldsymbol{D}_{AB}}{c^2}\\ &+\frac{D_{AB}}{2c^3}\left[\tilde{v}_A^2 + \left(\frac{\tilde{\boldsymbol{v}}_A\cdot\boldsymbol{D}_{AB}}{D_{AB}}\right)^2 - \tilde{\boldsymbol{a}}_A\cdot\boldsymbol{D}_{AB}\right]\\ &+\frac{1}{c^4}\left[(\tilde{\boldsymbol{v}}_A\cdot\boldsymbol{D}_{AB})(\tilde{v}_A^2 - \tilde{\boldsymbol{a}}_A\cdot\boldsymbol{D}_{AB}) + \frac{1}{6}D_{AB}^2\boldsymbol{b}_A\cdot\boldsymbol{D}_{AB}\right.\\ &\left.-\frac{1}{2}D_{AB}^2\boldsymbol{v}_A\cdot\boldsymbol{a}_A\right] + \frac{1}{c}\Delta_r(\tilde{\boldsymbol{x}}_A,t_B,\boldsymbol{x}_B) - \frac{D_{AB}}{c^2}\frac{\partial\Delta_r(\tilde{\boldsymbol{x}}_A,t_B,\boldsymbol{x}_B)}{\partial x_A^i}\tilde{v}_A^i\\ &+\frac{\tilde{\boldsymbol{v}}_A\cdot\boldsymbol{D}_{AB}}{c^2D_{AB}}\Delta_r(\tilde{\boldsymbol{x}}_A,t_B,\boldsymbol{x}_B) + \mathcal{O}(1/c^5)\,. \end{aligned} \tag{4.4}$$

This is no longer a PM expansion but becomes a PN one since the TTF is expanded in terms of quantities such as $\tilde{v}_A/c$, $(\tilde{\boldsymbol{D}}_{AB}\cdot\tilde{\boldsymbol{a}})/c^2$ that should be small to assure the convergence of the series. It should be noted that for this PN expansion $\Delta_r^{(1)}$ is considered of order G/c^2. This computation can be extended to higher orders if necessary. This analytical expansion makes clearly appear what is usually referred to as Sagnac terms. While being analytical, it has the disadvantage to be valid for small velocities/accelerations only (which is not problematic in the Solar System but can be limiting in other applications like binary pulsars).

4.1.2 Iterative procedure

Instead of using the analytical expansion presented above, one can use an iterative procedure. This procedure is standard and can be written as

$$\text{Start:} \quad t_A^{(0)} = t_B - \mathcal{T}_r(\boldsymbol{x}_A(t_B), t_B, \boldsymbol{x}_B(t_B)) \tag{4.5a}$$

$$\text{Loop:} \quad t_A^{(i+1)} = t_B - \mathcal{T}_r(\boldsymbol{x}_A(t_A^{(i)}), t_B, \boldsymbol{x}_B(t_B)) \tag{4.5b}$$

$$\text{End:} \quad \text{when } \left|t_A^{(i+1)} - t_A^{(i)}\right| < \varepsilon \tag{4.5c}$$

with ε the desired accuracy and (i) indexing the iteration steps. Each step of this iterative procedure requires to evaluate the TTF. In practice, in the Solar System this procedure converges very quickly after two or three iterations. The main advantage of this procedure is that no PN expansion is done and that it is really easy to implement.

The two procedures presented in section 4.1 allow one to compute t_A, the coordinate emission time of the signal emitted along the world line $\boldsymbol{x}_A(t)$, from the reception coordinate time t_B and the coordinate of the receiver $\boldsymbol{x}_B$. The analytical expansion (4.4) is a PN expansion of t_A up to $\mathcal{O}(1/c^4)$ while the iterative procedure (4.5) is valid at any order.

4.2 Doppler and astrometric observables from the Time Transfer Function

In this section, we give the relativistic formulae to compute the Doppler and astrometric observables as functions of the TTF and its partial derivatives. The expressions presented here make no expansion of any kind and are therefore very general.

4.2.1 Doppler observables

The one-way frequency shift

Let us note $\nu_{\mathcal{A}/\mathcal{B}}$ the proper frequency at which the signal was emitted/received. Then, the one-way frequency shift is defined by

$$\left.\frac{\Delta\nu}{\nu}\right|_{\mathrm{A}\to\mathrm{B}}^{\text{one-way}} = \frac{\nu_B}{\nu_A} - 1\,. \tag{4.6}$$

It is well-known that the ratio ν_B/ν_A can be expressed as [Synge 1960]

$$\frac{\nu_B}{\nu_A} = \frac{u_B^\mu k_\mu^B}{u_A^\nu k_\nu^A} = \frac{k_0^B}{k_0^A}\frac{u_B^0 + u_B^i\left(\hat{k}_i\right)_B}{u_A^0 + u_A^i\left(\hat{k}_i\right)_A} = \frac{u_B^0}{u_A^0}\mathcal{K}\frac{1+\beta_B^i\hat{k}_i^B}{1+\beta_A^i\hat{k}_i^A} = \left(\frac{d\tau}{dt}\right)_A \frac{dt_A}{dt_B}\left(\frac{dt}{d\tau}\right)_B, \tag{4.7}$$

where $u^\mu_{A/B} = (dx^\mu/ds)_{A/B}$ is the four-velocity of the observers $\mathcal{A}$ or $\mathcal{B}$, $\beta^i_{A/B} = c^{-1}\dfrac{dx^i_{A/B}}{dt}$ is their coordinate velocity, while $\mathcal{K} = \dfrac{k^B_0}{k^A_0}$ and $\hat{k}_i = \left(\dfrac{k_i}{k_0}\right)$ are the ratios of the null tangent vectors k^A and k^B at the point of emission x_A and at the point of reception x_B, respectively. Terms appearing in the right hand side of Eq. (4.7) can be expressed as

$$u^0_{A/B} = \left(\frac{d\tau}{dt}\right)_{A/B} = \left|g_{00} + 2g_{0i}\beta^i + g_{ij}\beta^i\beta^j\right|^{1/2}_{A/B} \quad \text{and} \quad \frac{dt_A}{dt_B} = \mathcal{K}\frac{1+\beta^i_B\left(\hat{k}_i\right)_B}{1+\beta^i_A\left(\hat{k}_i\right)_A}, \tag{4.8}$$

where the expressions of $\mathcal{K}$ and $\hat{k}^B_i$ are given by Eq. (2.36). It is then straightforward to define the one-way frequency shift (4.6) as a function of $\Delta_{e/r}$ and their partial derivatives. Substituting for $\left(\hat{k}_i\right)_{A/B}$ and $\mathcal{K}$ from Eq. (2.36) into Eq. (4.8) and inserting it in relation (4.7), one gets the exact expression [Teyssandier 2009, Hees *et al.* 2012b]

$$\boxed{\frac{\nu_B}{\nu_A} = \frac{\left|g_{00} + 2g_{0i}\beta^i + g_{ij}\beta^i\beta^j\right|^{1/2}_A}{\left|g_{00} + 2g_{0i}\beta^i + g_{ij}\beta^i\beta^j\right|^{1/2}_B} \times \frac{1 - N^i_{AB}\beta^i_B - \beta^i_B\frac{\partial\Delta_r}{\partial x^i_B} - \frac{1}{c}\frac{\partial\Delta_r}{\partial t_B}}{1 - N^i_{AB}\beta^i_A + \beta^i_A\frac{\partial\Delta_r}{\partial x^i_A}}}. \tag{4.9}$$

Multi-ways frequency shift

In this section, we consider a multi-ways frequency shift. For example, let us suppose that the signal is emitted by an observer $\mathcal{O}_\mathcal{A}$, transmitted by an observer $\mathcal{O}_\mathcal{B}$ and then received by an observer $\mathcal{O}_\mathcal{C}$ (which can eventually be $\mathcal{O}_\mathcal{A}$). The frequency shift is then defined as for the one-way

$$\left.\frac{\Delta\nu}{\nu}\right|_{\mathrm{A}\to\mathrm{C}} = \frac{\nu_C}{\nu_A} - 1, \tag{4.10}$$

where the ratio ν_C/ν_A can be expanded as follows

$$\boxed{\frac{\nu_C}{\nu_A} = \frac{\nu_C}{\nu_{B,e}}\delta\nu_B\frac{\nu_{B,r}}{\nu_A}}, \tag{4.11}$$

with $\nu_{B,r}$ the proper frequency received by the observer $\mathcal{O}_\mathcal{B}$ and $\nu_{B,e}$ the proper frequency emitted by the same observer. The factor $\delta\nu_B = \dfrac{\nu_{B,e}}{\nu_{B,r}}$ stands for any frequency shift introduced between the reception and re-emission of the signal in $\mathcal{B}$, for example due to the transponder of a probe.

The computation of the multi-ways frequency shift is then straightforward: the two terms $\nu_C/\nu_{B,e}$ and $\nu_{B,r}/\nu_A$ from (4.11) are one-way frequency shifts and can be computed using (4.9). This procedure can be easily generalized if more links are needed.

4.2.2 Astrometric observables

The goal of astrometry is to determine the position of celestial bodies from angular observations. We focus on two main approaches: the modeling of the direction of incidence of a light ray in a certain reference frame and the angular separation of two light sources.

Angular direction in the observer's reference frame

One way to get a covariant definition of this astrometric observable is to use the tetrad formalism [Brumberg 1991, Misner *et al.* 1973, Weinberg 1972, Klioner & Kopeikin 1992], thus giving the direction of observation of an incoming light ray in a particular tetrad comoving with the observer $\mathcal{O}_{\mathcal{B}}$.

Let us note $\lambda^{\mu}_{(\alpha)}$ the components of this tetrad, where (α) corresponds to the tetrad index (running between 0 and 3) and μ is a normal tensor index which can be lowered and raised by use of the metric. The fact that the basis vectors of the tetrad are orthonormal implies

$$g_{\mu\nu}\lambda^{\mu}_{(\alpha)}\lambda^{\nu}_{(\beta)} = \eta_{(\alpha)(\beta)} \,. \tag{4.12}$$

The components of the tetrad allow us to transform the coordinates of the wave vector from the global coordinate frame to the tetrad frame with

$$k_{(\alpha)} = \lambda^{\mu}_{(\alpha)} k_{\mu} \,, \tag{4.13}$$

where k_{μ} are the components of the wave vector in the global frame while $k_{(\alpha)}$ are the components of the same vector in the tetrad basis. The projection of the light ray in the tetrad frame is given by the normalization

$$n^{(i)} = \frac{k^{(i)}}{\sqrt{\delta_{jk}k^{(j)}k^{(k)}}} = \frac{k^{(i)}}{k^{(0)}} = -\frac{k_{(i)}}{k_{(0)}}, \tag{4.14}$$

where we used the properties of the null-vector $k^{(i)}$ and the fact that the metric is locally Minkowskian in the tetrad basis. The vector quantities defined by Eq. (4.14) represent the so called "director cosines" of an observation, *i.e.* the cosines of the angles formed by the projection of k_{μ} on the tetrad axes (which is a relativistic observable). Using the transformation law (4.13) into Eq. (4.14), one gets

$$\boxed{n^{(i)} = -\frac{\lambda^{0}_{(i)}k_0 + \lambda^{j}_{(i)}k_j}{\lambda^{0}_{(0)}k_0 + \lambda^{j}_{(0)}k_j} = -\frac{\lambda^{0}_{(i)} + \lambda^{j}_{(i)}\hat{k}_j}{\lambda^{0}_{(0)} + \lambda^{j}_{(0)}\hat{k}_j} \,,} \tag{4.15}$$

where $\hat{k}_j$ is the direction triple defined in (2.7). This expression is consistent with the one derived in [Klioner 2004, Crosta & Vecchiato 2010]. Using the relation (2.36),

one can then express the incoming direction of the light ray in terms of the reception delay function and its derivatives [Bertone & Le Poncin-Lafitte 2012] as

$$n^{(i)} = -\frac{\lambda^0_{(i)}\left(1-\frac{1}{c}\frac{\partial\Delta_r}{\partial t_B}\right) - \lambda^j_{(i)}N^j - \lambda^j_{(i)}\frac{\partial\Delta_r}{\partial x^j_B}}{\lambda^0_{(0)}\left(1-\frac{1}{c}\frac{\partial\Delta_r}{\partial t_B}\right) - \lambda^j_{(0)}N^j - \lambda^j_{(0)}\frac{\partial\Delta_r}{\partial x^j_B}}\,. \tag{4.16}$$

Again, this expression is very general and makes no assumption on the tetrad considered or any expansion of the involved quantities.

Angular separation of two sources

Some astrometric observations measure the angular distance between two celestial bodies instead of projecting the coordinate direction of the incident light ray in the observer's reference frame as described in the previous section. This observable can also be computed within the TTF formalism. Indeed, it was shown in [Teyssandier & Le Poncin-Lafitte 2006] that the angular distance ϕ between two incident light ray coming from two celestial bodies and observed by a moving observer $\mathcal{O}_B$ can be written as

$$\boxed{\sin^2\frac{\phi}{2} = -\frac{1}{4}\left[\frac{\left(g_{00}+2g_{0k}\beta^k+g_{kl}\beta^k\beta^l\right)g^{ij}(\hat{k}'_i-\hat{k}_i)(\hat{k}'_j-\hat{k}_j)}{(1+\beta^m\hat{k}_m)(1+\beta^l\hat{k}'_l)}\right]_B}\,, \tag{4.17}$$

where $\left(\hat{k}_j\right)_B$ and $\left(\hat{k}'_j\right)_B$ are the direction triples of the two incident light rays expressed in the global coordinates.

4.3 Applications

As an example, we use the equations presented in section 4.2 to give estimates of the relativistic corrections to BepiColombo and GAME-like observables. We shall work in the Schwarzschild metric due to the gravitational field of the Sun, neglecting all other gravitational sources.

4.3.1 Application to BepiColombo

BepiColombo mission will reach an impressive level of accuracy on its measurments: 10 cm on the Range and 10^{-6} m/s on the Doppler [Milani *et al.* 2002, Iess *et al.* 2009]. Such an accuracy needs to model the influence of some 2PM terms coming from the Sun on light propagation [Tommei *et al.* 2010]. As example of how the equations presented in this paper can be applied to a real measurement, we simulate a 1 year Mercury-Earth Doppler link taking into account only the gravitational contribution from the Sun. The Earth and Mercury orbits used here come from the JPL ephemerides [Folkner *et al.* 2009] obtained using the SPICE toolkit

[Acton 1996, Acton *et al.* 2011]. Substituting for the metric, Δ_r and its derivatives from Eq. (3.13), Eq. (3.15), Eq. (3.19) and Eq. (3.25), respectively into Eq. (4.9) one can write the expression of the Doppler around a spherical mass

$$\frac{\nu_B}{\nu_A} = \frac{\sqrt{1-2\frac{m}{r_A}+2\beta\frac{m^2}{r_A^2}-\frac{3}{2}\beta_3\frac{m^3}{r_A^3}-\frac{v_A^2}{c^2}-2\gamma\frac{v_A^2}{c^2}\frac{m}{r_A}-\frac{3}{2}\varepsilon\frac{m^2}{r_A^2}\frac{v_A^2}{c^2}}}{\sqrt{1-2\frac{m}{r_B}+2\beta\frac{m^2}{r_B^2}-\frac{3}{2}\beta_3\frac{m^3}{r_B^3}-\frac{v_B^2}{c^2}-2\gamma\frac{v_B^2}{c^2}\frac{m}{r_B}-\frac{3}{2}\varepsilon\frac{m^2}{r_B^2}\frac{v_B^2}{c^2}}}\times\frac{q_B}{q_A} \tag{4.18}$$

with

$$\begin{aligned} q_A = {} & 1-\frac{\boldsymbol{N}_{AB}\cdot\boldsymbol{v}_A}{c}-\frac{2(1+\gamma)m}{c\left[(r_A+r_B)^2-R_{AB}^2\right]}\left[(r_A+r_B)\boldsymbol{N}_{AB}\cdot\boldsymbol{v}_A+R_{AB}\boldsymbol{n}_A\cdot\boldsymbol{v}_A\right] \\ & +\frac{\kappa m^2}{cr_Ar_B}\left[\frac{\arccos\mu}{\sqrt{1-\mu^2}}\left(-\boldsymbol{N}_{AB}\cdot\boldsymbol{v}_A-\frac{R_{AB}\boldsymbol{n}_A\cdot\boldsymbol{v}_A}{r_A(1-\mu^2)}+\mu\frac{R_{AB}\boldsymbol{n}_B\cdot\boldsymbol{v}_A}{r_B(1-\mu^2)}\right)\right. \\ & \left.-\frac{R_{AB}}{r_A(1-\mu^2)}(\boldsymbol{n}_B\cdot\boldsymbol{v}_A-\mu\boldsymbol{n}_A\cdot\boldsymbol{v}_A)\right] \\ & +\frac{(1+\gamma)^2m^2}{cr_Ar_B(1+\mu)}\left[\boldsymbol{N}_{AB}\cdot\boldsymbol{v}_A+\frac{R_{AB}}{r_A(1+\mu)}(\boldsymbol{n}_A\cdot\boldsymbol{v}_A+\boldsymbol{n}_B\cdot\boldsymbol{v}_A)\right], \end{aligned} \tag{4.19a}$$

and

$$\begin{aligned} q_B = {} & 1-\frac{\boldsymbol{N}_{AB}\cdot\boldsymbol{v}_B}{c}-\frac{2(1+\gamma)m}{c\left[(r_A+r_B)^2-R_{AB}^2\right]}\left[(r_A+r_B)\boldsymbol{N}_{AB}\cdot\boldsymbol{v}_B-R_{AB}\boldsymbol{n}_B\cdot\boldsymbol{v}_B\right] \\ & +\frac{\kappa m^2}{cr_Ar_B}\left[\frac{\arccos\mu}{\sqrt{1-\mu^2}}\left(-\boldsymbol{N}_{AB}\cdot\boldsymbol{v}_B+\frac{R_{AB}\boldsymbol{n}_B\cdot\boldsymbol{v}_B}{r_B(1-\mu^2)}-\mu\frac{R_{AB}\boldsymbol{n}_A\cdot\boldsymbol{v}_B}{r_A(1-\mu^2)}\right)\right. \\ & \left.+\frac{R_{AB}}{r_B(1-\mu^2)}(\boldsymbol{n}_A\cdot\boldsymbol{v}_B-\mu\boldsymbol{n}_B\cdot\boldsymbol{v}_B)\right] \\ & +\frac{(1+\gamma)^2m^2}{cr_Ar_B(1+\mu)}\left[\boldsymbol{N}_{AB}\cdot\boldsymbol{v}_B-\frac{R_{AB}}{r_B(1+\mu)}(\boldsymbol{n}_A\cdot\boldsymbol{v}_B+\boldsymbol{n}_B\cdot\boldsymbol{v}_B)\right]. \end{aligned} \tag{4.19b}$$

We use relation (3.20) and Eq. (4.18)-(4.19) to estimate the order of magnitude of the first and second PM contribution to the Mercury-Earth Range and Doppler represented in Figure 4.1. The different peaks correspond to Solar conjunctions in the geometry of the observation. Moreover, we would like to stress the fact that the expression of the time transfer used in the standard modeling of radio-science measurements (see for example [Moyer 2000]) is only an approximation of the relation (3.20) and can be written as

$$\mathcal{T}_r(\boldsymbol{x}_A,t_B,\boldsymbol{x}_B)=t_B-t_A=\frac{R_{AB}}{c}+\frac{(\gamma+1)m}{c}\ln\left(\frac{r_A+r_B+R_{AB}+(1+\gamma)m}{r_A+r_B-R_{AB}+(1+\gamma)m}\right). \tag{4.20}$$

A comparison of Range and Doppler simulations obtained using expressions based on the approximation (4.20) and on expression (3.20), complete at the 2PM order, is

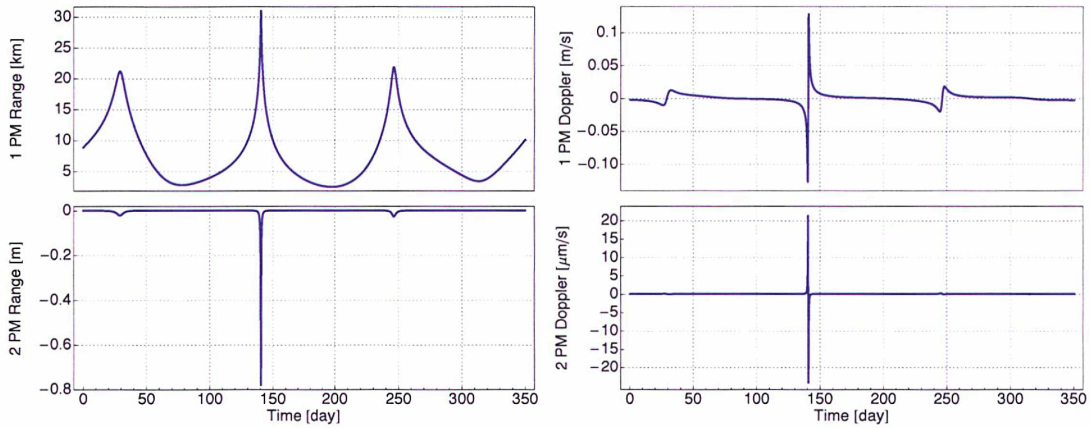

Figure 4.1: First and second PM contributions to the Range and the Doppler for a 1 year Mercury-Earth radio-science link. The peaks correspond to different conjunctions between the Earth, the Sun and Mercury.

illustrated in Fig. 4.2 to quantify the accuracy of the standard radio-science modeling. The order of magnitude of the error committed by using the simplified formula (4.20) instead of the complete 2PM formula (3.20) is just below BepiColombo accuracy. Nevertheless, future space missions are going to aim at increasing the level of accuracy on radioscience measurements so that the current modeling will have to be improved to include the full 2PM correction on light propagation.

4.3.2 Direction of a light ray emitted by a star and observed on Earth

A comoving kinematically nonrotating tetrad

In order to simulate an astrometric observable, one needs to specify the reference frame used for the projection of the incident direction of a light ray. As shown in section 4.2.2, this reference frame is mathematically modeled by a tetrad $\lambda^{\mu}_{(\alpha)}$, which explicitly appears in the computation of the astrometric observables (4.16).

In this paragraph, we will develop the expression of a kinematically nonrotating tetrad comoving with an observer in the case of a static spherically symmetric space-time described by the metric (3.1). This tetrad is called "kinematically nonrotating" in the sense that the spatial coordinates transformation between the global coordinate system and the local one does not depend on a time dependent orthogonal matrix [Klioner & Soffel 1998]. This type of local coordinate system is currently used in the definition of the GCRS [Soffel *et al.* 2003] or in the context of the Gaia mission [Klioner 2004].

We define ∂_α the vectors of the natural coordinate basis and $e_{(\alpha)}$ the basis vectors of the tetrad. The transformation matrix between these two basis is noted $\lambda^{\mu}_{(\alpha)}$ and

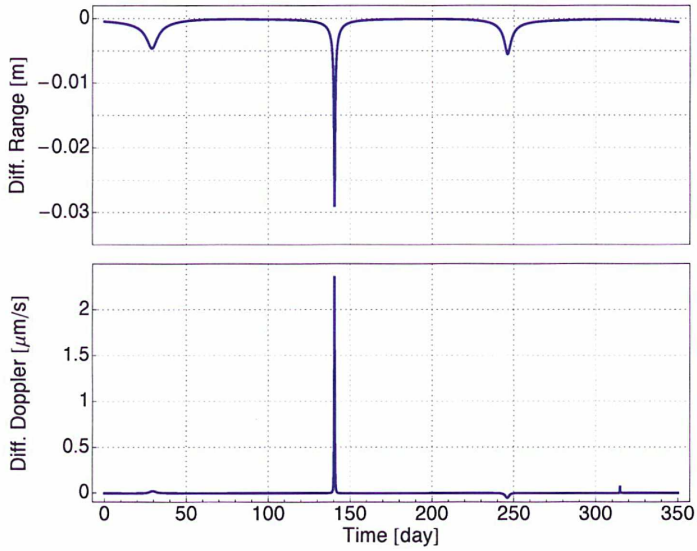

Figure 4.2: Difference between the standard formulation of the Range/Doppler used in radio-science modeling (4.20) and the exact 2PM expression (3.20). The peaks correspond to conjunctions of Earth, Sun and Mercury.

it is defined by

$$e_{(\alpha)} = \lambda^{\mu}_{(\alpha)} \partial_{\mu} \, . \tag{4.21}$$

The great advantage of such a basis is that the tetrad is locally orthonormal, so that the metric is locally Minkowskian. This transformation physically corresponds to a change of basis in the tangent space of the differential variety. From the point of view of the metric, we can easily show the link between the $g_{\mu\nu}$ of the natural coordinate basis and $\eta_{(\alpha)(\beta)}$ in the tetrad basis using Eq. (4.21) as

$$\eta_{(\alpha)(\beta)} = \boldsymbol{g}(\boldsymbol{e}_{(\alpha)}, \boldsymbol{e}_{(\beta)}) = \boldsymbol{g}(\lambda^{\mu}_{(\alpha)} \partial_{\mu}, \lambda^{\nu}_{(\beta)} \partial_{\nu}) = \lambda^{\mu}_{(\alpha)} \lambda^{\nu}_{(\beta)} \boldsymbol{g}(\partial_{\mu}, \partial_{\nu}) = \lambda^{\mu}_{(\alpha)} \lambda^{\nu}_{(\beta)} \boldsymbol{g}_{\mu\nu} \, . \tag{4.22}$$

Since in the tetrad basis the metric is locally Minkowskian, special relativity applies locally. In particular, all indexes related to the tetrad (between parenthesis) are upped and lowered using Minkowsky metric tensor, while natural coordinate basis indexes are set up and down using the $g_{\mu\nu}$ metric.

We can split the transformation between the natural coordinate basis and the local comoving basis of the tetrad in two parts $\lambda^{\mu}_{(\alpha)} = \Lambda^{\hat{\kappa}}_{(\alpha)} \tilde{\Lambda}^{\mu}_{\hat{\kappa}}$ [Misner *et al.* 1973]. The first step (parametrized by $\tilde{\Lambda}^{\mu}_{\hat{\kappa}}$) consists in orthogonalizing the natural coordinate basis to obtain a local orthonormal coordinate basis static with respect to the chosen coordinate system. The second part of the transformation (parametrized by $\Lambda^{\hat{\kappa}}_{(\alpha)}$) consists in applying a Lorentz boost to this orthonormal basis to make it comoving with the observer. Quantities related to the final tetrad will be denoted

with indices into parentheses, while quantities expressed in the intermediate tetrad will be denoted with a hat.

Since the space-time metric (3.1) is diagonal, it is straightforward to orthonormalize the basis

$$\tilde{\Lambda}^{0}_{\hat{0}} = \frac{1}{\sqrt{A(r)}} \quad , \quad \tilde{\Lambda}^{i}_{\hat{0}} = \tilde{\Lambda}^{0}_{\hat{i}} = 0 \quad , \quad \tilde{\Lambda}^{j}_{\hat{i}} = \frac{\delta^{j}_{i}}{\sqrt{B(r)}} \, . \tag{4.23}$$

The second step consists then in a Lorentz boost of the previous tetrad in order to make it comoving with the observer. We will note the four-velocity of the observer (expressed in the global coordinate system) by $u^\alpha = dx^\alpha/ds$. This velocity can also be expressed in terms of coordinates related to the intermediate tetrad $\hat{u}^{\hat{\alpha}} = d\hat{x}^{\hat{\alpha}}/ds = \tilde{\Lambda}^{\hat{\alpha}}_{\mu} u^\mu = \left(\sqrt{A(r)}u^0, \sqrt{B(r)}u^i\right)$. Finally, the coordinate velocity of the observer will be denoted by $\beta^i = \frac{1}{c}\frac{dx^i}{dt}$. The same quantity expressed in the intermediate tetrad is $\hat{\beta}^i = \frac{1}{c}\frac{d\hat{x}^i}{d\hat{t}} = \sqrt{\frac{B(r)}{A(r)}}\beta^i$. The second matrix transformation is thus simply provided by a standard Lorentz transformation matrix whose inverse is provided by

$$\Lambda^{\hat{0}}_{(0)} = \hat{\gamma} \quad , \quad \Lambda^{\hat{0}}_{(i)} = \Lambda^{\hat{i}}_{(0)} = -\hat{\gamma}\hat{\beta}^i \quad , \quad \Lambda^{\hat{i}}_{(j)} = \delta_{ij} + \frac{\hat{\gamma}^2}{\hat{\gamma}+1}\hat{\beta}^i\hat{\beta}^j \tag{4.24}$$

with

$$\hat{\gamma} = \left(1-\hat{\beta}^2\right)^{-1/2} = \left(1 - \frac{B(r)}{A(r)}\beta^2\right)^{-1/2} \, . \tag{4.25}$$

Combining Eq. (4.23) and Eq. (4.24) we get

$$\lambda^{0}_{(0)} = \frac{\hat{\gamma}}{\sqrt{A(r)}} = \frac{1}{\sqrt{A(r) - B(r)\beta^2}} \, , \tag{4.26a}$$

$$\lambda^{i}_{(0)} = -\frac{\hat{\gamma}\hat{\beta}^i}{\sqrt{B(r)}} = -\frac{\beta^i}{\sqrt{A(r) - B(r)\beta^2}} \, , \tag{4.26b}$$

$$\lambda^{0}_{(j)} = -\frac{\hat{\gamma}\hat{\beta}^j}{\sqrt{A(r)}} = -\sqrt{\frac{B(r)}{A(r)}}\frac{\beta^j}{\sqrt{A(r) - B(r)\beta^2}} \, , \tag{4.26c}$$

$$\lambda^{i}_{(j)} = \frac{\delta_{ij} + \frac{\hat{\gamma}^2}{\hat{\gamma}+1}\hat{\beta}^i\hat{\beta}^j}{\sqrt{B(r)}} = \frac{\delta_{ij}}{\sqrt{B(r)}} + \frac{\sqrt{B(r)}\beta^i\beta^j}{\sqrt{A^2(r) - A(r)B(r)\beta^2} + A(r) - B(r)\beta^2} \, . \tag{4.26d}$$

Eq. (4.26) is the exact expression of a kinematically nonrotating tetrad in a static, spherically symmetric space-time and it can be expanded to 2PM order if necessary using Eqs. (3.13)-(3.14).

Application: incident light ray emitted from a star observed on Earth
As a further example, we consider a hypothetical star located far away from the Solar System and nearly in the Earth orbital plane. We compute the incident direction of the light ray emitted by this star and observed on Earth. The reference frame used to project the incident direction is given by a comoving kinematically nonrotating tetrad. The only gravitational interaction considered here is the one of the Sun described by the metric (3.13). The incident direction of the light ray can be computed using Eq. (3.15c) and Eq. (3.25b) into Eq. (4.16), and the expression of the tetrad (4.26). The incident direction of the light ray with respect to the tetrad is denoted by $n^{(i)}$ and can be parametrized by two angles α and δ, usually called right ascension and declination

$$n^{(i)} = (\cos\alpha\cos\delta, \sin\alpha\cos\delta, \sin\delta) \; . \tag{4.27}$$

Figure 4.3 represents the 1PM and 2PM contributions to α and δ as well as the total deflection angle. As one can see from relation (3.25b) and Eq. (4.16), the 2PM correction to the angular measurement depends on two terms: a first term proportional to κ and a second one proportional to $(1+\gamma)^2$, both of them being formally of order 2PM. Nevertheless, it is known that the term proportional to $(1+\gamma)^2$ can be absorbed in the 1PM term by a change of variable and it is therefore usually called "enhanced post-post-Newtonian term" (for further details about this, see [Klioner & Zschocke 2010, Teyssandier 2012]). The enhanced post-post-Newtonian term has an important contribution of the order of few mas while the 2PM contribution proportional to κ has a contribution of 10 μas only even for signals grazing the Sun.

4.3.3 Angular distance between two stars as measured from Earth

For this application, we consider two hypothetical stars located far away from the Solar System nearly in the Earth orbital plane and we compute the angular separation between them as measured from Earth. This representation can be used as a very simplified model of the GAME space mission [Vecchiato *et al.* 2009, Gai *et al.* 2012]. The only gravitational interaction considered here is the one of the Sun described by the space-time metric (3.13). Relation (4.17), giving the angular separation between two incident light rays, can be simplified in the case of static and spherically geometry described by the space-time metric (3.1). It can then be written as

$$\sin^2\frac{\phi}{2} = \frac{1}{4}\left[\frac{(A(r_B) - B(r_B)\beta^2)\,|\hat{\boldsymbol{k}}' - \hat{\boldsymbol{k}}|^2}{B(r_B)(1+\beta^m\hat{k}_m)(1+\beta^l\hat{k}'_l)}\right]_B \; , \tag{4.28}$$

where $\left(\hat{k}_j\right)_B$ and $\left(\hat{k}'_j\right)_B$ are the components of the direction triple of the two incident light rays expressed in global coordinates that can be computed using Eq. (2.7) with Eq. (3.15c) , $A(r)$ and $B(r)$ are the functions parametrizing the metric (3.1) and

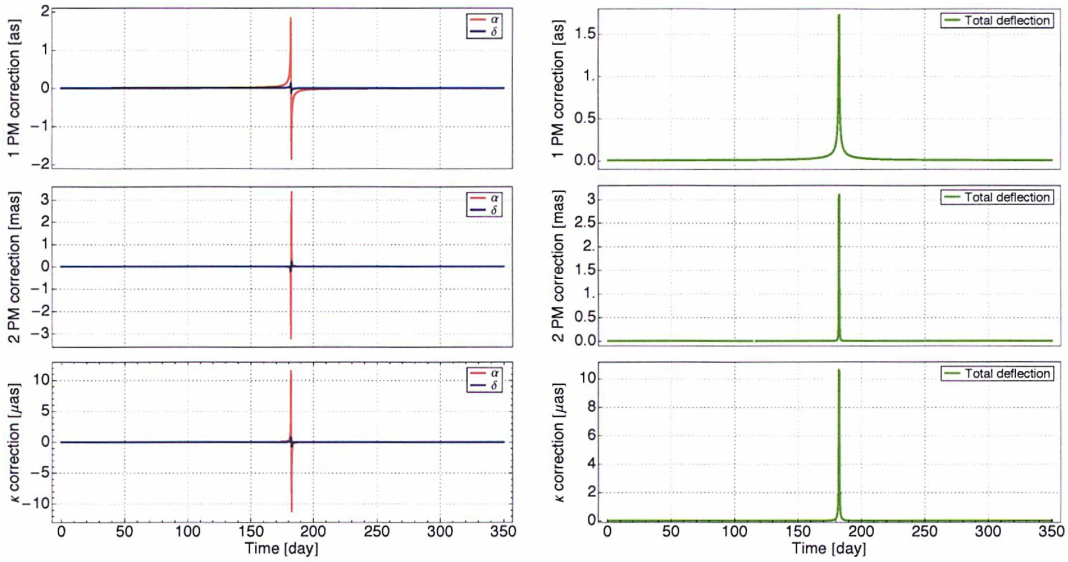

Figure 4.3: Contributions to the observed direction of an incident light ray coming from a star over one year of observations from the Earth. The central peak corresponds to the Earth, Sun, star conjunction. Left: contributions expressed for the right ascension and declination in the tetrad (see relation (4.27)) - Right: contribution to the total angular deflection. The 2PM contribution is the total formal 2PM contribution of around 3 *mas* (included the so-called "enhanced post-post Newtonian" terms). The κ contribution of around 10 μas is the due to the terms proportional to κ in (3.25b).

$\beta^i = v^i/c$ is the coordinate velocity of the observer. We apply the last expression in a Schwarzschild geometry. The functions $A(r)$ and $B(r)$ are then given by (3.13) and the $\hat{k}_i$ are determined by (2.36), once we consider Eq. (3.15c). Figure 4.4 represents the evolution of the angular separation (4.28) with respect to time and the contribution of the 1 and 2 PM corrections. As for the direction of the incident light ray (see previous section), the 2PM correction to the angular measurement depends on two terms: a first term proportional to κ and a second one proportional to $(1+\gamma)^2$. In this case too, the so called enhanced post-post-Newtonian term has an important contribution of the order of few mas for signals grazing the Sun, while the 2PM contribution proportional to κ has a contribution of 10 μas only.

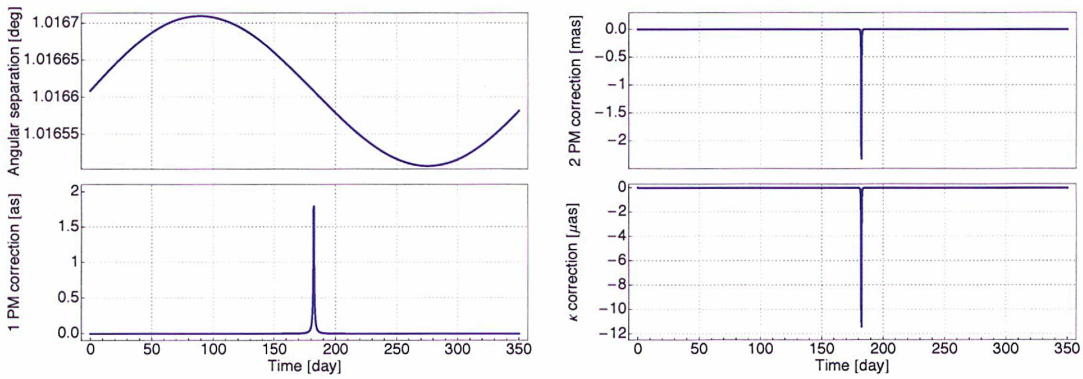

Figure 4.4: Contributions to the angular separation between two incident light rays coming from two stars as observed from Earth over one year. The central peak in the relativistic corrections correspond to the Earth, Sun, star conjunction. The 2PM contribution is the total formal second order contribution of around 10 *mas* (included the so-called "enhanced post-post Newtonian" terms). The κ contribution, not exceeding some μas for signals grazing the Sun, is proportional to the κ term in (3.25b).

4.4 Conclusions

In this chapter we provided general equations to define the Doppler observable used in radio-science and two kinds of astrometric observables using the results presented in chapters 2. The expressions we present make no expansions of any kind and can therefore be applied to any space-time metric. Moreover, we presented to methods to treat the case of a relativistic observation between a moving emitter and receiver. As an example, we also provided applications of these formulas to the simulation of high-precision observations of the kind of BepiColombo and GAME within the Schwarzschild field of the Sun up to the 2PM order. To provide a full description of the incoming direction of the light signal in the observer's reference frame, we also define a kinematically nonrotating tetrad valid at 2PM. These results have been presented at [Bertone *et al.* 2012a] and will be summarized in [Hees *et al.* 2013]. In the next chapters, we will focus our attention on the modeling of high-precision astrometric observations in the context of Gaia. The formulae presented in this chapter will be of capital importance in the development of the Gaia observable based on our model. This observable will be first compared to the approaches chosen for the data analysis of the Gaia mission (see chapter 5) and then implemented in the GSR software (see chapter 6).

CHAPTER 5

TTF model for relativistic astrometry in the context of Gaia

Contents

From now on, we focus our attention on relativistic astrometry and the Gaia mission. In section 5.1, we present the two approaches developed for the analysis of Gaia observations, namely the Gaia RElativity Model (GREM) and the Relativistic Astrometric MODel (RAMOD). In section 5.2, we present the set-up of our astrometric observable, defined in Eq. (4.15), in the Gaia context. Finally, in section 5.3 we present a procedure to compute the time transfer and the direction triples in GREM and RAMOD, in order to get a cross-check between the three model at the accuracy required for the Gaia mission.

5.1 The Gaia astrometric models

The data analysis of the Gaia mission (see section 1.1.1) is a complex task requiring a precise understanding of the observation process. For this reason, two independent relativistic models have been developed to analyze and interpret the observations.

The first model, GREM [Klioner 2003], has been formulated according to a PPN scheme accurate to the μas level. Basically, this approach solves the light trajectory using a matching technique that links the perturbed internal solution inside the near zone of the Solar System (where the observer is located) with the assumed asymptotically flat external one (where the source is located, at arbitrary distance). It allows to transform the observed light ray in a suitable coordinate direction and

to read off the aberration terms and light deflection effects, evaluated at the point of observation. This model is considered as baseline for the Gaia data reduction.

The second model, RAMOD [de Felice *et al.* 2004], is an astrometric model conceived to solve the inverse ray-tracing problem in a general relativistic framework not constrained by a priori approximations and according to the precepts of measurement in GR [de Felice & Bini 2010]. The full development to the μas level imposes to consider the retarded distance effects introduced by the motion of the Solar System bodies. The RAMOD full solution requires the integration of a set of differential equations, which allows the light trajectory to be traced back to the initial position of the star and which naturally entangles the contribution of the aberration and of the curvature from the background geometry. In this section, we shall detail the definition of the Gaia astrometric observable in these two models.

5.1.1 GREM

GREM is actually the most complete relativistic model of light propagation and the basis for the reduction of Gaia observations. The author sets several steps for the conversion of the observed quantities into the coordinate ones, from the observed direction of light to the spatial position of the source of emission in the BCRS [Klioner 2003]. These steps and the associated vectors are illustrated in Fig. 5.1 and described hereafter:

1. the aberration due to the motion of the observing satellite is subtracted from the observed direction $\boldsymbol{s}$ of the star which is converted into the barycentric direction $\boldsymbol{n}$ at observation coordinates;

2. the gravitational influence of Solar System bodies is taken into account. The deflecting bodies are considered to be in linear uniform motion during the propagation of the photon through the Solar System while the influence of the quadrupole moment of the giant planets is computed at the moment of the closest approach of the photon to the planet. Resulting from this, vector $\boldsymbol{n}$ is transformed in $\boldsymbol{\sigma}$, representing the direction of the light ray at past null infinity, $t \to -\infty$;

3. nevertheless, since the source is at finite distance from the observer, one should solve the boundary problem relating $\boldsymbol{\sigma}$ to the coordinate direction $\boldsymbol{k}$, going from the star to the observer;

4. the following step corrects the parallax effect due to the distance of the source. Vector $\boldsymbol{k}$ is then converted into the barycentric direction to the source $\boldsymbol{l}$;

5. the final step sets a model for the proper motion of the star and the variation of $\boldsymbol{l}$ during the several years of Gaia mission.

In the following, we shall detail step 1 to present how the Gaia observables is computed from the BCRS spatial coordinate direction of the light ray $\boldsymbol{n}$. We define

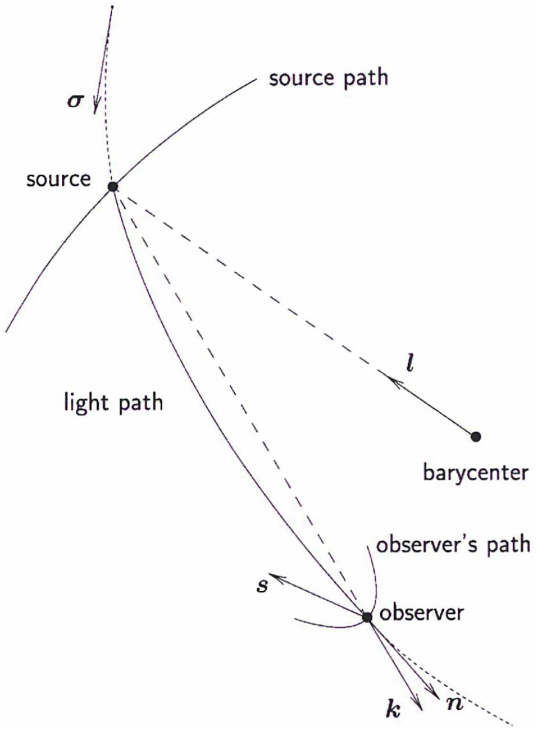

Figure 5.1: Five principal vectors used in the GREM model : $\boldsymbol{s}, \boldsymbol{n}, \boldsymbol{\sigma}, \boldsymbol{k}$ and $\boldsymbol{l}$. (from [Klioner 2003])

the unit "aberration free direction" $\boldsymbol{n} \equiv \boldsymbol{p}/|\boldsymbol{p}|$ and

$$p^i \equiv c^{-1}\dot{x}^i = \sigma + c^{-1}\Delta\dot{x}_P(t) \ , \tag{5.1}$$

with $\dot{x}^i = dx^i/dt$ the coordinate velocity of the photon and $\Delta\dot{x}_P(t)$ the deflection of the light ray from past null infinity. In section 5.3.1 we will present explicit relations between p^i and the direction triple $\hat{k}_i$ defined in our model.

The coordinate quantities $\boldsymbol{p}$ and $\boldsymbol{n}$ are obviously not directly observables; the observed vector towards the light source is the four-vector $s^\alpha = (1, s^i)$, defined with respect to the local inertial frame of the observer as

$$s^i = -\frac{d\mathcal{X}^i}{d\mathcal{X}^0} \ , \tag{5.2}$$

where $\mathcal{X}^\alpha$ are the coordinates in the Center-of-Mass Reference System (CoMRS [Klioner 2004]), comoving with the satellite. Then, to deduce $\boldsymbol{s}$ from the coordinate light direction $\boldsymbol{p}$ we need to compute the infinitesimal transformation Λ^α_β defined by the relation

$$d\mathcal{X}^\alpha = \Lambda^\alpha_\beta dx^\beta \ . \tag{5.3}$$

Combining Eqs.(5.2)-(5.3) it is then straightforward to write

$$s^i = -\frac{\Lambda_0^i + \Lambda_j^i p^j}{\Lambda_0^0 + \Lambda_j^0 p^j} \,. \tag{5.4}$$

Adopting the IAU resolution B1.3 [Soffel *et al.* 2003] for the BCRS and the CoMRS, it is then possible to explicit the transformation matrix Λ_β^α and to expand Eq. (5.4) to obtain the coordinate transformation between n^i and s^i with 1 μas accuracy as [Klioner 2003]

$$\begin{aligned} s^i &= -n^i + c^{-1}\Big[\boldsymbol{n}\times(\boldsymbol{v}_s\times\boldsymbol{n})\Big]^i \\ &\quad +c^{-2}\left\{(\boldsymbol{n}\cdot\boldsymbol{v}_s)\Big[\boldsymbol{n}\times(\boldsymbol{n}\times\boldsymbol{v}_s)\Big]^i + \frac{1}{2}\Big[\boldsymbol{v}_s\times(\boldsymbol{n}\times\boldsymbol{v}_s)\Big]^i\right\} \\ &\quad +c^{-3}\left\{\Big[(\boldsymbol{v}_s\cdot\boldsymbol{n})^2 + (1+\gamma)w(\boldsymbol{x})\Big]\Big[\boldsymbol{n}\times(\boldsymbol{v}_s\times\boldsymbol{n})\Big]^i\right. \\ &\quad \left.+\frac{1}{2}(\boldsymbol{v}_s\cdot\boldsymbol{n})\Big[\boldsymbol{v}_s\times(\boldsymbol{n}\times\boldsymbol{v}_s)\Big]^i\right\} + \mathcal{O}(c^{-4}) \,, \end{aligned} \tag{5.5}$$

containing the aberrational effects up to $1/c^{-3}$ and where $v_s^i = dx_s^i/dt$ is the coordinate velocity of the observing satellite, $w(\boldsymbol{x})$ is the PPN gravitational potential and γ is a PPN parameter.

5.1.2 RAMOD

The development of RAMOD is proceeding by evolution steps (see Fig. 5.2) since the project was launched in 1998 by a group of Italian astronomers from the Observatory of Turin and the University of Padua.

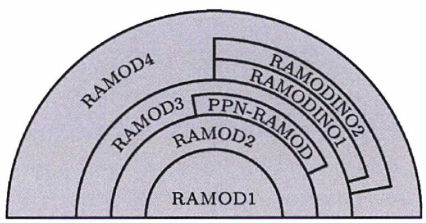

Figure 5.2: RAMOD identifies a family of astrometric models with increasing accuracies. The attitude models belonging to the project are called RAMODINO1 and RAMODINO2. The present relativistic model implemented in GSR (see chapter 6) is an adaptation of PPN-RAMOD to Gaia. (from [Bucciarelli *et al.* 2005])

The first version of the model, RAMOD1, represents a non-perturbative approach to the astrometric problem with the Sun as only field source [de Felice *et al.* 1998].

In a Schwarzschild's spacetime, the observer is placed on a circular orbit and the light sources are supposed to be at space infinity. Its first evolution, RAMOD2 [de Felice *et al.* 2001], takes into account the parallax and proper motion of stars, supposed at finite distance, by setting different boundary conditions to the model. The current evolution of the project is represented by RAMOD3 [de Felice *et al.* 2004], based on a perturbative approach of Minkowski space-time. Sources of the field are the planets and major bodies of the Solar System, with their position fixed at the closest approach with the photon. The influence of the quadrupole moment of the major planets would also be taken into account. The aim of the model would be the accuracy of the μas level on the star positioning, sufficient for the reduction of Gaia's data. The next step is RAMOD4, whose aim is to describe light propagation in a system with non-null vorticity [de Felice *et al.* 2006]. Several extensions have been explored by the authors. Among them we shall note PPN-RAMOD [Vecchiato *et al.* 2003], developed to test the parameters of the PPN solution of GR and currently used to describe light propagation within the GSR data reduction software (see chapter 6), and RAMODINO1 and RAMODINO2 [Bini *et al.* 2003] are the attitude models of the project.

Based on a fully dynamical post-Minkowskian background [Crosta 2011], RAMOD has been solved explicitly in the 1PM static approximation [Crosta 2013] needed for GSR. RAMOD always relies on measurable quantities with respect to a local barycentric observer along the light ray [de Felice *et al.* 2004]. The unknown is the local line-of-sight, quoted $\bar{\ell}^\alpha$ in RAMOD and measured by the fiducial observer u along the null-geodesic

$$\bar{\ell}^\alpha = -\frac{k^\alpha}{u_\beta k^\beta} - u^\alpha \,, \tag{5.6}$$

where k^μ represents the tangent vectors and u^α is the four-velocity of u (see Fig. 5.3). In this formalism, the null-geodesic equation transforms, according to the measurement protocol procedure [de Felice & Bini 2010], into a set of coupled nonlinear differential equations, called "master equations"

$$\frac{d\bar{\ell}^0}{d\zeta} - \bar{\ell}^i\bar{\ell}^j h_{0j,i} - \frac{1}{2}h_{00,0} = 0 \,, \tag{5.7a}$$

$$\begin{aligned}\frac{d\bar{\ell}^k}{d\zeta} &- \frac{1}{2}\bar{\ell}^k\bar{\ell}^i\left(\bar{\ell}^j h_{ij,0} - h_{00,i}\right) + \bar{\ell}^i\bar{\ell}^j\left(h_{kj,i} - \frac{1}{2}h_{ij,k}\right) \\ &+\bar{\ell}^i\left(h_{k0,i} + h_{ki,0} - h_{0i,k}\right) - \frac{1}{2}h_{00,k} - \bar{\ell}^k\bar{\ell}^i h_{0i,0} + h_{k0,0} = 0 \,,\end{aligned} \tag{5.7b}$$

where ζ is a parameter along the null-geodesic.

Once solved for $\bar{\ell}^\alpha$, the astrometric observable (*i.e.* the direction of the light ray in the reference frame of the observer) is defined by its projection on a tetrad comoving with the observer [Bini *et al.* 2003] as

$$n_{(i)} = \frac{(\bar{\ell}_{(B)\beta} - \nu_\beta)E^\beta_{\hat{a}}}{\gamma(1 - \nu_\alpha\bar{\ell}^\alpha_{(B)})} \,, \tag{5.8}$$

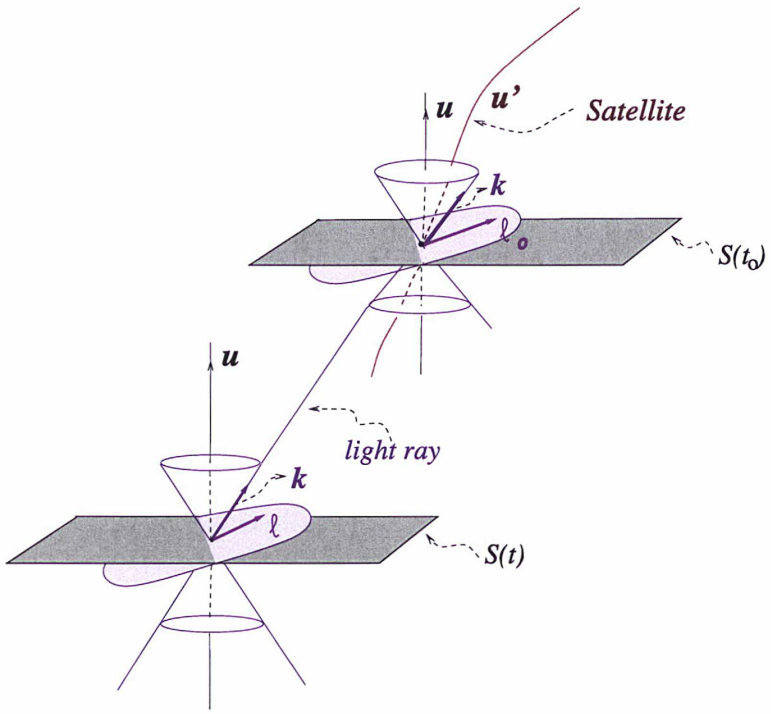

Figure 5.3: The light trajectory, identified by the 4-vector k, propagates in space-time until it is intercepted by the Gaia-like satellite at observation time $t_0 \equiv t_B$. At each point on the trajectory, the light signal strikes the locally barycentric observer u which identifies, in its instantaneous rest space (light gray), the local line of sight ℓ. The surfaces $S(t)$ such that $t = const$ do not in general coincide with the local rest space of u. [de Felice *et al.* 2006]

where ν_α is the four-velocity of the satellite u_s relatively to the local barycentric observer u, $\gamma = -u_s^\alpha u_\alpha$, $E_{\hat{a}}^\beta$ is the tetrad comoving with the observer (*i.e.* the satellite) with the index $\hat{a}$ representing each axis of the tetrad and $\overline{\ell}_{(B)}$ represents the local line-of-sight of the photon as seen by u at the moment of observation.

The satellite reference frame defining the transformation $E_{\hat{a}}^\beta$ is obtained by successive transformations of the local BCRS tetrad [Bini *et al.* 2003]

$$\lambda_{\hat{a}}^\alpha = h_{0\alpha}\delta_0^\alpha + \left(1 - \frac{h_{00}}{2}\right)\delta_a^\alpha + \mathcal{O}(h^2)\,. \tag{5.9}$$

In particular, the vectors of the triad $\boldsymbol{\lambda}_{\hat{a}}$ (defined as the spatial part of $\lambda_{\hat{a}}^\alpha$) are boosted to the satellite rest-frame by means of an instantaneous Lorentz transformation identified by the four-velocity of the observer u_s with respect to the local BCRS. The boosted tetrad $\boldsymbol{\lambda}_{\hat{a}}^{bs}$ obtained in this way represents a CoMRS , similar to the one defined in section 5.1.1. In addition, one of the axes of the system is Sun-locked, i.e. one axis points toward the Sun at any point of its Lissajous orbit around L2. The Gaia attitude frame is finally obtained by applying the following

rotations to the Sun-locked frame [Crosta & Vecchiato 2010]

1. by an angle $\omega_p t$ about the four-vector $\lambda^{\alpha}_{bs(\hat{1})}$ which constantly points towards the Sun (where ω_p is the angular velocity of precession of Gaia);
2. by a fixed angle θ about the image of the four-vector $\lambda^{\alpha}_{bs(\hat{2})}$ after the previous rotation (where θ represents the Sun aspect angle of 45^o - see Fig. 1.1);
3. by an angle $\omega_r t$ about the image of the four-vector $\lambda^{\alpha}_{bs(\hat{1})}$ after the previous two rotations (where ω_r is the spin angular velocity).

The triad resulting from these transformations, detailed in [Crosta & Vecchiato 2010], establishes Gaia attitude triad given by

$$\boldsymbol{E}_{\hat{a}} = \mathcal{R}_1(\omega_r t)\mathcal{R}_2(\theta)\mathcal{R}_1(\omega_p t)\boldsymbol{\lambda}^{bs}_{\hat{a}} \tag{5.10}$$

The transformations between the barycentric coordinate time and the observer's proper time complete the process.

It has been showed in [Crosta & Vecchiato 2010] that the PN expansion of Eq. (5.10) up to the order needed at Gaia accuracy yields the equivalence with the observable defined in Eq. (5.5) for GREM.

5.2 TTF observable for Gaia

In chapter 4 we presented a general formula to compute the astrometric observable, *i.e.* the incoming direction of the light ray in the reference system comoving with the observer, using the knowledge of the direction triple $\hat{k}_i$ at observation coordinates in combination with a generic tetrad $\lambda^{j}_{(i)}$ comoving with the observer. We used our formulation in the Schwarzschild field of the Sun with a generic kinematically non-rotating tetrad comoving with the Earth in order to compute the gravitational and aberration corrections for a series of observations. We now intend to apply the same formula (4.15) to model Gaia observations. For this, we need a tetrad adapted to model the motion of Gaia. Due to the generality of our model, both transformation matrix $E^{\beta}_{\hat{a}}$ (defined at Eq. (5.10)) and Λ^{β}_{α} (defined at Eq. (5.3)) can be used at this scope, depending on the convenience.

The interest of such observable would be double. First, it would represent an additional tool to check the models currently adopted for Gaia; second, this observable would be based on the well-developed TTF formalism allowing for its further development beyond Gaia accuracy using the results presented in chapters 2 and 3.

5.3 Analytical comparison of the three models

The comparison of GREM and RAMOD is considered as a priority for the Gaia mission [Crosta & Vecchiato 2010, Crosta 2011] since they will both concur to create a

catalog of one billion positions, parallaxes and proper motions based on measurements of absolute astrometry. Any inconsistency in the relativistic models would then invalidate the quality and reliability of the estimates, hence all related scientific output.

Despite their differences, both models aim for the reconstruction of light trajectory from the star to the observer in order to build the astrometric observable. This makes our TTF model a completely new and independent approach to the problem, particularly adapted to further cross-check the current relativistic solutions for astrometry.

In this section, we present a procedure to cross-check the relativistic description of light propagation in GREM, RAMOD and our TTF model on the basis of their solutions for the time of flight $\mathcal{T}$ and direction triple $\hat{k}_i$ of a light ray propagating between two points at finite distance.

5.3.1 GREM to compute $\mathcal{T}$ and $\hat{k}_i$

In section 5.1.1 we presented GREM observable (5.5). In this section we will explore the relation between p^i (5.1), and hence the photon velocity $\dot{x}^i$, and the quantities defined in our TTF model. GREM itself is based on KK92 [Klioner & Kopeikin 1992], a seminal study describing light propagation in the field of multiple axisymmetric and rotating bodies in translational motion. We will use KK92 to validate our model of light propagation in the field of moving spherical bodies. The results of this section can then easily be reduced to GREM by posing the coordinate velocity of the perturbing bodies $\boldsymbol{v}_P = 0$.

Considering only the terms relevant for our purpose and using our notation, the trajectory of the photon in KK92 can be written as

$$x^i(t) = x^i(t_B) + c\sigma^i(t - t_B) + \Delta x^i(t, x^i, t_B, x^i_B) \,, \tag{5.11}$$

where $(t_B, x^i(t_B))$ are the reception coordinates, $\boldsymbol{\sigma}$ is a normalized vector giving the unperturbed direction of light at past null infinity and the gravitational perturbation is given by

$$\begin{aligned} \Delta x^i \;=\; -\frac{2G}{c^2}\sum_P \mathcal{M}_P \Bigg\{ g_P^i \ln\left[\frac{\boldsymbol{g}_P\cdot\boldsymbol{R}_P(t) + g_P R_P(t)}{\boldsymbol{g}_P\cdot\boldsymbol{R}_{PB} + g_P R_{PB}}\right] + \frac{(\boldsymbol{\sigma}\times\boldsymbol{R}_P(t)\times\boldsymbol{g}_P)^i}{g_P R_P(t) - \boldsymbol{g}_P\cdot\boldsymbol{R}_P(t)} \\ - \frac{(\boldsymbol{\sigma}\times\boldsymbol{R}_{PB}\times\boldsymbol{g}_P)^i}{g_P R_{PB} - \boldsymbol{g}_P\cdot\boldsymbol{R}_{PB}} \Bigg\} \,, \end{aligned} \tag{5.12}$$

where we use the definitions in Eq. (3.49)-(3.50).

The TTF formalism being designed for light propagation between two points located at finite distance, one first has to set the boundary condition

$$\boldsymbol{x}(\boldsymbol{x}_B, \boldsymbol{\sigma}, \Delta t) = \boldsymbol{x}_A \tag{5.13}$$

in Eq. (5.11) to provide the "crossing trajectory equation"

$$x^i(t_A) = x^i(t_B) - c\,\Delta t\,\sigma^i + \Delta x^i(\Delta t, x^i_B, \sigma^i)\ , \tag{5.14}$$

where $\Delta t \equiv t_B - t_A$ represents the lapse of coordinate time between the emission and reception of the signal. In the following, Eqs. (5.11)-(5.14) will be used to find the equivalence between KK92 and TTF for the coordinate time of flight and the tangent vectors.

Coordinate time of flight

Let us state the formal development

$$\Delta t = \sum_i \Delta t_{(i)}\ , \tag{5.15}$$

where $\Delta t_{(n)}$ is of order $\mathcal{O}(c^{-n})$. Substituting for Δt from Eq. (5.15) into Eq. (5.14) and identifying terms of the same order, we get

$$\begin{aligned}
\Delta t_{(1)} &= \frac{R_{AB}}{c}\ , && \text{(5.16a)}\\
\Delta t_{(2)} &= \boldsymbol{N}_{AB}\cdot\boldsymbol{\Delta x}(\Delta t, x^i_B, \sigma^i) && \text{(5.16b)}\\
&= -\frac{2G}{c^2}\sum_P \mathcal{M}_P\,(\boldsymbol{g}_P\cdot\boldsymbol{N}_{AB})\ln\left[\frac{\boldsymbol{g}_P\cdot\boldsymbol{R}_{PA}+g_PR_{PA}}{\boldsymbol{g}_P\cdot\boldsymbol{R}_{PB}+g_PR_{PB}}\right]\ ,
\end{aligned}$$

where we used the property $\boldsymbol{\sigma}\cdot\boldsymbol{\sigma}=1$ and noted that $\boldsymbol{N}_{AB}\cdot(\boldsymbol{N}_{AB}\times\boldsymbol{R}_X\times\boldsymbol{g}_P)=0$. Using Eq. (3.54) shows that Eq. (5.16) is strictly equivalent to Eq. (2.13) when the gravitational delay is given by Eq. (3.51) with $\gamma=1$.

Light direction triple

The relation between the tangent vectors to the null-geodesic $k^\mu = \dfrac{dx^\mu}{d\lambda}$ and the photon velocity $\dot{x}^i$ used in KK92 is obtained by noting that $\dfrac{\dot{x}^i}{c} = \dfrac{dx^i/d\lambda}{dx^0/d\lambda} = \dfrac{k^i}{k^0}$. It follows that

$$\begin{aligned}
\hat{k}_i &= \frac{k_i}{k_0} = \frac{g_{ij}k^j + g_{0i}k^0}{g_{00}k^0 + g_{0i}k^i} = \left(g_{0i}+g_{ij}\hat{k}^j\right)\left(g_{00}+g_{0i}\hat{k}^i\right)^{-1}\\
&= -\frac{\dot{x}^i}{c} - 2h_{00}\sigma^i - (\delta_{ij}+\sigma^i\sigma^j)h_{0j} + \mathcal{O}(c^{-4})\ . && \text{(5.17)}
\end{aligned}$$

The computation of $\frac{\dot{x}^i}{c}$ is obtained by deriving the photon trajectory in Eq. (5.11) with respect to coordinate time. Its application at $(t_B, \boldsymbol{x}_B)$ gives

$$\frac{\dot{x}^i_B}{c} = \sigma^i + \frac{\Delta\dot{x}^i_B}{c} , \tag{5.18}$$

where $\Delta\dot{x}^i$ represents the gravitational perturbation to the photon direction

$$\frac{\Delta\dot{x}^i_B}{c} = -\frac{2G}{c^2}\sum_P \mathcal{M}_P \frac{g_P}{R_{PB}}\left\{g^i_P + \frac{(\boldsymbol{N}_{AB}\times\boldsymbol{R_{PA}}\times\boldsymbol{g}_P)^i}{g_P R_{PB} - \boldsymbol{g}_P\cdot\boldsymbol{R_{PB}}}\right\} . \tag{5.19}$$

Let us state the formal development

$$\boldsymbol{\sigma} = \sum_i \boldsymbol{\sigma}_{(i)} , \tag{5.20}$$

where $\boldsymbol{\sigma}_{(i)}$ is of order $\mathcal{O}(c^{-n})$. Substituting for $\boldsymbol{\sigma}$ from Eq. (5.20) into Eq. (5.14) and identifying all terms of the same order, we get

$$\sigma^i_{(1)} = \frac{x^i_B - x^i_A}{R_{AB}} = N^i_{AB} , \tag{5.21a}$$

$$\sigma^i_{(2)} = -\frac{1}{R_{AB}}\left[\delta_{ij} - N^i_{AB}N^j_{AB}\right]\Delta x^j(\Delta t, x^j_B, \sigma^j) , \tag{5.21b}$$

where we used the property $\sigma^i\sigma^i = 1$. Using Eq. (3.54) and after some algebra, we get the following relation

$$\frac{(\boldsymbol{\sigma}\times\boldsymbol{R}_{PA}\times\boldsymbol{g}_P)^i}{g_P R_{PA} - (\boldsymbol{g}_P\cdot\boldsymbol{R}_{PA})} - \frac{(\boldsymbol{\sigma}\times\boldsymbol{R}_{PB}\times\boldsymbol{g}_P)^i}{g_P R_{PB} - (\boldsymbol{g}_P\cdot\boldsymbol{R}_{PB})} = \frac{g_P(\boldsymbol{\sigma}\times\boldsymbol{R}_{PB}\times\boldsymbol{g}_P)^i}{R^2_{PA}R^2_{PB} - (\boldsymbol{R}_{PA}\cdot\boldsymbol{R}_{PB})^2}\left[R_{PA} - R_{PB} - g_P R_{AB}\right] . \tag{5.22}$$

Substituting for Δx^i from Eq. (5.12) into Eq. (5.21) and using the relation given in Eq. (5.22), we obtain

$$\sigma^i = N^i_{AB} - \frac{2G}{c^2}\sum_P \frac{\mathcal{M}_P}{R_{AB}}\left[\frac{(\boldsymbol{N}_{AB}\times\boldsymbol{R}_{PB}\times\boldsymbol{g}_P)^i}{g^2_P R^2_{PB} - (\boldsymbol{g_P}\cdot\boldsymbol{R}_{PB})^2}\left(g_P R_{PA} - g_P R_{PB} - g^2_P R_{AB}\right)\right.$$
$$\left. + (g^i_P - N_{AB}{}^i N_{AB}{}^j g^j_P)\ln\left(\frac{g_P R_{PB} - \boldsymbol{g}_P\cdot\boldsymbol{R}_{PB}}{g_P R_{PA} - \boldsymbol{g}_P\cdot\boldsymbol{R}_{PA}}\right)\right] + \mathcal{O}(c^{-4}) . \tag{5.23}$$

It is then straightforward to check that Eq. (3.57) is equivalent to Eq. (5.17) when using Eq. (5.18), Eq. (5.19), Eq. (5.23), the metric tensor (3.26) and the potentials in Eq. (3.38) at reception event.

5.3.2 RAMOD to compute $\mathcal{T}$ and $\hat{k}_i$

Comparisons between RAMOD and other PM/PN light propagation models can be found in [Crosta 2011], where the author shows how RAMOD master equations recover the analytical linearized case used in [Kopeikin & Schäfer 1999] once converted in a coordinate form, while in [Crosta & Vecchiato 2010] the authors present a study of the aberration in RAMOD and GREM. An analytical cross-check of the coordinate time of flight and direction triple has not been done yet with the TTF. We perform it in the static case, *i.e.* in the case of a fully analytical solution of RAMOD3 [Crosta 2013, Bini *et al.* 2013], where space-time is described by the gravitational perturbation

$$h_{00} = \frac{2G}{c^2}\sum_P \frac{\mathcal{M}_P}{r_P(\zeta)} \quad , \quad h_{0i} = 0 \quad , \quad h_{ij} = \delta_{ij}\,\gamma\, h_{00} \tag{5.24}$$

and where $\boldsymbol{r}_P(\zeta) = \boldsymbol{x}(\zeta) - \boldsymbol{x}_P(t_C)$ is the distance between the positions of the photon $\boldsymbol{x}(\zeta) = \boldsymbol{x}_B - \zeta \boldsymbol{R_{AB}}$ and of the deflecting body $\boldsymbol{x}_P(t_C)$ while γ is a PPN parameter.

Coordinate time of flight

The computation of the coordinate time of flight Δt can be obtained within RAMOD by considering the time component of the fiducial observer u [de Felice *et al.* 2006]

$$u^0 \equiv \frac{cdt}{d\zeta} = 1 + \frac{h_{00}}{2} + O(c^{-4})\,. \tag{5.25}$$

Inserting Eq. (5.24) into Eq. (5.25) and integrating between the emission ζ_A and the reception ζ_B, we get

$$\begin{aligned} c\Delta t &= \int_{\zeta_A}^{\zeta_B} \left(1 + \frac{G}{c^2}\sum_P \mathcal{M}_P \frac{1}{r_P(\zeta)}\right) d\zeta + \mathcal{O}(c^{-4}) \\ &= \Delta\zeta + \frac{G}{c^2}\sum_P \mathcal{M}_P \ln \frac{R_{PB} + \boldsymbol{N_{AB}}\cdot\boldsymbol{R_{PB}}}{R_{PA} + \boldsymbol{N_{AB}}\cdot\boldsymbol{R_{PA}}} + \mathcal{O}(c^{-4})\,, \end{aligned} \tag{5.26}$$

where $\Delta\zeta \equiv \zeta_B - \zeta_A$ and we used definitions (3.49)-(3.50) with $\boldsymbol{\beta_P} = 0$. We need now an explicit expression for $\Delta\zeta$. First, we rewrite Eq. (18) of [Crosta 2013] following our notation as

$$\begin{aligned} \bar{\ell}_B^k &= \frac{x_B^k - x_A^k}{\Delta\zeta} + \frac{2G}{c^2}\sum_P \mathcal{M}_P \left\{ \frac{{N_{AB}}^k}{2}\left[\frac{1}{\Delta\zeta}\ln\left[\frac{\boldsymbol{N_{AB}}\cdot\boldsymbol{R_{PB}} + R_{PB}}{\boldsymbol{N_{AB}}\cdot\boldsymbol{R_{PA}} + R_{PA}}\right] - \frac{1}{R_{PB}}\right]\right. \\ &\left. + \frac{d_B^k}{d_B^2}\left[-\frac{\boldsymbol{N_{AB}}\cdot\boldsymbol{R_{PB}}}{R_{PB}} + \frac{R_{PB} - R_{PA}}{\Delta\zeta}\right]\right\} + O\left(c^{-4}\right)\,, \end{aligned} \tag{5.27}$$

with $\boldsymbol{d}_B = \boldsymbol{R_{PB}} - \boldsymbol{N}_{AB}(\boldsymbol{R_{PB}} \cdot \boldsymbol{N}_{AB})$. Then, using the relation $\boldsymbol{d}_B \cdot \boldsymbol{N}_{AB} = 0$ and the normalisation condition $\bar{\ell}^\alpha \bar{\ell}_\alpha = g_{\alpha\beta}\bar{\ell}^\alpha\bar{\ell}^\beta = 1$ on Eq. (5.27), we obtain

$$\begin{aligned} \bar{\ell}^k_B \bar{\ell}^k_B &= 1 - h_{00}|_B + \mathcal{O}(c^{-4}) = \frac{{R_{AB}}^2}{\Delta\zeta^2} + \frac{2G}{c^2}\sum_P \mathcal{M}_P \\ &\times\left\{\frac{R_{AB}}{\Delta\zeta^2}\ln\left[\frac{(\boldsymbol{N}_{AB}\cdot\boldsymbol{R_{PB}}) + R_{PB}}{(\boldsymbol{N}_{AB}\cdot\boldsymbol{R_{PA}}) + R_{PA}}\right] - \frac{R_{AB}}{R_{PB}\Delta\zeta}\right\} + \mathcal{O}\left(c^{-4}\right) . \end{aligned} \tag{5.28}$$

Following Eq. (5.26), we assume that $\Delta\zeta$ admits a PN expansion

$$\Delta\zeta = R_{AB} + \Delta\zeta_{(2)} + \mathcal{O}(c^{-3}) , \tag{5.29}$$

where $\Delta\zeta_{(2)}$ is of order $\mathcal{O}(c^{-2})$. Substituting for $\Delta\zeta$ from Eq. (5.29) into Eq. (5.28) and identifying the terms of the same order, we get straightforwardly

$$\Delta\zeta_{(2)} = \frac{G}{c^2}\sum_P \mathcal{M}_P \ln\left[\frac{R_{PB} + \boldsymbol{N}_{AB}\cdot\boldsymbol{R_{PB}}}{R_{PA} + \boldsymbol{N}_{AB}\cdot\boldsymbol{R_{PA}}}\right] . \tag{5.30}$$

Finally, substituting for $\Delta\zeta$ from Eq. (5.29) and Eq. (5.30) into Eq. (5.26) we retrieve the Shapiro term of Eq. (3.51) with $\boldsymbol{\beta_P} = 0$.

Light direction triple

The relation between the tangent vectors $\hat{k}_i$ of the TTF formalism and the local line-of-sight $\bar{\ell}^i$ is obtained by expanding Eq. (5.6) with the metric (5.24) and Eq. (5.25), so that

$$\begin{aligned} \bar{\ell}^i = -\frac{k^i}{u^0 k_0} &= -\hat{k}_i\left[1 - \frac{3}{2}h_{00}\right] + \mathcal{O}(c^{-3}) \\ &= -\hat{k}_i\left[1 - \frac{3G}{c^2}\sum_P \frac{\mathcal{M}_P}{r_P(\zeta)}\right] + \mathcal{O}(c^{-3}) . \end{aligned} \tag{5.31}$$

Substituting for $\bar{\ell}^i$ from Eq. (5.27) into Eq. (5.31) and using Eq. (5.29)-(5.30), the reader can easily retrieve Eq. (3.57) with $\boldsymbol{\beta_P} = 0$.

5.4 Conclusions

In this chapter we presented the relativistic models developed for the analysis of Gaia observations, namely GREM and RAMOD. We also described the procedure to follow to apply the astrometric observable defined in Eq. (4.15) to the specific case of the Gaia mission. We conclude that both Gaia tetrads used in the GREM and RAMOD approaches would be suitable for our model. Then, we studied the relations between the solution proposed by the three models for the coordinate direction

of the observed light ray. In particular, we provide a procedure to relate them by computing the time of flight $\mathcal{T}$ and the direction triple $\hat{k}_i$ in GREM and RAMOD and then comparing the results to Eq. (2.13) and Eq. (2.36). The outcome of this comparison shows that the three models are equivalent at the accuracy required for Gaia. These results are summarized in [Bertone *et al.* 2013a] and have been presented at [Bertone *et al.* 2013b]. This study, developed during the time spent with the group of "fundamental astronomy" of the Astrophysical Observatory of Torino, also allowed me to interact in the final phase of the development of RAMOD3, preparing for its implementation to the reduction of Gaia observations and opening the road to possible future collaborations.

CHAPTER 6

Implementation for the reduction of astrometric observations

Contents

We illustrated in chapter 5 the equivalence of our astrometric observable with GREM and RAMOD approaches at the accuracy required by the Gaia mission. In section 6.1, we present the infrastructure in place for the data treatment of the Gaia mission, focusing on the astrometric solution which shall provide a new, more accurate stellar catalog at the end of the 5 years nominal mission. Two main pipelines have been developed for this scope: the Astrometric Global Iterative Solution (AGIS) and its verification counterpart Global Sphere Reconstruction (GSR). In section 6.2 we present our contribution on the GSR software developed at the Astrophysical Observatory of Torino. Using the tools provided by the Gaia Data Processing and Analysis Consortium (DPAC), we implemented our model for the Gaia observable in the GSR software and compared our results with those of GREM and RAMOD. Finally, we use our model to write the linearized observation equations to be solved in the astrometric solution and give some preliminary results of its application to a series of simulated observations.

6.1 Reduction pipelines of GAIA's observations

The Gaia space mission presented in section 1.1.1 will perform absolute astrometry, aiming at the definition of a global astrometric reference frame at visual wavelengths. In a certain sense, this is more like the definition of a unit of measure rather than a pure measurement of a certain quantity. It is for this reason that, within this procedure, it will be very difficult to identify possible errors in the measurements or

in the data reduction process leading to the definition of the final catalog. Moreover, because of its size and complexity, it will be nowadays nearly impossible to produce a verification catalog at comparable accuracies by means of ground-based measurements.

Gaia inherits many ideas from its "parent" mission HIPPARCOS whose goal was also to produce a catalogue of absolute positions. Therefore, HIPPARCOS has faced the same kind of problems as above, but at a much smaller scale because of its lower precision and the much smaller size of its catalog. The data reduction process in HIPPARCOS was carried out by two consortia, FAST and NDAC, which operated independently on the same data. Their two results were then compared and appropriately merged in order to obtain the final catalogue. This ideal solution cannot be applied to the case of Gaia. Due to the size of the problem and to the connection between the different kind of data (astrometric, photometric, spectroscopic), the data reduction task is much demanding both in terms of resources and manpower. To retain as much as possible the HIPPARCOS approach, without requiring excessive resources, the Gaia Data Processing and Analysis Consortium (DPAC) [Mignard *et al.* 2008] decided to replicate some of the most delicate tasks in the so-called Astrometric Verification Unit (AVU) [Abbas *et al.* 2011].

One of these concerns the core task of the Gaia mission, *i.e.* the solution of the Global Astrometric Sphere, providing the materialization of the astrometric reference frame for the Gaia catalog which will constitute the main outcome of the mission. For this task the main solution process, the Astrometric Global Iterative Solution (AGIS), and its verification counterpart Global Sphere Reconstruction (GSR) will run in parallel on the main Gaia data reduction pipeline. While AGIS puts its efforts in maximizing the number of objects of the reduced sphere, GSR focuses on a fully iterative implementation of the astrometric sphere solution with well-defined stopping conditions and based on an independent astrometric model [Vecchiato *et al.* 2012].

6.1.1 AGIS

The sphere reconstruction consists in the least-squares solution of a large system of linearized equations where each equation corresponds to an observation. One member contains the measurement, the known term, while the other is function of the unknowns to be estimated. These include the astrometric parameters (at least for the subset of stars representing the reference frame), the satellite attitude (in order to have the accurate celestial pointing of the instruments at each epoch) and the geometric instrument calibration (necessary to convert the pixel measurements on the CDD into angular directions). In addition, one can solve some global parameters, such as the PPN γ which appears in each equation of the system [Lindegren *et al.* 2012].

The main pipeline process for the reconstruction of the global sphere is called AGIS (Astrometric Global Iterative Solution) and takes its name after the iterative

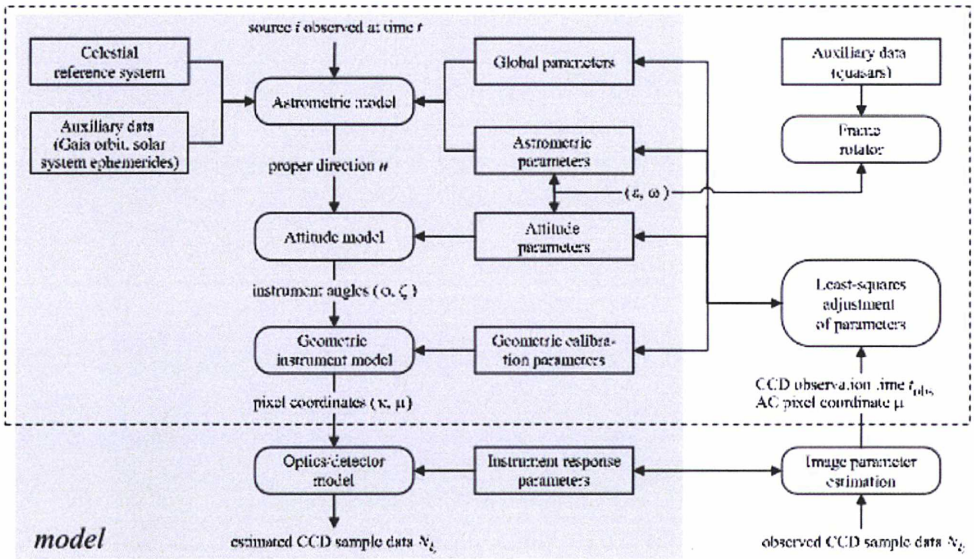

Figure 6.1: Schematic representation of the main elements of the astrometric data analysis. In the shaded area is the mathematical model that allows to calculate the position of the stellar image for any given set of model parameters. To the right are the processes that fit this model to the observed CCD data by adjusting the parameters in the rectangular boxes along the middle. [Lindegren *et al.* 2012]

method used to solve the system of equations. It consists in treating each type of parameter (astrometric, attitude, calibration and global) separately : when one of them is solved, the others are fixed at their previous estimation to compute the known terms ; then the following parameter is solved using the new estimations and the process is iterated until convergence is reached. This approach makes the code easy to parallelize, which is helpful and maybe necessary to solve a system of equations of such a size. As prescribed by the Gaia DPAC, AGIS is entirely written in the object-oriented Java programming language [O'Mullane *et al.* 2011]. Each of these parameters relies on a specific mathematical formulation, as we present in the following.

- Reference system - both light propagation and the orbit of Gaia, as well as the motion of stars, Solar System and extragalactic bodies are entirely modeled in the Barycentric Celestial Reference System (BCRS) whose spatial axes are aligned with the International Celestial Reference Frame (ICRF [Feissel & Mignard 1998]) and whose associated time coordinate is the barycentric coordinate time (TCB). To describe the attitude of Gaia and the direction of light as observed by Gaia, one also defines the Centre-of-Mass Reference System (CoMRS). This is a celestial reference system comoving with the satellite, originated at its center of mass, kinematically nonrotating and with the proper time of Gaia (G.T.) as coordinate time [Klioner 2004];

- Astrometric model - is the procedure for calculating the proper direction to a source at any time in terms of its astrometric parameters. It involves taking into account the proper motion of the source, gravitational light deflection by Solar System bodies and Lorentz transformations to the co-moving frame of the observer. This whole procedure is based on GREM (outlined in Section 5.1.1 and detailed in [Klioner 2003]);

- Attitude model - provides the instantaneous orientation of the Gaia instrument in the BCRS as specified by the Nominal Scanning Law (NSL [de Bruijne *et al.* 2010]) in terms of a finite number of attitude parameters;

- Geometric instrument model - defines the relation between the layout of the CCDs and the field angles. It depends on the physical geometry of each CCD, its position and alignment in the focal place and on the conventions adopted for the optical system. It should include the chosen "Time, Delay and Integrate" (TDI) scanning mode and the selection rules on the basis of star brightness [Lindegren *et al.* 2012].

The input of AGIS shall be a set of pre-processed data from the GAIA telemetry including up to 10^8 stars. To verify its results, a counterpart to AGIS has been set in the AVU subsystem : it is the Global Sphere Reconstruction (GSR).

6.1.2 GSR

The basic requirement of a fully iterative solution for the Global Sphere Reconstruction (GSR) [Vecchiato *et al.* 2012] was adopted to have a rigorously defined set of stopping conditions for the solution algorithm, as well as the opportunity to compute the full variance-covariance matrix of the system of equations. Such an approach was potentially more demanding from the computational point of view and could not be adapted to the simple structure of an embarrassingly parallel algorithm. For these reasons, GSR was originally designed to operate on a selection of 10^7 stars chosen from the AGIS dataset. However, recent developments in the algorithm implementation and in the available hardware [Bandieramonte *et al.* 2012] made it possible to overcome this limitation so that, in its present form, GSR is able to reduce the same number of objects than AGIS.

In order to keep the two reductions as independent as possible, GSR implements its own astrometric model, based on the definition of an abscissa-based observable including the relativistic modeling of both light propagation and the satellite attitude. The first one is taken from the RAMOD project described in section 5.1.2. The actual version, GSR1+, implements an extended version of PPN-RAMOD [Vecchiato *et al.* 2003] based on the Schwarzschild metric to describe light propagation. As a consequence, all observations too close to the Earth or the giant planets have to be rejected to respect the accuracy required by GAIA. The next

version of the software, in preparation, will implement the fully accurate RAMOD3 model, overcoming the limitations of GSR1. On the other hand, the attitude of the satellite is realized by the reference system co-moving with Gaia described in [Crosta & Vecchiato 2010] and adapted to the PPN-Schwarzschild metric. Instead of a block-iterative procedure, GSR uses a new parallelized version of the least squares (LSQR) algorithm designed by [Paige & Saunders 1982]. Based on a conjugate-gradient for solving sparse systems of linear equations, it allows GSR to solve all the unknowns in a single iteration. The general algorithm of GSR data reduction is illustrated in Fig. 6.2.

The results of the two pipelines shall be compared using a series of tests (mainly based on the Spherical Harmonics decomposition in its Scalar and Vectorial forms and the Infinite Overlapping Circle - IOC - test) each sensitive to a particular kind of problem. If everything behaves as expected, all tests will give the same result, while in case of problems they will allow the user to identify and isolate those coming from one or more sets of observations.

In the following, we present the development of a version of GSR modified to implement the TTF for the definition of the astrometric observable, thus allowing for a more accurate description of light propagation within the Solar System.

6.2 GSR-TTF

The final step of this work is to simulate an astrometric observation made by Gaia using the director cosines we defined in chapter 4 within the TTF formalism. To do it, we implement our model in the GSR software developed at Turin Observatory and we use it to generate a series of simulated observations. A brief overview of our activity on the GSR code is given in Fig. 6.2. We mainly focused on the computation of the Gaia observable and on writing the linearized observation equations necessary to evaluate the astrometric coordinates of the observed star from a series of observations. The result is a "GSR-TTF" code, still in a preliminary phase but already well integrated, adapted to give indications for the further development of the GSR code and useful to investigate the results of AGIS and GSR.

Before presenting the details of the implementation of our model in GSR, a brief overview of the astrometric problem for Gaia and how it is treated in the software is necessary. The input of the code are *packets*, each containing a single observation characterized by : the coordinate time of observation (necessary to get Gaia state vector and the planetary ephemerides), the catalog coordinates of the observed source and all quantities used in the solution of the astrometric problem, which we are going to detail in the following. The values contained in the packet are then updated by the processing of the observation.

As shown in Fig. 6.3, each point of the celestial sphere can be fixed in the reference system of the Gaia spacecraft by three direction cosines $n_{(i)} = (\cos\alpha, \cos\beta, \cos\delta)$. From a geometrical point of view, Gaia will measure the abscissa of such a point,

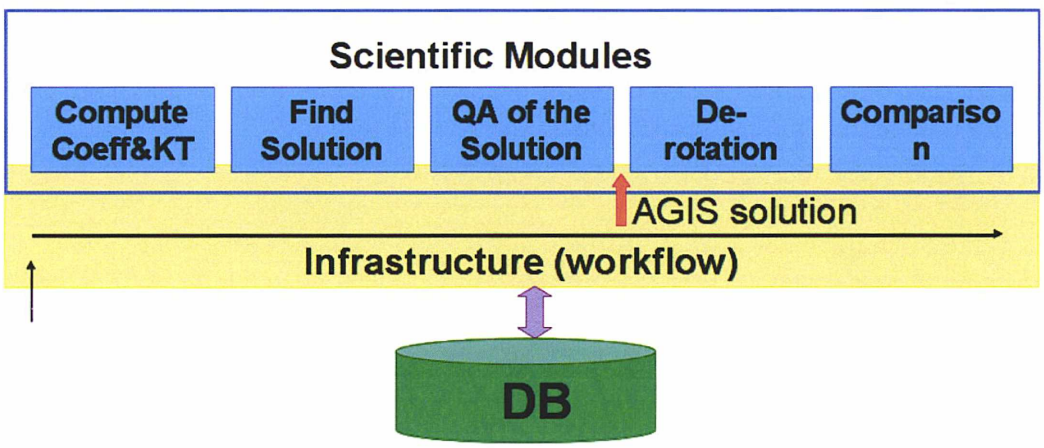

Figure 6.2: Schematic representation of GSR architecture [Vecchiato *et al.* 2012]. During this thesis, we focused on the first two scientific modules, namely "compute Coeff&KT" and "Find solution". In particular, we first computed a "calculated observable" ϕ_{calc} using our formula (4.16) with the RAMOD tetrad (5.10) and compared it with a "nominal" observed value ϕ_{obs} computed using the GREM model. The result of $\phi_{obs} - \phi_{calc}$ provided an indication of the accuracy of our model in the Gaia context. Then, we focused on writing the linearized observation equations $\sin\phi d\phi = -\sum_i \frac{\partial F}{\partial p^i}|_{\bar{p}^i} \delta p^i$, where p^i are the unknowns to be determined by a least-squares procedure in the "Find solution" part.

i.e. the angle ϕ between the x-axis of the spacecraft and the projection of the point in the $x-y$ plane. This angle is related to the director cosines $n_{(i)}$ by the following relations

$$\cos\phi = \frac{n_{(1)}}{\sqrt{1-n_{(3)}^2}}, \tag{6.1a}$$

$$\sin\phi = \frac{n_{(2)}}{\sqrt{1-n_{(3)}^2}}. \tag{6.1b}$$

As illustrated in section 1.1.1, Gaia spacecraft has two fields of view (FOV) called f_+ and f_- whose pointing directions are separated by a fixed base angle of 106.5^o and which are symmetric with respect to the x-axis. Since the angular amplitude of each FOV is about 0.3^o, the abscissae range is fixed in the intervals 53.25 ± 0.15 degrees for f_+ and 103.25 ± 0.15 degrees for f_-. Therefore, one of Eq. (6.1a) is enough to determine a univocal correspondence between the value of ϕ and that of the direction cosines. The usual choice is $\cos\phi$, so that the direction cosines with respect to the x and z axes are sufficient to completely determine the observation. The abscissa is generally expressed as function of the astrometric parameters $(\alpha_*, \delta_*, \varpi_*, \mu_{\alpha*}, \mu_{\delta*})$ and of the satellite attitude. The latter has to be considered unknown since the satellite attitude cannot be determined by other independent measures at the accuracy required by the mission. For a similar reason Eq. (6.1a) also depends on a set of instrument parameters $\{c_l\}$ to provide a sort of long-term calibration. Moreover, when working within the PPN formalism, one should add the parameter γ to the unknowns of Eq. (6.1a). A better determination of γ, which measures the amount of curvature induced by the mass-energy on space-time, shall be one of the important scientific contributions of Gaia. As consequence, each of the Gaia observations can be resumed to a non-linear function of these four classes of unknown included in a suitable model of the abscissa ϕ

$$\cos\phi \equiv \mathcal{F}\left(\alpha_*, \delta_*, \varpi_*, \mu_{\alpha*}, \mu_{\delta*}, a_1^{(j)}, a_2^{(j)}, ..., c_1, c_2, ..., \gamma\right). \tag{6.2}$$

The Gaia mission will perform several billions of observations during its operation years, resulting in a very large system of equations (up to $10^{10} \times 10^8$ in the case of Gaia).

Solving such a big system of non linear equations is not feasible, so the observation equations (6.2) are linearized about a convenient starting point, *i.e.* the current best available estimate of the required unknowns. The problem is then converted in a very big system of linear equations

$$\begin{aligned} -\sin\phi d\phi = {} & \frac{\partial\mathcal{F}}{\partial\alpha_*}|_{\bar{\alpha}_*}\delta\alpha_* + \frac{\partial\mathcal{F}}{\partial\delta_*}|_{\bar{\delta}_*}\delta\delta_* + \frac{\partial\mathcal{F}}{\partial\varpi_*}|_{\bar{\varpi}_*}\delta\varpi_* + ... \\ & + \sum_{ij}\frac{\partial\mathcal{F}}{\partial a_i^{(j)}}|_{\bar{a}_i^{(j)}}\delta a_i^{(j)} + \sum_i \frac{\partial\mathcal{F}}{\partial c_i}|_{\bar{c}_i}\delta c_i + \frac{\partial\mathcal{F}}{\partial\gamma}|_{\bar{\gamma}}\delta\gamma + ..., \end{aligned} \tag{6.3}$$

where the unknown are the corrections δx to the starting catalog values while the derivatives of $\mathcal{F}$ are the coefficients of the system matrix. The known-terms are then represented by the left-hand side of Eq. (6.3) as

$$-\sin\phi_{calc}(\phi_{obs}-\phi_{calc})\ , \tag{6.4}$$

where ϕ_{obs} represents the observed abscissa and formally includes the measurement errors so that it can be written $\phi_{obs}=\phi_{true}+\Delta\phi$, while ϕ_{calc} is the computed value given by $\arccos(\mathcal{F})$ at the starting point of the linearization (generally speaking, the value contained in the astrometric catalog).

The resulting system of equations is quite sparse since each observation refers to a single star among the millions considered in the reconstruction problem (and then only to its astrometric parameters). A similar reasoning is valid for the attitude and calibration parameters, while γ is a global parameter in the sense that it appears in each equation of the system. The number of observations being far larger than the number of unknown parameters, the system is over-determined and can be solved by a least-squares procedure.

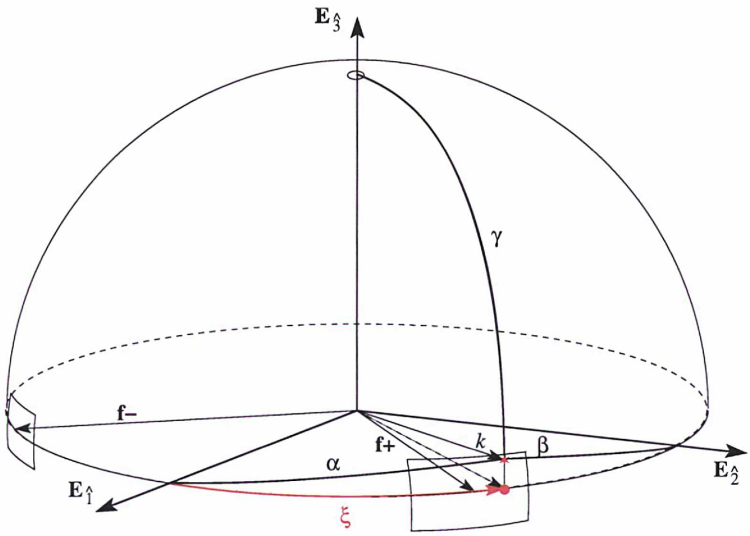

Figure 6.3: Fundamental angles in the Gaia reference frame $E_{\hat{a}}$. The two Fields of View (FOV) directions are indicated by f_+ and f_- while the measured abscissa is given by $n_{(i)}\ =\ (\alpha,\beta,\gamma)$ (from [Vecchiato *et al.* 2012])

The final goal of the entire procedure is then to get better estimates of all the intervening parameters but for that, we first need to provide an accurate model of the director cosines of the observation. The GSR software is built so that the director cosines are provided using the RAMOD model (more precisely, the version actually implemented is PPN-RAMOD [Vecchiato *et al.* 2003]). Since the software is built in a modular structure, it is nevertheless possible to use other models to treat light propagation, the aberration corrections, etc.

In particular, we implemented Eq. (4.16) to compute the director cosines at the accuracy required by the Gaia mission using our model : we populated the equation using a PN expansion of the direction triple $\hat{k}_i$ (similarly to what shown in section 3.2.3) and the RAMOD tetrad (5.10) for the transformation from the BCRS to the CoMRS of Gaia. We used the director cosines $n_{(i)}$ so defined to build the abscissae ϕ, necessary to write the so called known-terms at the left-hand side of Eq. (6.3). Then, we compared our results to those obtained using the GREM and PPN-RAMOD models on the same data-set of observations. Once the abscissae have been validated, it is necessary to compute the partial derivatives appearing at the right-hand-side of Eq. (6.3), constituting the coefficient of the linearized observation equations to be used to solve the celestial sphere.

These steps required to modify the following sections of the GSR code, keeping as much as possible its original structure in order to take advantage of the many functionalities already implemented. For each processed *packet*, the following steps are computed

DataTakersSeqTest.java Charges the observations packets and launches the analysis routines;

BeforeCoeffDataTaker.java Calls, for each observation, the routines defining all needed quantities for the computation of the the astrometric observable;

CommonTermsRod.java Defines all needed vectors (star-observer, perturbing body-observer, ...) and tensors (tetrad components, metric, ...) and computes the director cosines $n_{(i)}$ and the abscissae ϕ as well as the coefficients of the linearized equations;

KnownTermsDataTaker.java Calls, for each observation, the routine computing the known-terms (6.4);

KnownTermsExtract.java Defines ϕ_{obs} and ϕ_{calc}, computes the known-terms (6.4) and updates the information in the *packet*;

CoeffDataTaker.java Calls, for each observation, the routine computing the coefficients of the linearized equations and populates the coefficients vector in the *packet*;

CoeffExtract.java Computes the coefficients of the linearized observation equation (6.3);

AfterCoeffDataTaker.java Reads and checks the values of all coefficients stocked in the *packet*.

In the following sections, we will detail the procedure followed to implement the astrometric model presented in this thesis into the GSR software as well as the tests performed on our results. First, we will use our model to compute the observation abscissa (6.1a) and we will compare our results to those of RAMOD and GREM.

This will allow us to validate our implementation and explore the residual differences between the different models. Once this first phase is fulfilled, we will focus on the implementation of the linearized observation equation (6.3) and on testing the procedure of reconstruction of the celestial sphere. This preliminary study should give a global overview of how our model can be applied to the complex task of processing the observations of an astrometric space mission.

6.2.1 Simulation of the observation abscissae

As presented above, the implementation of our observable in GSR concerns the development of both sides of Eq. (6.3). In this section we will focus on building and testing the known terms (6.4).

Let us show the procedure followed to build the abscissa ϕ using our astrometric model. First we need to define the director cosines appearing in Eq. (6.1a) using Eq. (4.15) taken at the observation point x_B

$$n_B^{(i)} = -\left.\frac{\lambda^0_{(i)} + \lambda^j_{(i)}\hat{k}_j}{\lambda^0_{(0)} + \lambda^j_{(0)}\hat{k}_j}\right|_B , \tag{6.5}$$

where we shall choose the direction triple $\hat{k}_i$ (defining the barycentric direction of light) and the tetrad $\lambda^\alpha_{(\beta)}$ (*i.e.* the transformation matrix to the reference system comoving with the observer) according to the accuracy required by the Gaia mission.

Concerning light deflection, for most observation we shall consider the PN gravitational potentials of all Solar System bodies (see Table 1.2). Moreover, it has been shown in [Klioner 2003] and confirmed by our study in section 3.2.3, that computing the positions of the gravitating bodies at the retarded moment of time

$$t_C = t_B - c^{-1}\,|\boldsymbol{x}_B - \boldsymbol{x}_P(t_B)| + \mathcal{O}(c^{-2}) , \tag{6.6}$$

where t_B is the coordinate time of observation and $\boldsymbol{x}_P(t_B)$ is the position of body P at t_B, allows us to neglect the effects due to the velocities of the bodies. Then, we effectively use a constant value $\boldsymbol{x}_P = \boldsymbol{x}_P(t_C)$ in our computations so that the metric tensor writes $g_{\mu\nu} = \eta_{\mu\nu} + h_{\mu\nu}$ with

$$h_{00} = \frac{2G}{c^2}\sum_P \frac{\mathcal{M}_P}{r_P(t_C)} , \qquad h_{0i} = 0 , \qquad h_{ij} = \delta_{ij}\,\gamma\,h_{00} , \tag{6.7}$$

where $\boldsymbol{r}_P = \boldsymbol{x}_B - \boldsymbol{x}_P(t_C) - \lambda R_{AB}\boldsymbol{N}_{AB}$. For this preliminary study, we neglect the multipole terms appearing in Eq. (3.31) since their implementation in the code would be quite cumbersome and their influence would be observable only for observations grazing the giant planets (1 μas at 152" from Jupiter). Finally, the direction triple to be used in Eq. (6.5) is (remembering Eqs. (3.35)-(3.37a))

$$\begin{aligned}(\hat{k}_i^B)(\boldsymbol{x}_A, \boldsymbol{x}_B) = {} & N^i_{AB} - (\gamma+1)\sum_P \frac{G\mathcal{M}_P}{c^2 R_{PB}}\,\frac{1}{1+\boldsymbol{N}_{PA}\cdot\boldsymbol{N}_{PB}} \\ & \times\left[\frac{R_{AB}}{R_{PA}}\boldsymbol{N}_{PB} - \left(1+\frac{R_{PB}}{R_{PA}}\right)\boldsymbol{N}_{AB}\right] ,\end{aligned} \tag{6.8}$$

where we used

$$\boldsymbol{R}_{PX} = \boldsymbol{x}_X - \boldsymbol{x}_P(t_C), \tag{6.9a}$$

$$R_{PX} = |\boldsymbol{R}_{PX}|, \qquad \boldsymbol{N}_{PX} = \frac{\boldsymbol{R}_{PX}}{R_{PX}}\,, \tag{6.9b}$$

$$\boldsymbol{R}_{AB} = \boldsymbol{x}_B - \boldsymbol{x}_A, \quad R_{AB} = |\boldsymbol{R}_{AB}|, \quad \boldsymbol{N}_{AB} = \frac{\boldsymbol{R}_{AB}}{R_{AB}}\,. \tag{6.9c}$$

Concerning the Gaia tetrad, the simplest choice is to use Eq. (5.10), presented in [Crosta & Vecchiato 2010] and already used in GSR. This completes the implementation in GSR of an abscissa ϕ based on our model. We shall now compare our results to those of PPN-RAMOD (actually implemented in GSR) and of GREM (the model implemented in AGIS).

First, we launch a simulation over one day of observations using the three models to generate the abscissae ϕ. The results are illustrated in Fig. 6.4 and Fig. 6.5 (produced using the GaiaTools library provided by the Gaia DPAC), where the models are compared one to each other. The numbers on the left axis have a double meaning: they mark (1) the difference in μas between the two models - represented by the red plot - and (2) the distance in degrees/10 between a given planet and the observation - the blue, green and yellow plot representing Jupiter, Saturn and Mars, respectively. In particular, the periodic oscillation of the distance planet-observation illustrated in the plots is due to the Gaia scanning law (see section 1.1.1) setting a rotation period of approximately 6 h. Let us analyze each comparison, noting that we can generally separate the observations in "near" and "far" from the planets with respect to the maximum impact parameter to get 1 μas gravitational deflection:

- (PPN-)RAMOD vs TTF - we observe huge differences (up to 500 μas, the y-axis is limited to ± 20 μas to help a better visualization) for the observations near Jupiter. This is expected since PPN-RAMOD is based on a "parametrized" Schwarzschild model of the Solar System, while our TTF model includes the contribution of all major Solar System bodies. On the other hand, since both models implement the same description for the observer, the comparison shows no differences for most of the observations "far" from the planets.

- TTF vs GREM - both the modelings of light propagation and the aberration caused by the motion of the observer are different. Nevertheless, in chapter 5 we showed the equivalence between our approach and GREM, so that we would expect not to observe sensible differences in the plot. Indeed, the difference between the abscissae is confined in the interval ± 2.5 μas but (1) the shape of the plot far from the planets suggests the presence of a systematic discrepancy in the description of the aberration in the two models or codes; (2) the sudden shift corresponding to the maximum approach to Jupiter suggests an erroneous treatment of the satellite attitude.

- RAMOD vs GREM - we observe the combined effects of a different treatment of gravitational light deflection (near Jupiter) and aberration (far from the

planets). One can see how our TTF model can be of help to decorrelate the two effects, especially near Solar System bodies, where the differences due to light deflection cover the rest of the signal.

Once the basic structure of the signal on one day of observations is understood, it is interesting to observe a simulation over 50 days. In Fig. 6.6 we still represent in red the difference between the abscissae computed by the three models and with other colors the angular distance between some planets and the observation. The modulation in the distance of the planets reflects the combination of Gaia attitude and with the relative orbital motion of the Earth and other Solar System planets. One can note that for almost all observations, the difference between the abscissae computed by GREM and our model is less than 2.5 μas, well below the required accuracy of around 10 μas; however, the same systematic discrepancy observed over one day is still present. This effect is probably related to a slightly different implementation of the aberration effect in the two approaches (let us remember that our model implements the RAMOD approach to describe the observer) and it opens interesting questions: a preliminary study is presented in Appendix B but further analysis are in progress with the GSR team in Turin. On the other hand, we can observe that the differences between the abscissae of RAMOD and our model, exclusively related to gravitational light deflection, are concentrated around the conjunction with the planets (making it necessary to reject approximately 1/3 of the observations over the considered period). The observations far from the planets are as expected less "noisy", which confirms the origin of the discrepancies with GREM results. Another possible visualization of these results is an histogram illustrating the number of observations for which different models produce abscissae with a given difference. In Fig. 6.7 we show that, for the vast majority of the observations, the difference between the abscissae produced by our model are less then $1 - 2$ μas away from what expected by GREM. As comparison, in Fig. 6.8 we show the same histogram for the PPN-RAMOD model actually implemented in GSR (always with respect to GREM). The number of abscissae differing for more than 2 μas (and up to 450 μas) is far larger, confirming the necessity for a more complete model to reach the level of accuracy required by Gaia. Nevertheless, further investigations are needed to completely understand the influence of the accuracy on the single measurement when such models are used in the framework of a more complex problem such as the reconstruction of the celestial sphere.

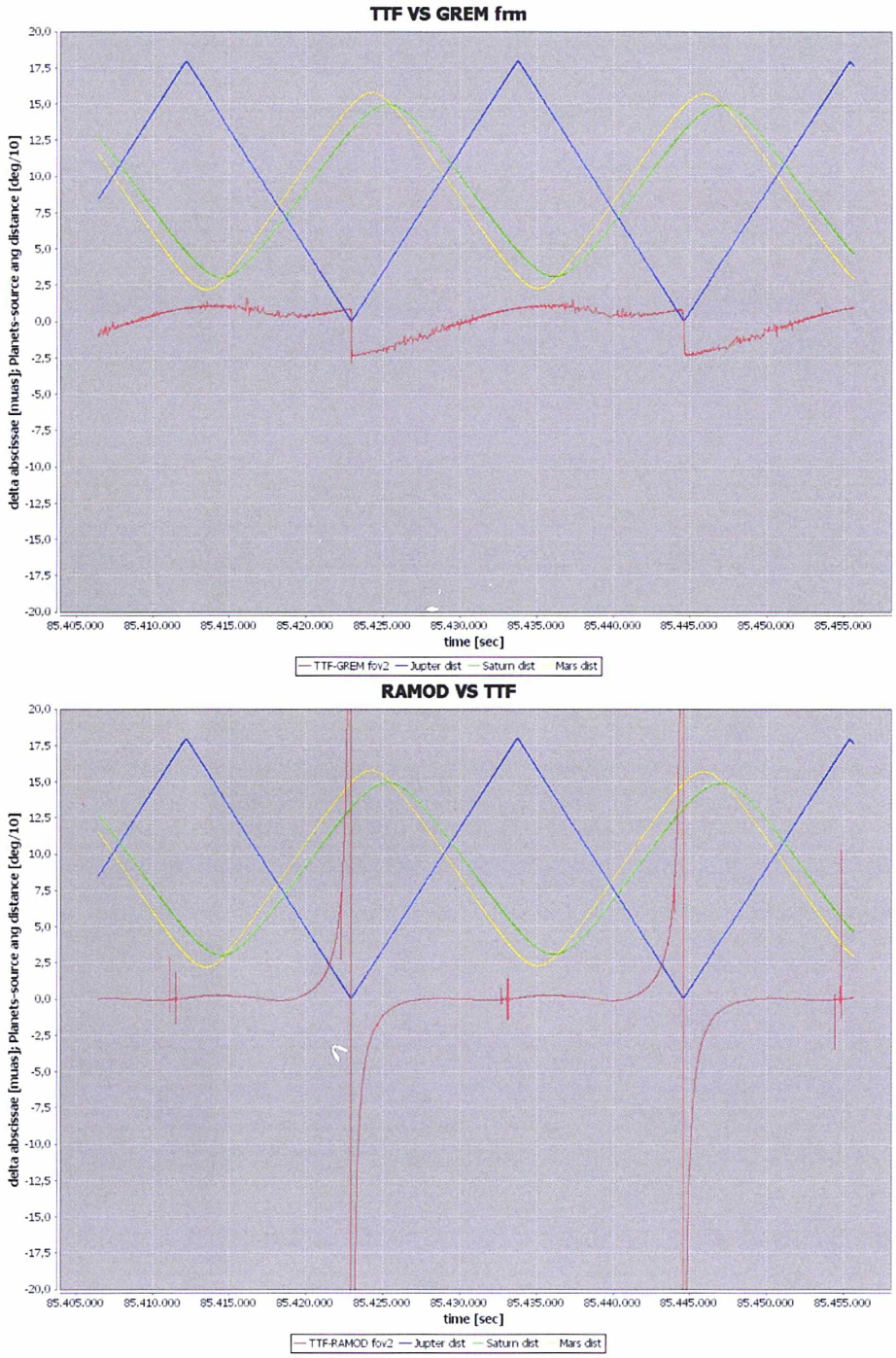

Figure 6.4: Difference between the abscissae resulting from our TTF model and the GREM (**top**) and PPN-RAMOD (**bottom**) models. The numbers on the left axis have a double meaning: they mark (1) the difference in μas between the two models - represented by the red plot - and (2) the distance in degrees/10 between a given planet and the observation - the blue, green and yellow plot representing Jupiter, Saturn and Mars, respectively. The y-axis is limited to ± 20 μas to help a better visualization.

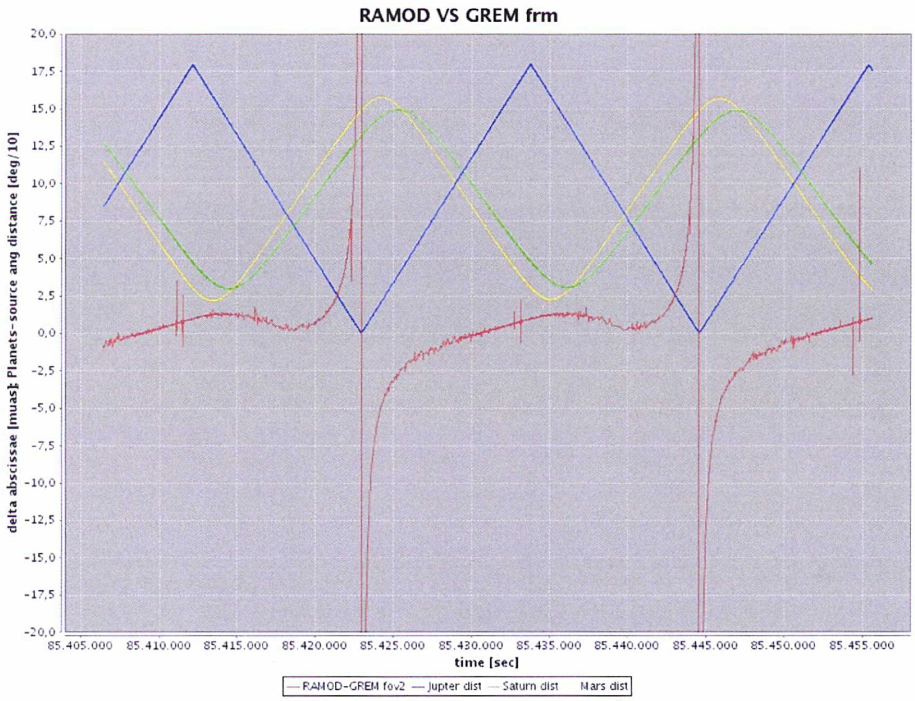

Figure 6.5: Difference between the abscissae resulting from the GREM and PPN-RAMOD models. The numbers on the left axis have a double meaning: they mark (1) the difference in μas between the two models - represented by the red plot - and (2) the distance in degrees/10 between a given planet and the observation - the blue, green and yellow plot representing Jupiter, Saturn and Mars, respectively. The y-axis is limited to ± 20 μas to help a better visualization.

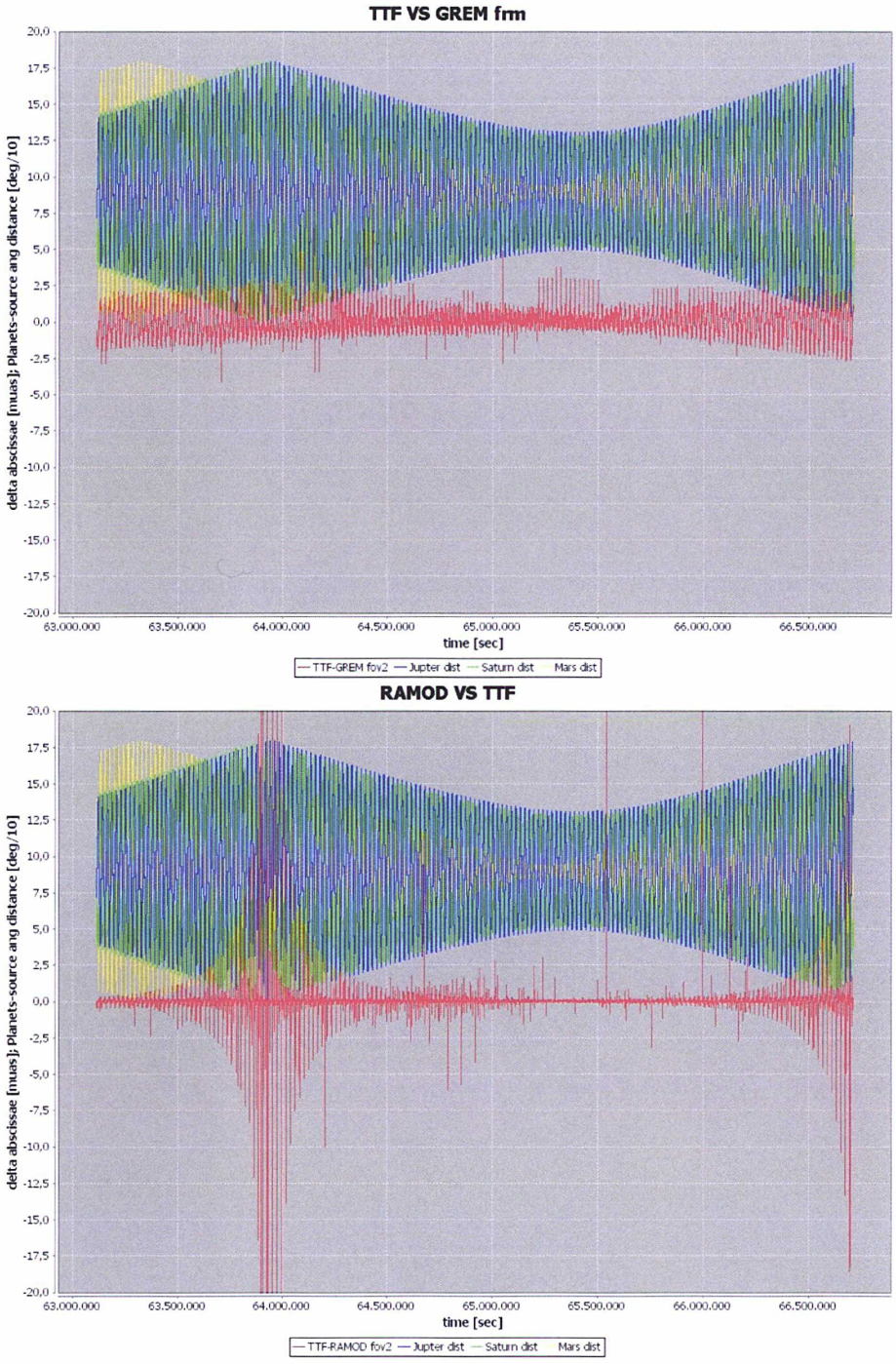

Figure 6.6: Difference between the abscissae resulting from the GREM (**top**) and PPN-RAMOD (**bottom**) models. The numbers on the left axis have a double meaning: they mark (1) the difference in μas between the two models - represented by the red plot - and (2) the distance in degrees/10 between a given planet and the observation - the blue, green and yellow plot representing Jupiter, Saturn and Mars, respectively. The y-axis is limited to ± 20 μas to help a better visualization.

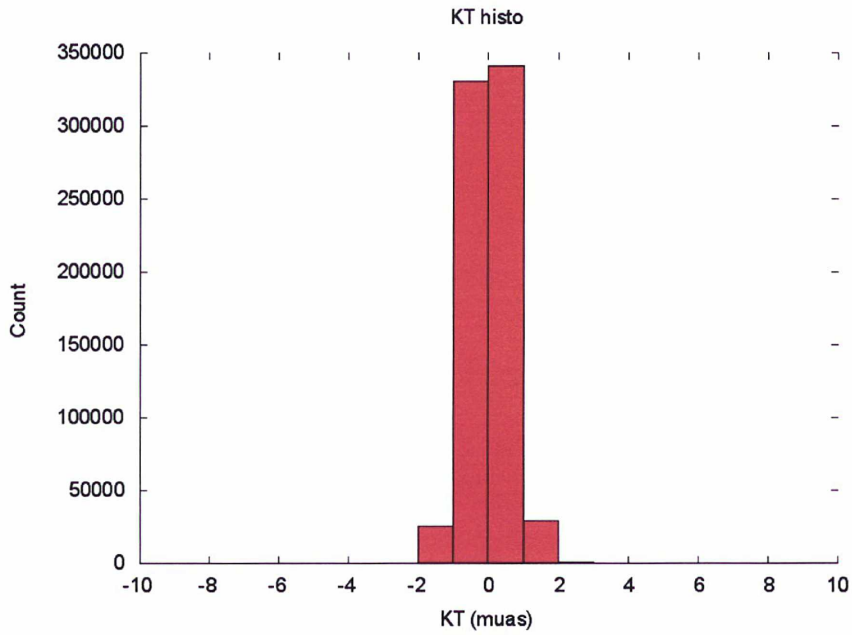

Figure 6.7: Histogram of the abscissae difference between the TTF and GREM models. The vast majority of the observations show differences in the interval of $1-2\ \mu as$, well below the accuracy required by Gaia.

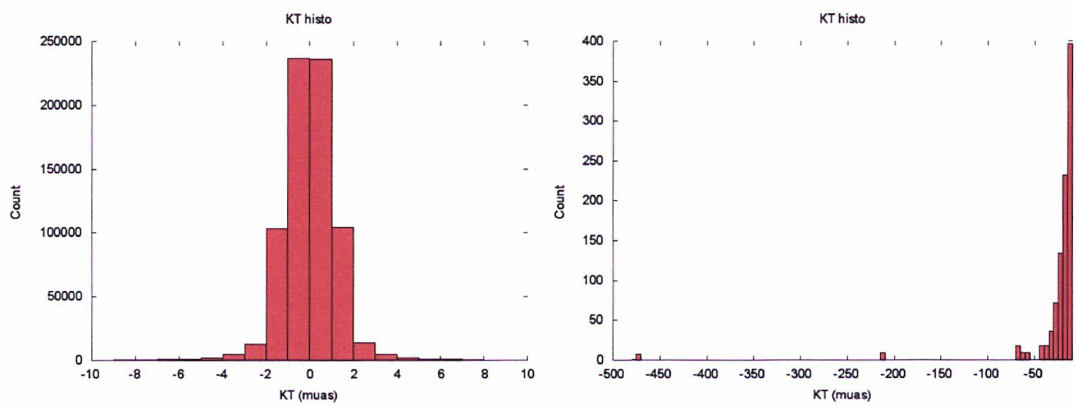

Figure 6.8: Histogram of the abscissae difference between the PPN-RAMOD and GREM models. The splitting emphasize the number of observations within $\pm 10\mu as$ and with differences of more than $10\mu as$. The chart being reasonably symmetric, only the negative values side is shown.

6.2.2 Towards the celestial sphere reconstruction

The validation of the abscissae computed with our model presented in section 6.2.1 has two goals: evaluating its accuracy in the specific case of the Gaia mission and setting the basis for the computation of the linearized observation equations and the reconstruction of a celestial sphere. First, let us make clear what do we intend by "reconstruction of the celestial sphere". The main goal of the Gaia mission is to improve the quality of the stellar catalogs for the coordinates, parallaxes and proper motions of the observed stars. This will be done by comparing Gaia observations to simulated observations built using the catalog data and a theoretical model of the observation: minimizing the difference between the real and simulated observation will provide better estimates of the astrometric parameters. For this scope, we use Eq. (6.3), containing at its left-hand-side the difference between the measured and simulated observations and at its right-hand-side the sensitivity of the observable with respect to each parameter we want to estimate. Since the problem is largely over-determined (Gaia will provide around 700 observations for each star [Mignard *et al.* 2008]) a least-square solution will be used.

Nevertheless, (1) by now we have no observational data from Gaia (it will be launched in late 2013), (2) even after launch, we will not know the "real" star parameters but only the approximation contained in the actual catalogs. We should then find a way to test our models and procedures. One solution is to simulate both the "real" and "simulated" observation from stellar catalogs : to produce the "real" observations $\cos\phi_{obs}$, we will first add some noise to the catalog data (in order to simulate the measuring error), while the simulated observations $\cos\phi_{calc}$ will be produced after adding a constant error to the catalog. If our procedure is well conceived, it should be able to retrieve the initial catalog value.

At this preliminary phase of the implementation, we content ourselves of estimating the astrometric coordinates α_* and δ_* so that all other parameters are assumed to be known and we consider the following simplified version of Eq. (6.3)

$$-\sin\phi_{calc}d\phi = \left.\frac{\partial\mathcal{F}}{\partial\alpha_*}\right|_{\bar{\alpha}_*}\delta\alpha_* + \left.\frac{\partial\mathcal{F}}{\partial\delta_*}\right|_{\bar{\delta}_*}\delta\delta_* \,. \tag{6.10}$$

The coefficients $\partial\mathcal{F}/\partial\alpha_*$ and $\partial\mathcal{F}/\partial\delta_*$ can be computed analytically since the function $\mathcal{F} = \cos\phi_{calc}$, defined by Eq. (6.1a), is known. We get

$$\frac{\partial\cos\phi}{\partial v} = \frac{\partial_v(\cos\psi_{(1)})}{\sqrt{1-\cos^2\psi_{(3)}}} + \frac{\cos\psi_{(1)}\cos\psi_{(3)}\partial_v(\cos\psi_{(3)})}{(1-\cos^2\psi_{(3)})^{3/2}} \,, \tag{6.11}$$

where v can take the values α_* or δ_* and

$$\partial_v\cos\psi \equiv \frac{\partial\cos\psi_{(i)}}{\partial v} = -\frac{E^j_{(i)}\partial_v\hat{k}_j(E^0_{(0)}+E^l_{(0)}\hat{k}_l) + (E^0_{(i)}+E^j_{(i)}\hat{k}_j)E^l_{(0)}\partial_v\hat{k}_l}{(E^0_{(0)}+E^l_{(0)}\hat{k}_l)^2} \,. \tag{6.12}$$

The partial derivatives of the direction triple appearing in Eq. (6.12) are given by

$$\begin{aligned}\frac{\partial \hat{k}_i}{\partial v} &= \partial_v N^i_{AB} - (\gamma+1)\sum_P \frac{G\mathcal{M}_P}{c^2 R_{PB}} \frac{1}{1+\boldsymbol{N}_{PA}\cdot\boldsymbol{N}_{PB}} \Bigg\{ -\frac{\partial_v \boldsymbol{N}_{PA}\cdot\boldsymbol{N}_{PB}}{1+\boldsymbol{N}_{PA}\cdot\boldsymbol{N}_{PB}} \\ &\times \left[N^i_{AB}\frac{R_{AB}}{R_{PA}} - N^i_{AB}\left(1+\frac{R_{PB}}{R_{PA}}\right)\right] + \frac{N^i_{PB}}{R^2_{PA}}\left(R_{PA}\partial_v R_{AB} - R_{AB}\partial_v R_{PA}\right) \\ &-\partial_v N^i_{AB}\left(1+\frac{R_{PB}}{R_{PA}}\right) + N^i_{AB} R_{PB}\frac{\partial_v R_{PA}}{R^2_{PA}}\Bigg\}\,, \end{aligned} \tag{6.13}$$

where we used the definitions (6.9) and

$$\partial_v N^i_{AB} = -\frac{(\boldsymbol{N}_{AB}\times\partial_v\boldsymbol{x}_A\times\boldsymbol{N}_{AB})^i}{R_{AB}}\,, \tag{6.14a}$$

$$\partial_v R_{AB} = -\frac{\boldsymbol{R_{AB}}\cdot\partial\boldsymbol{x}_A}{R_{AB}}\,, \tag{6.14b}$$

$$\partial_v R_{PA} = \frac{\boldsymbol{R_{PA}}\cdot\partial_v\boldsymbol{x}_A}{R_{PA}}\,, \tag{6.14c}$$

$$\partial_v \boldsymbol{N}_{PA}\cdot\boldsymbol{N}_{PB} = \frac{\boldsymbol{R_{PB}}}{R_{PB}R_{PA}}\cdot\left[\partial_v\boldsymbol{x}_A - \frac{\boldsymbol{R_{PA}}}{R^2_{PA}}\boldsymbol{R_{PA}}\cdot\partial_v\boldsymbol{x}_A\right]. \tag{6.14d}$$

Finally, remembering that the incoming direction $\boldsymbol{n}$ can be expressed in terms of right ascension and declination as in Eq. (4.27), we shall write

$$\partial_{\alpha_*} x^i_A = (-r_A\sin\alpha\cos\delta, r_A\cos\alpha\cos\delta, 0)\,, \tag{6.15a}$$

$$\partial_{\delta_*} x^i_A = (-r_A\cos\alpha\sin\delta, -r_A\sin\alpha\sin\delta, r_A\cos\delta)\,. \tag{6.15b}$$

The problem of solving Eq. (6.10) for a given star can be put in the form

$$\boldsymbol{b} = O\boldsymbol{x}\,, \tag{6.16}$$

where $\boldsymbol{x} = (\delta\alpha_*, \delta\delta_*)$ is the unknown vector that we want to estimate, $\boldsymbol{b}$ contains the known-terms (6.4) for each observation of the star and O is the coefficient matrix of size (number of observations $\times$ number of unknowns). The goal of the least squares solution is then to minimize the "error" $|O\boldsymbol{x}-\boldsymbol{b}|$. The standard method to solve this problem [Meyer 2001], and the one we will use here, is to rewrite Eq. (6.16) as $O^TO\boldsymbol{x} = O^T\boldsymbol{b}$ and then, if the matrix O^TO is invertible, to solve as

$$\boldsymbol{x} = (O^TO)^{-1}O^T\boldsymbol{b}\,. \tag{6.17}$$

The astrometric solution we performed is a solution of this equation for 200 stars along the whole mission period of 5 years. We used a data-set elaborated by the Gaia Coordination Unit 2 (CU2) responsible for data simulation, in order to produce

1. the measured abscissa $\cos\phi_{obs}$ with a white Gaussian noise of $\sigma = 2$ *mas* previously added to the astrometric coordinates α_* and δ_*;

2. the computed abscissa $\cos\phi_{calc}$ after having corrected the catalog values of a constant value of $\Delta\alpha_* = 100\ mas$ and $\Delta\delta_* = 50\ mas$.

The final goal of the procedure is to retrieve as much as possible the catalog values α_* and δ_* for the 200 treated stars. In Fig. 6.9 we illustrate the results of the least squares (6.17) solution: for most stars we improve our initial solution for α_* and δ_* by two orders of magnitude. The efficiency of the least-squares solution depends on the number of observations N_{obs} for a given star as its square root $\sqrt{N_{obs}}$, which depends on the Gaia nominal scanning law (see Fig. 6.10). As expected, stars with ≈ 150 observations show an improvement double than stars with ≈ 40 observations, as illustrated in Fig. 6.10.

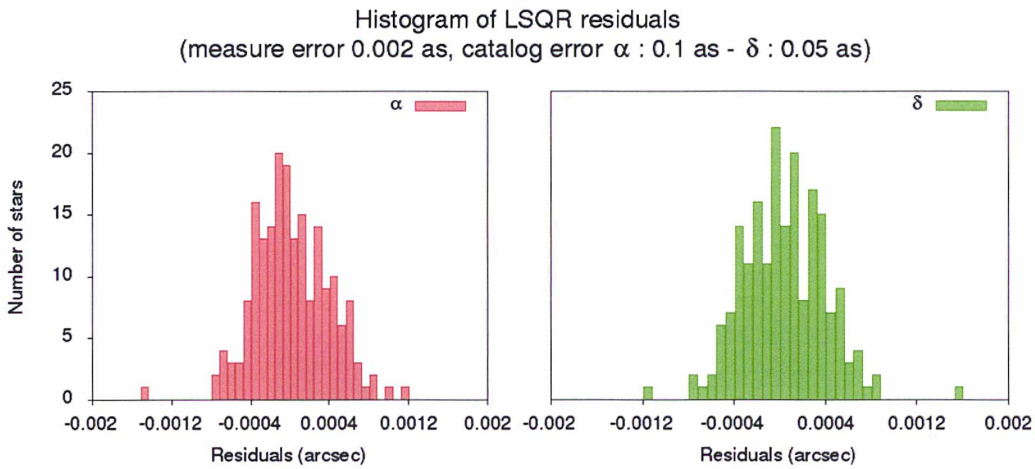

Figure 6.9: Histogram of LSQR residuals (post-fit values minus initial catalog values) on the astrometric coordinates. Initial values: measure error $\sigma = 2\ mas$, catalog error $\alpha = 100\ mas$ - $\delta = 50\ mas$. After one iteration the residuals have improved of a factor ≈ 10, depending on the number of observations for a given star.

The problem treated in GSR is much more complex since it includes the estimation of global (γ) and time-dependent (*i.e.* the attitude) parameters preventing from treating the observation of each star as separate problems. For this reason, solving the full version of this problem would require more powerful machines and a more complex algorithm. Nevertheless, this preliminary analysis is sufficient to get an overview of how our model could be applied to such a problem.

6.3 Conclusions

In this chapter, we applied the astrometric model developed in the thesis to a set of Gaia simulated observations. Thanks to the collaboration with the GSR team in Torino, we implemented our equations into the GSR Java code to compute the observation abscissae at the accuracy required by the Gaia mission: we populated the

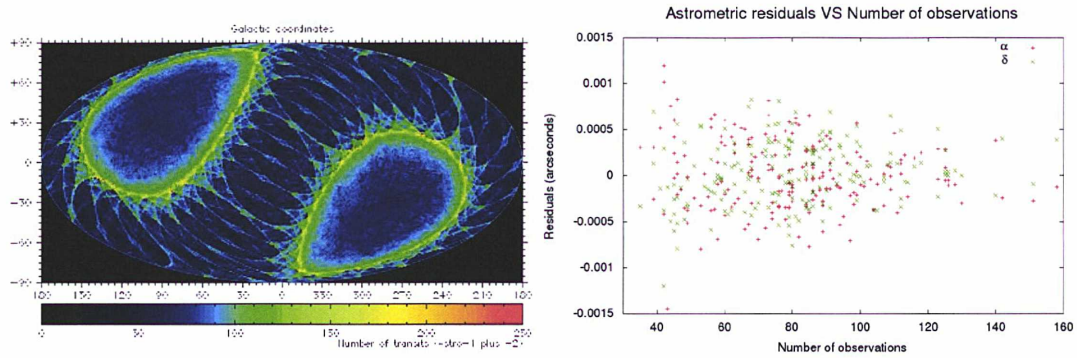

Figure 6.10: **Left:** Frequency of observations as function of celestial coordinates due to Gaia scanning law (blue $\approx$ 50 - yellow $\approx$ 200) - **Right:** Astrometric residuals after one iteration as function of the number of observations for the star (α_* residuals in red - α_* residuals in green)

equation using a PN expansion of the direction triple $\hat{k}_i$ (similarly to what shown in section 3.2.3) and the RAMOD tetrad (5.10) for the transformation from the BCRS to the CoMRS of Gaia. We used this model to check the reliability of our results in a real Gaia configuration by comparing them with those of PPN-RAMOD (already implemented in GSR) and GREM (taken as reference model) using the GaiaTools library provided by the Gaia DPAC. Once the model was implemented and tested, we could use it to assist the GSR team in detecting and analyzing possible differences in the data treatment with respect to AGIS: some interesting results have arisen, requiring further analysis. These preliminary results have been presented at the *GAIA REMAT #12 Meeting* in July 2013. Finally, our model of the observation abscissa has been applied to the reconstruction of a small celestial sphere. This required to compute and implement in the code the linearized equations of our observable and a least-squares procedure. The preliminary results presented in this chapter are a first step in building a full software for the reduction of astrometric observations based on our TTF model.

CHAPTER 7

Conclusions and perspectives

Contents

This thesis is the result of a Vinci fellowship proposal to the French-Italian University based on a project in five steps:

1. the theoretical development of a model of astrometric observable;

2. this model shall be based on the Time Transfer Functions formalism to account for gravitational light deflection by Solar System bodies;

3. the adaptation of the model to the satellite attitude tetrad developed within the RAMOD project;

4. the development of a software implementing steps 1 and 2;

5. the simulation, from an existing star catalog and the nominal satellite orbit, of a set of observations.

The proposal also mentioned some secondary goals including high precision orbit determination by the improvement of the relativistic Doppler modeling. It is worth noting that all the primary goals and some secondary goals of the proposal have been completed in the nominal three years duration of the Ph.D. thesis.

7.1 Relativistic light propagation and observables

In the first part of this thesis, we focused on the development of explicit formulae to describe relativistic light propagation up to 2PM. Then, we used these formulae to build a relativistic model of the observables required for the data analysis of modern high-precision space missions.

Relativistic light propagation up to 2PM

We founded our study on the mathematical formalism of the Time Transfer Function, which models the coordinate time of flight of an EM wave propagating between two events x_A and x_B. A key-point of this formalism are the relations providing $\mathcal{K}$ and $\widehat{k}_i$ (the ratios of the covariant components of the tangent vectors to the light ray) once the Time Transfer function is explicitly known.

Our contribution is the construction of these ratios, fundamental in the modeling of relativistic observables, within the post-Minkowskian approximation of GR as closed form integrals, *i.e.* as function of a metric tensor and its derivatives only, taken along the straight Minkowskian line between x_A and x_B. The main interests of such general formulae is the opportunity of solving them both analytically or numerically for any weak field metric, which has also applications for testing alternative metric theories of gravity.

We developed our formalism up to the second post-Minkowskian order to be able to account for the so called "enhanced terms" [Klioner 2003]. We applied then our formulae to a 2PM Schwarzschild metric in order to analytically retrieve the solution presented by [Teyssandier 2012], thus validating our general formulation.

Closed form equations of relativistic observables

Based on our closed form formulae for $\mathcal{T}$, $\mathcal{K}$ and $\widehat{k}_i$, we built a relativistic modeling for the Range and Doppler observables used in radio-science as well as for the angular separation between two light sources and the incident direction of an incoming light ray, which are the basic ingredients of any astrometric measurement.

We expressed these modelings using general formulae that we apply then to several interesting examples. Within the Schwarzschild field of the Sun, we provided estimates of the 1PM and 2PM relativistic corrections on the Doppler effect for BepiColombo. Similarly, in a GAME-like configuration, we developed a 2PM kinematically nonrotating tetrad and provided estimates of the relativistic contributions to simulated astrometric observations. We then provided an estimate of the effect of the second order "enhanced terms" on radio-science and astrometric observables.

7.2 Application to the Gaia μas astrometry

One of the main goals of this work was to apply our theoretical formulation to the Gaia mission, developing a model of Gaia observations to be implemented in the GSR data reduction software. Nevertheless, to provide our model with solid bases, we first needed to validate it analytically by comparing to the relativistic models developed for Gaia.

Comparison to the Gaia models

To ensure a correct interpretation of Gaia observations, two parallel relativistic models have been developed, GREM and RAMOD. A good knowledge of the relations between the quantities defined in the two models is then mandatory and a comparison effort is already in place, focusing on the modeling of the astrometric observable and the aberration [Crosta & Vecchiato 2010].

We contributed to this study by establishing an original procedure to cross-check our results on the gravitational deflection of light with those of the Gaia models. Concerning GREM, we compared our model to its seminal study [Klioner & Kopeikin 1992] considering the case of gravitational sources in translational motion. Our study shows that the three models are consistent at the accuracy level required by Gaia. Finally, an unexpected outcome of this analysis was an alternative coordinate form of RAMOD3 solution, potentially better suited for the implementation in the current version of the GSR software.

GSR-TTF

Once validated, the astrometric observable developed in this thesis can be applied to a tetrad comoving with Gaia to get an accurate model of its observations. The collaboration with the GSR team, responsible for the verification of the astrometric core processing, allowed us to implement our model into the GSR Java code and to compare our results to those of PPN-RAMOD and GREM using the tools provided by the Gaia DPAC. This first validation of our results opened the way to the computation of the linearized observation equations necessary to estimate the astrometric parameters from a set of simulated observations.

The main interest of such a study was to prove the applicability of our model to a complex matter like the treatment of Gaia observations and to provide the GSR team with an additional tool to check the final phases of development of the code as presented in the Gaia REMAT#12 meeting in July 2013.

7.3 Open questions and perspectives

The results of this thesis naturally bring up some interesting openings. First, the cross-check procedure presented in chapter 5 includes most, but not all, of the gravitational contributions to light deflection required at Gaia accuracy. This procedure should then be extended to include all effects actually treated by the GREM model, including the gravitational deflection due to the quadrupole moment of Solar System bodies.

Moreover, an analytical solution of RAMOD4 is under development at Turin Observatory, extending the previous version of the model to a non-vorticity free environment. A study by [Crosta 2011] shows that additional terms appear with respect to the standard PN/PM approaches to gravitational light propagation. It

would be then interesting to explore the impact of the strict measurement protocol followed by RAMOD by comparing this new solution to GREM and to our model.

Then, the development of our model up to 2PM allowed us to retrieve the so called second order "enhanced terms" [Klioner & Zschocke 2010]. Recently [Linet & Teyssandier 2013] developed a new procedure to compute the light travel time up to the 3PM order, highlighting the presence of supplementary "enhanced terms". It would be then of interest to extend our formulation up to 3PM and to provide an estimation of the influence of these terms on the radio-science and astrometric observables.

In the context of Gaia, the improvement of GSR-TTF is a perspective work by itself. In particular, the further analysis of the mismodeling effects put in evidence by our preliminary comparison to GREM and the implementation of the quadrupole terms in the software is a short term priority.

On a larger perspective, a ray tracing model called GYOTO has been developed by [Vincent *et al.* 2011] at Paris Observatory. Finding a common basis for a comparison of the two models would be a first step towards further collaborations.

Appendix A

Publications

A.1 Peer-Reviewed Articles

Bertone S. and Le Poncin-Lafitte C. **Light deflection for relativistic space astrometry in closed form.** *Memorie della Società Astronomica Italiana*, 83(1020), 2012. `arXiv:1111.1325 [gr-qc]`.

Bertone, S.; Minazzoli, O.; Crosta, M.; Le Poncin-Lafitte, C.; Vecchiato, A.; Angonin, M.C. **Time Transfer functions as a way to validate light propagation solutions for space astrometry.** Under revision for publication in *Classical and Quantum Gravity*. `arXiv:1306.2367 [gr-qc]`.

Bertone, S. and Le Poncin-Lafitte, C. and Lainey, V., **Transponder delay effect in light time calculations for deep space navigation**. Under revision for publication in *Proceedings of the International Symposium on Orbit Propagation and Determination, arXiv:1305.1950 [astro-ph.IM]*.

A.2 Other publications

A. Hees, S. Bertone, and C. Le Poncin-Lafitte, ***Frequency shift up to the 2PM approximation.*** SF2A-2012: Proceedings of the Annual meeting of the French Society of Astronomy and Astrophysics, *2012, arXiv:1210.2577 [gr-qc]*.

Bertone S. and Le Poncin-Lafitte C. **Relativistic astrometry and Time Transfer functions.** *SF2A-2011: Proceedings of the Annual meeting of the French Society of Astronomy and Astrophysics*, 635-638, 2011.

Bertone, S. and Le Poncin-Lafitte, C. and Lainey, V., **Light time calculations for deep space navigation**. *Proceedings of the Journées 2010 "Systèmes de Référence Spatio-Temporels"*. N. Capitaine (ed.), Observatoire de Paris, 2011.

Bertone, S. and Le Poncin-Lafitte, C. and Angonin, M.-C., **Relativistic modeling for high precision space astrometry at post-post Minkowskian approximation**. *IAU Joint Discussion*, 2012.

A.3 Articles in preparation

Hees, A. and Bertone, S. and Le Poncin-Lafitte, C. **Relativistic formulation of Doppler and astrometric observables up to the second post-Minkoswian order using the Time Transfer Functions.** *To be submitted to Physical Review D.*

Le Poncin-Lafitte C., Bertone S. and Lainey V. **Revisiting light-time and frequency shift calculations for Deep Space Navigation.** In preparation.

Bertone, S.; Minazzoli, O ; Crosta, M. ; Le Poncin-Lafitte, C.; Vecchiato, A ; Angonin, M.C. **The relativistic models for Gaia at the (cross)check-point.** In preparation for *SF2A-2013: Proceedings of the Annual meeting of the French Society of Astronomy and Astrophysics.*

A.4 Gaia Meetings

Relativistic astrometry and Time Transfer Functions. **GAIA REMAT #9 meeting**, ESTEC, Noordwijk, NL, 08/2011.

Latest advances in an astrometric model based on the Time Transfer Functions formalism. **GAIA REMAT #12 meeting**, Observatoire de Paris, France, 07/2013.

Appendix B

GSR-TTF: additional analysis

In this appendix, we present the results of some preliminary analysis made possible by the implementation of our TTF model in the GSR software.

B.1 Retarded times for gravitational potentials

In chapter 5, we illustrated that, in order to neglect the orbital motion of the sources of the gravitational field in our model, we should take their ephemerides at the retarded time corresponding to their maximum approach with the photon as in [Klioner 2003]. This time t_C can be computed as

$$t_C = t_B - c^{-1} \left| \boldsymbol{x}_B - \boldsymbol{x}_P(t_B) \right| + \mathcal{O}(c^{-2}), \tag{B.1}$$

where t_B is the coordinate time of observation and $\boldsymbol{x}_P(t_B)$ is the position of perturbing body P at t_B. Then, we effectively use a constant position $\boldsymbol{x}_P = \boldsymbol{x}_P(t_C)$ for the deflecting bodies in our computations. Fig. B.1 illustrates the difference between implementing the gravitational potentials with respect to the body position at observation time t_B or at retarded time t_C. In the first case (no retarded time) the difference between GREM and our model for observations almost in conjunction with Jupiter can be more than 200 μas, also adding noise to the rest of the plot.

B.2 Early contributions of GSR-TTF

The first abscissae comparison we made between our model and GREM followed the guidelines used for the tests of PPN-RAMOD. Fig. B.2 illustrates the results of these first TTF vs GREM analysis and the same comparison with PPN-RAMOD. The peaks of $\approx$ 20 μas in the top plot (PPN-RAMOD vs GREM) could be due to the difference between the gravitational field considered in GREM (a system of extended bodies corresponding to Solar System planets and the Sun) and PPN-RAMOD (the spherically symmetric field of the Sun). The comparison with our model clearly shows that this is not possible, since the main differences appear "far" from the planets. Further analysis solicited by this finding showed that we were using an out-dated version of GREM for our analysis. The comparison with the current version of GREM in Fig. B.1, indeed does not show these peaks but it shows an unexpected bias and unexpected discontinuities needing further analysis. All these effects would have not been observed without the contribution of GSR-TTF.

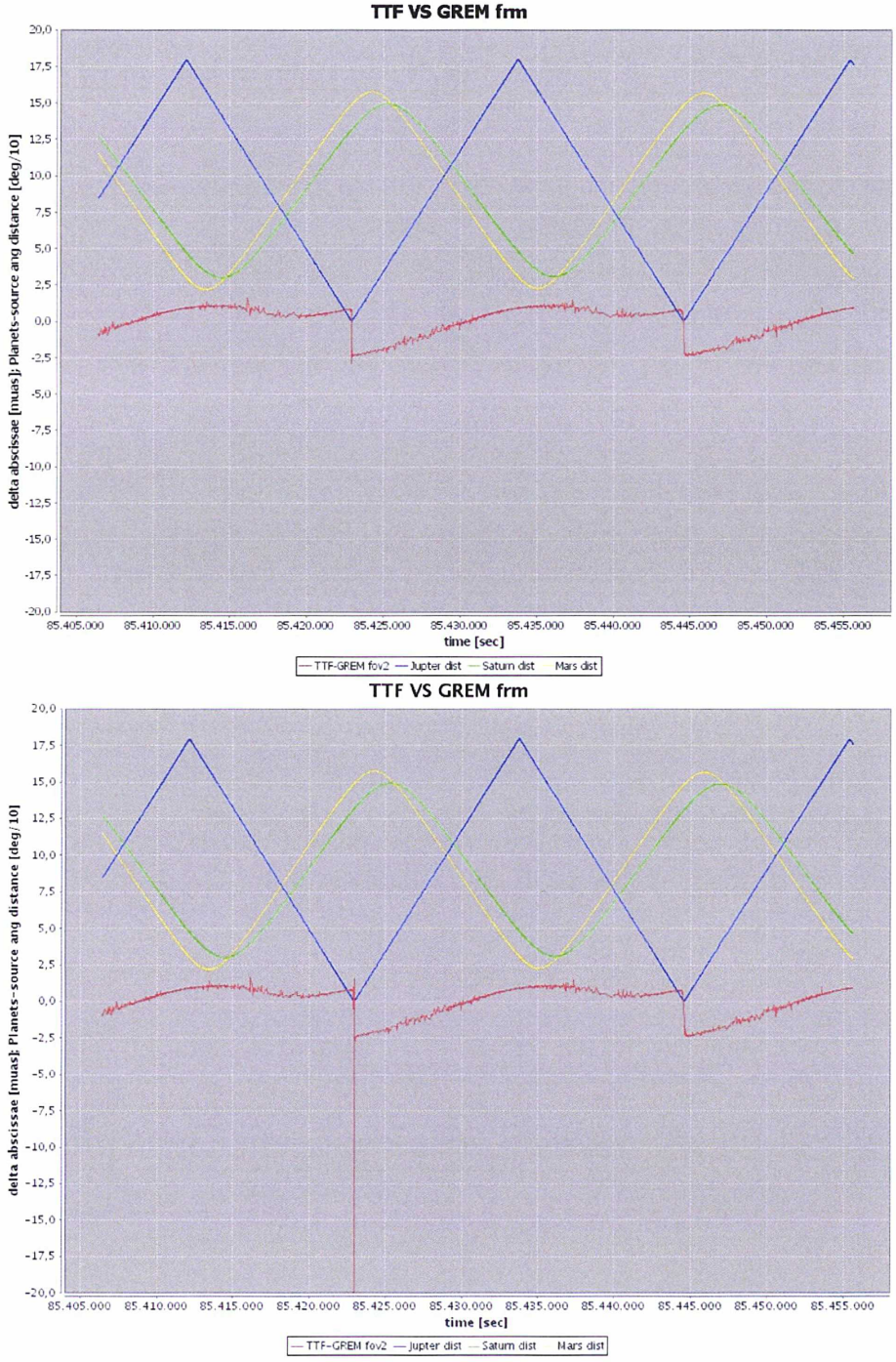

Figure B.1: Difference between the abscissae resulting from our TTF model -with (**top**) and without (**bottom**) retarded potentials- and the GREM. The numbers on the left axis have a double meaning: they mark (1) the difference in μas between the two models - represented by the red plot - and (2) the distance in degrees/10 between a given planet and the observation - the blue, green and yellow plot representing Jupiter, Saturn and Mars, respectively.

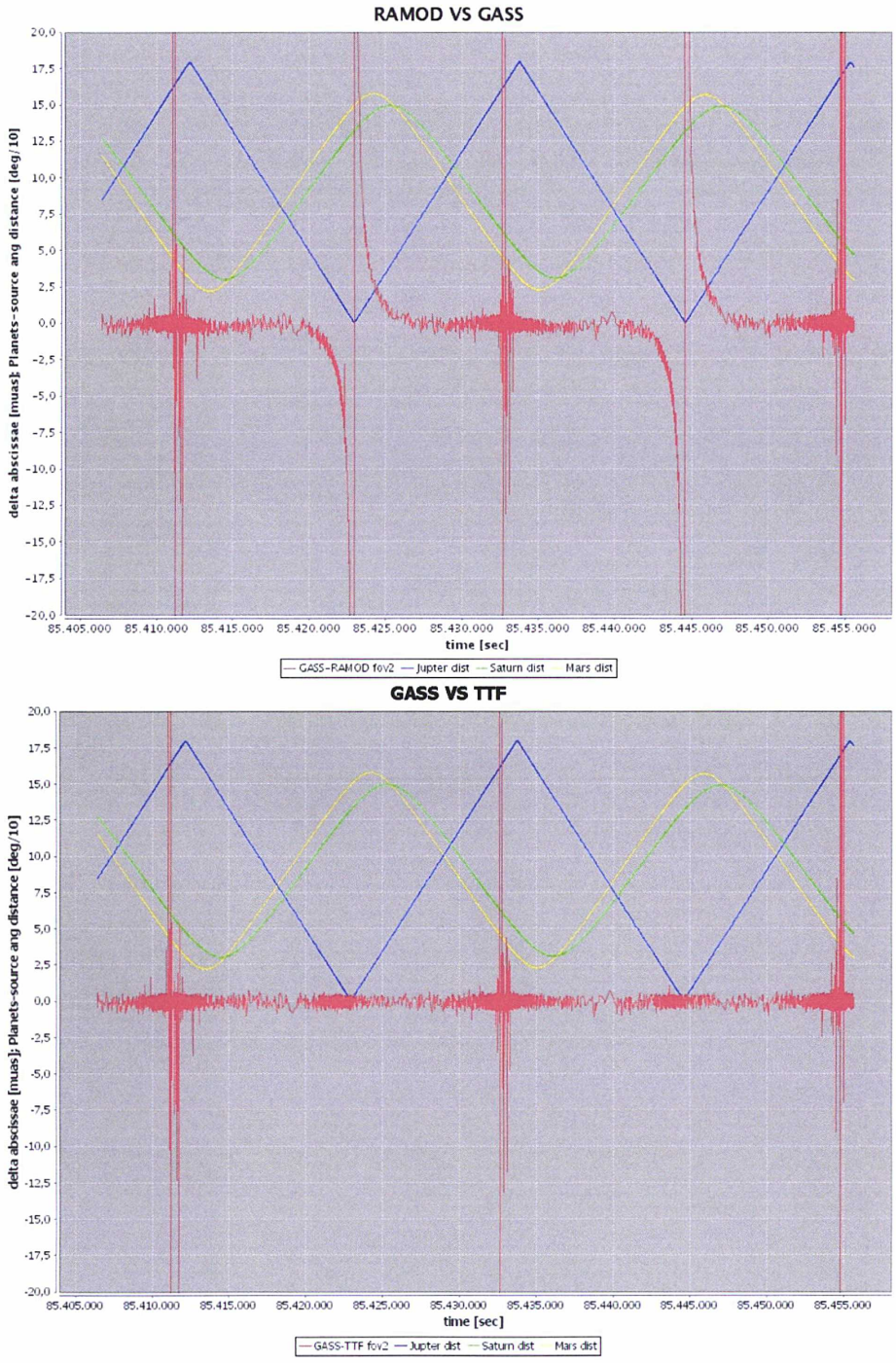

Figure B.2: Difference between the abscissae resulting from the old GREM model (here called GASS) and PPN-RAMOD (**Top**) and the TTF (**Bottom**) models. The numbers on the left axis have a double meaning : they mark the difference in μas between the two models, represented by the red curve; they mark the distance in degrees/10 between a given planet and the observation - the blue curve represents Jupiter, the green Saturn and the yellow represents Mars. The peaks far from Jupiter were confused with errors due to the gravitational deflection of some planet not included in the PPN-RAMOD model. After comparison with our model, it became clear that this was a mismodeling in the software implementation.

Bibliography

[Abbas *et al.* 2011] U. Abbas, A. Vecchiato, B. Bucciarelli, M. G. Lattanzi and R. Morbidelli. *Global Sphere Reconstruction in the Astrometric Verification Unit.* In EAS Publications Series, volume 45 of *EAS Publications Series*, pages 127–132, February 2011. (Cited on page 80.)

[Acton *et al.* 2011] C. Acton, N. Bachman, J. Diaz Del Rio, B. Semenov, E. Wright and Y. Yamamoto. *SPICE: A Means for Determining Observation Geometry.* In EPSC-DPS Joint Meeting 2011, page 32, October 2011. (Cited on page 56.)

[Acton 1996] C. H. Acton. *Ancillary data services of NASA's Navigation and Ancillary Information Facility.* Planetary and Space Science, vol. 44, pages 65–70, January 1996. (Cited on page 56.)

[Ashby & Bertotti 2010] N. Ashby and B. Bertotti. *Accurate light-time correction due to a gravitating mass.* Classical and Quantum Gravity, vol. 27, no. 14, page 145013, July 2010. (Cited on pages 17 and 37.)

[Bandieramonte *et al.* 2012] M. Bandieramonte, U. Becciani, A. Vecchiato, M. Lattanzi and B. Bucciarelli. *AVU-GSR Gaia Mission: A Hybrid Solution for HPC and Grid-MPI Infrastructures.* 2012 IEEE 21st International Workshop on Enabling Technologies: Infrastructure for Collaborative Enterprises, vol. 0, pages 167–172, 2012. (Cited on page 82.)

[Benkhoff *et al.* 2010] J. Benkhoff, J. van Casteren, H. Hayakawa, M. Fujimoto, H. Laakso, M. Novara, P. Ferri, H. R. Middleton and R. Ziethe. *BepiColombo - Comprehensive exploration of Mercury: Mission overview and science goals.* Planetary and Space Science, vol. 58, pages 2–20, January 2010. (Cited on pages 4 and 8.)

[Bertone & Le Poncin-Lafitte 2012] S. Bertone and C. Le Poncin-Lafitte. *Light deflection for relativistic space astrometry in closed form.* Memorie della Società Astronomica Italiana, vol. 83, page 1020, 2012. (Cited on pages 47 and 55.)

[Bertone *et al.* 2012a] S. Bertone, C. Le Poncin-Lafitte and M.-C. Angonin. *Relativistic modeling for high precision space astrometry at post-post Minkowskian approximation.* In IAU Joint Discussion, volume 7 of *IAU Joint Discussion*, page 3P, August 2012. (Cited on page 63.)

[Bertone *et al.* 2012b] S. Bertone, C. Le Poncin-Lafitte and V. Lainey. *Transponder delay effect in light time calculations for deep space navigation.* In Proceedings of the "International Symposium on Orbit Propagation and Determination, Lille 2011", 2012. (Cited on page 50.)

[Bertone *et al.* 2013a] S. Bertone, O. Minazzoli, M. Crosta, C. Le Poncin-Lafitte, A. Vecchiato and M.-C. Angonin. *Time Transfer functions as a way to validate light propagation solutions for space astrometry.* ArXiv e-prints, June 2013. accepted with reviews by Classical and Quantum Gravity. (Cited on pages 20, 42, 47 and 77.)

[Bertone *et al.* 2013b] S. Bertone, O. Minazzoli, M. Crosta, C. Le Poncin-Lafitte, A. Vecchiato and M.C. Angonin. *The relativistic models for Gaia at the (cross)check-point.* In SF2A-2013: Proceedings of the Annual meeting of the French Society of Astronomy and Astrophysics, 2013. in preparation. (Cited on page 77.)

[Bertotti *et al.* 2003] B. Bertotti, L. Iess and P. Tortora. *A test of general relativity using radio links with the Cassini spacecraft.* Nature, vol. 425, pages 374–376, September 2003. (Cited on page 8.)

[Bienayme & Turon 2002] O. Bienayme and C. Turon. *GAIA : a European space project.* EAS Publications Series, vol. 2, 2002. (Cited on pages 4 and 5.)

[Bini *et al.* 2003] D. Bini, M. T. Crosta and F. de Felice. *Orbiting frames and satellite attitudes in relativistic astrometry.* Classical and Quantum Gravity, vol. 20, pages 4695–4706, November 2003. (Cited on pages 9, 69 and 70.)

[Bini *et al.* 2013] D. Bini, M. Crosta, F. de Felice, A. Geralico and A. Vecchiato. *The Erez-Rosen metric and the role of the quadrupole on light propagation.* Classical and Quantum Gravity, vol. 30, no. 4, page 045009, February 2013. (Cited on page 75.)

[Blanchet *et al.* 2001] L. Blanchet, C. Salomon, P. Teyssandier and P. Wolf. *Relativistic theory for time and frequency transfer to order c^{-3}.* Astronomy and Astrophysics, vol. 370, pages 320–329, April 2001. (Cited on pages 16 and 37.)

[Brumberg 1987] V. A. Brumberg. *Light propagation in the Schwarzschild field based in the post-post-Newtonian approximation.* Kinematika i Fizika Nebesnykh Tel, vol. 3, pages 8–13, February 1987. (Cited on pages 3 and 37.)

[Brumberg 1991] V. A. Brumberg. Essential relativistic celestial mechanics. 1991. (Cited on page 54.)

[Bucciarelli *et al.* 2005] B. Bucciarelli, M. T. Crosta, F. de Felice, M. G. Lattanzi and A. Vecchiato. *Relativistic Astrometry: the RAMOD Project.* In C. Turon, K. S. O'Flaherty and M. A. C. Perryman, editeurs, The Three-Dimensional Universe with Gaia, volume 576 of *ESA Special Publication*, page 259, January 2005. (Cited on page 68.)

[Čadež & Kostić 2005] A. Čadež and U. Kostić. *Optics in the Schwarzschild spacetime.* Physical Reviews D, vol. 72, no. 10, page 104024, November 2005. (Cited on page 17.)

[Chandrasekhar 1983] S. Chandrasekhar. The mathematical theory of black holes. 1983. (Cited on page 17.)

[Chauvineau *et al.* 2005] B. Chauvineau, T. Regimbau, J.-Y. Vinet and S. Pireaux. *Relativistic analysis of the LISA long range optical links.* Physical Reviews D, vol. 72, no. 12, page 122003, December 2005. (Cited on page 16.)

[Crosta & Vecchiato 2010] M. Crosta and A. Vecchiato. *Gaia relativistic astrometric models. I. Proper stellar direction and aberration.* Astronomy and Astrophysics, vol. 509, page A37, January 2010. (Cited on pages 20, 54, 71, 75, 83, 89 and 101.)

[Crosta 2011] M. Crosta. *Tracing light propagation to the intrinsic accuracy of spacetime geometry.* Classical and Quantum Gravity, vol. 28, no. 23, page 235013, December 2011. (Cited on pages 69, 71, 75 and 101.)

[Crosta 2013] M. Crosta. *Tracing a relativistic Milky Way within the RAMOD measurement protocol.* ArXiv e-prints, May 2013. (Cited on pages 69 and 75.)

[Damour *et al.* 1991] T. Damour, M. Soffel and C. Xu. *General relativistic celestial mechanics. I. Method and definition of reference systems.* Physical Review D, vol. 43, pages 3273–3307, October 1991. (Cited on page 3.)

[de Bruijne *et al.* 2010] J. de Bruijne, H. Siddiqui, U. Lammers, J. Hoar, W. O'Mullane and T. Prusti. *Optimising the Gaia scanning law for relativity experiments.* In S. A. Klioner, P. K. Seidelmann and M. H. Soffel, editeurs, IAU Symposium, volume 261 of *IAU Symposium*, pages 331–333, January 2010. (Cited on page 82.)

[de Felice & Bini 2010] F. de Felice and D. Bini. Classical measurements in curved space-times. Cambridge Monographs on Mathematical Physics, 2010. (Cited on pages 17, 18, 66 and 69.)

[de Felice & Clarke 1992] F. de Felice and C.J.S. Clarke. Relativity on curved manifolds. Cambridge Monographs on Mathematical Physics, 1992. (Cited on page 17.)

[de Felice *et al.* 1998] F. de Felice, M. G. Lattanzi, A. Vecchiato and P. L. Bernacca. *General relativistic satellite astrometry. I. A non-perturbative approach to data reduction.* Astronomy and Astrophysics, vol. 332, pages 1133–1141, April 1998. (Cited on page 68.)

[de Felice *et al.* 2001] F. de Felice, B. Bucciarelli, M. G. Lattanzi and A. Vecchiato. *General relativistic satellite astrometry. II. Modeling parallax and proper motion.* Astronomy and Astrophysics, vol. 373, pages 336–344, July 2001. (Cited on page 69.)

[de Felice *et al.* 2004] F. de Felice, M.T. Crosta, A. Vecchiato, M.G. Lattanzi and B. Bucciarelli. *A General Relativistic Model of Light Propagation in the Gravitational Field of the Solar System: The Static Case.* Astrophysical Journal, vol. 607, pages 580–595, May 2004. (Cited on pages 17, 66 and 69.)

[de Felice *et al.* 2006] F. de Felice, A. Vecchiato, M. T. Crosta, B. Bucciarelli and M. G. Lattanzi. *A General Relativistic Model of Light Propagation in the Gravitational Field of the Solar System: The Dynamical Case.* Astrophysical Journal, vol. 653, pages 1552–1565, December 2006. (Cited on pages 19, 69, 70 and 75.)

[Einstein 1916] A. Einstein. *Die Grundlage der allgemeinen Relativitäts theorie.* Annalen der Physik, vol. 354, pages 769–822, 1916. English translation by Lorentz et al. [1923]. (Cited on page 10.)

[Feissel & Mignard 1998] M. Feissel and F. Mignard. *The adoption of ICRS on 1 January 1998: meaning and consequences.* Astronomy & Astrophysics, vol. 331, pages L33–L36, March 1998. (Cited on page 81.)

[Fienga *et al.* 2009] A. Fienga, J. Laskar, T. Morley, H. Manche, P. Kuchynka, C. Le Poncin-Lafitte, F. Budnik, M. Gastineau and L. Somenzi. *INPOP08, a 4-D planetary ephemeris: from asteroid and time-scale computations to ESA Mars Express and Venus Express contributions.* Astronomy and Astrophysics, vol. 507, pages 1675–1686, December 2009. (Cited on page 14.)

[Fienga *et al.* 2011] A. Fienga, J. Laskar, P. Kuchynka, H. Manche, G. Desvignes, M. Gastineau, I. Cognard and G. Theureau. *The INPOP10a planetary ephemeris and its applications in fundamental physics.* Celestial Mechanics and Dynamical Astronomy, vol. 111, pages 363–385, November 2011. (Cited on page 14.)

[Folkner *et al.* 2009] W. M. Folkner, J. G. Williams and D. H. Boggs. *The Planetary and Lunar Ephemeris DE 421.* Interplanetary Network Progress Report, vol. 178, page C1, August 2009. (Cited on pages 14 and 55.)

[Fujita & Hikida 2009] R. Fujita and W. Hikida. *Analytical solutions of bound timelike geodesic orbits in Kerr spacetime.* Classical and Quantum Gravity, vol. 26, no. 13, page 135002, July 2009. (Cited on page 17.)

[Gai *et al.* 2012] M. Gai, A. Vecchiato, S. Ligori, A. Sozzetti and M. G. Lattanzi. *Gravitation astrometric measurement experiment.* Experimental Astronomy, vol. 34, pages 165–180, October 2012. (Cited on pages 4, 7, 9 and 60.)

[Hagihara 1931] Y. Hagihara. *Theory of the relativistic trajectories in a gravitational field of Schwarzschild.* Japanese Journal of Astronomy and Geophysics, vol. 8, p. 67-176 (1931), vol. 8, pages 67–176, 1931. (Cited on page 17.)

[Hees *et al.* 2012a] A. Hees, S. Bertone and C. Le Poncin-Lafitte. *Frequency shift up to the 2-PM approximation.* In S. Boissier, P. de Laverny, N. Nardetto, R. Samadi, D. Valls-Gabaud and H. Wozniak, editeurs, SF2A-2012: Proceedings of the Annual meeting of the French Society of Astronomy and Astrophysics, pages 145–148, December 2012. (Cited on page 32.)

[Hees *et al.* 2012b] A. Hees, B. Lamine, S. Reynaud, M.-T. Jaekel, C. Le Poncin-Lafitte, V. Lainey, A. Füzfa, J.-M. Courty, V. Dehant and P. Wolf. *Radioscience simulations in general relativity and in alternative theories of gravity.* Classical and Quantum Gravity, vol. 29, no. 23, page 235027, December 2012. (Cited on pages 29 and 53.)

[Hees *et al.* 2013] A. Hees, S. Bertone and C. Le Poncin-Lafitte. *Relativistic formulation of Doppler and astrometric observables up to the second post-Minkoswian order using the Time Transfer Functions.* 2013. to be submitted to Physical Reviews D. (Cited on pages 19, 28, 32, 47 and 63.)

[Hobbs *et al.* 2010] D. Hobbs, B. Holl, L. Lindegren, F. Raison, S. Klioner and A. Butkevich. *Determining PPN γ with Gaia's astrometric core solution.* In S. A. Klioner, P. K. Seidelmann and M. H. Soffel, editeurs, IAU Symposium, volume 261 of *IAU Symposium*, pages 315–319, January 2010. (Cited on pages 7 and 9.)

[Iess *et al.* 2009] L. Iess, S. Asmar and P. Tortora. *MORE: An advanced tracking experiment for the exploration of Mercury with the mission BepiColombo.* Acta Astronautica, vol. 65, pages 666–675, September 2009. (Cited on pages 4, 8, 9 and 55.)

[Klioner & Kopeikin 1992] S. A. Klioner and S. M. Kopeikin. *Microarcsecond astrometry in space - Relativistic effects and reduction of observations.* Astronomical Journal, vol. 104, pages 897–914, August 1992. (Cited on pages 3, 43, 47, 54, 72 and 101.)

[Klioner & Peip 2003] S. A. Klioner and M. Peip. *Numerical simulations of the light propagation in the gravitational field of moving bodies.* Astronomy and Astrophysics, vol. 410, pages 1063–1074, November 2003. (Cited on page 44.)

[Klioner & Soffel 1998] S. A. Klioner and M. Soffel. *Nonrotating astronomical relativistic reference frames.* Astronomy and Astrophysics, vol. 334, pages 1123–1135, June 1998. (Cited on pages 14 and 57.)

[Klioner & Soffel 2000] S. A. Klioner and M. H. Soffel. *Relativistic celestial mechanics with PPN parameters.* Physical Review D, vol. 62, no. 2, page 024019, July 2000. (Cited on pages 12 and 39.)

[Klioner & Zschocke 2010] S.A. Klioner and S. Zschocke. *Numerical versus analytical accuracy of the formulae for light propagation.* Classical and Quantum Gravity, vol. 27, no. 7, page 075015, April 2010. (Cited on pages 16, 60 and 102.)

[Klioner *et al.* 2008] S. A. Klioner, M. H. Soffel and C. Le Poncin-Lafitte. *Towards the relativistic theory of precession and nutation.* In N. Capitaine, editeur, Journées Systèmes de Référence Spatio-temporels 2007, page 139, April 2008. (Cited on page 14.)

[Klioner 2000] S. Klioner. *Relativity in Modern Astrometry and Celestial Mechanics - Overview.* In K. J. Johnston, D. D. McCarthy, B. J. Luzum and G. H. Kaplan, editeurs, IAU Colloq. 180: Towards Models and Constants for Sub-Microarcsecond Astrometry, page 265, 2000. (Cited on page 14.)

[Klioner 2003] S. A. Klioner. *A Practical Relativistic Model for Microarcsecond Astrometry in Space.* Astronomical Journal, vol. 125, pages 1580–1597, March 2003. (Cited on pages 15, 19, 42, 44, 47, 65, 66, 67, 68, 82, 88, 100 and 105.)

[Klioner 2004] S. A. Klioner. *Physically adequate proper reference system of a test observer and relativistic description of the GAIA attitude.* Physical Review D, vol. 69, no. 12, page 124001, June 2004. (Cited on pages 9, 13, 54, 57, 67 and 81.)

[Klioner 2005] S. A. Klioner. *Relativistic Formulation and Reference Frame.* In C. Turon, K. S. O'Flaherty and M. A. C. Perryman, editeurs, The Three-Dimensional Universe with Gaia, volume 576 of *ESA Special Publication*, page 207, January 2005. (Cited on page 10.)

[Klioner 2012] S. A. Klioner. *Astronomical relativistic reference systems and their application for astrometry.* Memorie della Societa Astronomica Italiana, vol. 83, page 994, 2012. (Cited on page 16.)

[Kopeikin & Schäfer 1999] S. M. Kopeikin and G. Schäfer. *Lorentz covariant theory of light propagation in gravitational fields of arbitrary-moving bodies.* Physical Review D, vol. 60, no. 12, page 124002, December 1999. (Cited on pages 16 and 75.)

[Kopeikin & Xie 2010] S. Kopeikin and Y. Xie. *Celestial reference frames and the gauge freedom in the post-Newtonian mechanics of the Earth-Moon system.* Celestial Mechanics and Dynamical Astronomy, vol. 108, pages 245–263, November 2010. (Cited on page 13.)

[Kopeikin 1997] S. M. Kopeikin. *Propagation of light in the stationary field of multipole gravitational lens.* Journal of Mathematical Physics, vol. 38, pages 2587–2601, May 1997. (Cited on page 41.)

[Kostić 2012] U. Kostić. *Analytical time-like geodesics in Schwarzschild space-time.* General Relativity and Gravitation, vol. 44, pages 1057–1072, April 2012. (Cited on page 17.)

[Le Poncin-Lafitte & Teyssandier 2008] C. Le Poncin-Lafitte and P. Teyssandier. *Influence of mass multipole moments on the deflection of a light ray by an isolated axisymmetric body.* Physical Review D, vol. 77, no. 4, page 044029, February 2008. (Cited on pages 19, 33, 40, 41 and 42.)

[Le Poncin-Lafitte *et al.* 2004] C. Le Poncin-Lafitte, B. Linet and P. Teyssandier. *World function and time transfer: general post-Minkowskian expansions.* Classical and Quantum Gravity, vol. 21, pages 4463–4483, September 2004. (Cited on pages 17, 21, 23, 37 and 45.)

[Le Poncin-Lafitte 2010] C. Le Poncin-Lafitte. *Practical relativistic clock synchronization for high-accuracy space astrometry.* In S. A. Klioner, P. K. Seidelmann, & M. H. Soffel, editeur, IAU Symposium, volume 261 of *IAU Symposium*, pages 334–336, January 2010. (Cited on page 14.)

[Lindegren *et al.* 2012] L. Lindegren, U. Lammers, D. Hobbs, W. O'Mullane, U. Bastian and J. Hernández. *The astrometric core solution for the Gaia mission. Overview of models, algorithms, and software implementation.* Astronomy & Astrophysics, vol. 538, page A78, February 2012. (Cited on pages 80, 81 and 82.)

[Linet & Teyssandier 2002] B. Linet and P. Teyssandier. *Time transfer and frequency shift to the order $1/c^4$ in the field of an axisymmetric rotating body.* Physical Review D, vol. 66, no. 2, page 024045, July 2002. (Cited on pages 17, 19, 21, 22, 32, 41 and 45.)

[Linet & Teyssandier 2013] B. Linet and P. Teyssandier. *New method for determining the light travel time in static, spherically symmetric spacetimes. Calculation of the terms of order G^3.* ArXiv e-prints, April 2013. (Cited on pages 34 and 102.)

[Meyer 2001] Carl D. Meyer. Matrix analysis and applied linear algebra. SIAM, 2001. (Cited on page 96.)

[Mignard *et al.* 2008] F. Mignard, C. Bailer-Jones, U. Bastian, R. Drimmel, L. Eyer, D. Katz, F. van Leeuwen, X. Luri, W. O'Mullane, X. Passot, D. Pourbaix and T. Prusti. *Gaia: organisation and challenges for the data processing.* In W. J. Jin, I. Platais and M. A. C. Perryman, editeurs, IAU Symposium,

volume 248 of *IAU Symposium*, pages 224–230, July 2008. (Cited on pages 80 and 95.)

[Milani *et al.* 2002] A. Milani, D. Vokrouhlický, D. Villani, C. Bonanno and A. Rossi. *Testing general relativity with the BepiColombo radio science experiment.* Physical Reviews D, vol. 66, no. 8, page 082001, October 2002. (Cited on page 55.)

[Minazzoli & Chauvineau 2009] O. Minazzoli and B. Chauvineau. *Post-Newtonian metric of general relativity including all the c^{-4} terms in the continuity of the IAU2000 resolutions.* Physical Reviews D, vol. 79, no. 8, page 084027, April 2009. (Cited on page 40.)

[Minazzoli & Chauvineau 2011] O. Minazzoli and B. Chauvineau. *Scalar-tensor propagation of light in the inner solar system including relevant c^{-4} contributions for ranging and time transfer.* Classical and Quantum Gravity, vol. 28, no. 8, page 085010, April 2011. (Cited on page 16.)

[Misner *et al.* 1973] C.W. Misner, K.S. Thorne and J.A. Wheeler. Gravitation. San Francisco: W. H. Freeman, 1973. (Cited on pages 9, 10, 15, 54 and 58.)

[Mouret 2011] S. Mouret. *Tests of fundamental physics with the Gaia mission through the dynamics of minor planets.* Physical Reviews D, vol. 84, no. 12, page 122001, December 2011. (Cited on pages 7 and 9.)

[Moyer 2000] Moyer. Formulation for observed and computed values of deep space network data types for navigation monograph 2. Deep Space Communications and Navigation Series. 2000. (Cited on pages 9 and 56.)

[O'Mullane *et al.* 2011] W. O'Mullane, U. Lammers, L. Lindegren, J. Hernandez and D. Hobbs. *Implementing the Gaia Astrometric Global Iterative Solution (AGIS) in Java.* Experimental Astronomy, vol. 31, pages 215–241, October 2011. (Cited on page 81.)

[Paige & Saunders 1982] C. C. Paige and M. A. Saunders. *LSQR, An algorithm for sparse linear equations and sparse least squares.* ACM Trans. Math. Software, Volume 8, p. 43-71, vol. 8, pages 43–71, 1982. (Cited on page 83.)

[Perlick 1990] V. Perlick. *On Fermat's principle in general relativity. I. The general case.* Classical and Quantum Gravity, vol. 7, pages 1319–1331, August 1990. (Cited on page 26.)

[Perryman & ESA 1997] M. A. C. Perryman and ESA, editeurs. The hipparcos and tycho catalogues. astrometric and photometric star catalogues derived from the esa hipparcos space astrometry mission, volume 1200 of *ESA Special Publication*, 1997. (Cited on page 4.)

[Petit & Wolf 2005] G. Petit and P. Wolf. *Relativistic theory for time comparisons: a review.* Metrologia, vol. 42, page 138, June 2005. (Cited on page 50.)

[Pitjeva 2005] E. V. Pitjeva. *High-Precision Ephemerides of Planets - EPM and Determination of Some Astronomical Constants.* Solar System Research, vol. 39, pages 176–186, May 2005. (Cited on page 14.)

[Richter & Matzner 1983] G. W. Richter and R. A. Matzner. *Second-order contributions to relativistic time delay in the parametrized post-Newtonian formalism.* Physical Reviews D, vol. 28, pages 3007–3012, December 1983. (Cited on page 37.)

[San Miguel 2007] A. San Miguel. *Numerical determination of time transfer in general relativity.* General Relativity and Gravitation, vol. 39, pages 2025–2037, December 2007. (Cited on page 17.)

[Shapiro 1964] I. I. Shapiro. *Fourth Test of General Relativity.* Physical Review Letters, vol. 13, pages 789–791, December 1964. (Cited on pages 37 and 41.)

[Soffel *et al.* 1991] M. H. Soffel, X. Wu, C. Xu and J. Mueller. *Consistent relativistic VLBI theory with picosecond accuracy.* Astronomical Journal, vol. 101, pages 2306–2310, June 1991. (Cited on page 9.)

[Soffel *et al.* 2003] M. Soffel, S. A. Klioner, G. Petit, P. Wolf, S. M. Kopeikin, P. Bretagnon, V. A. Brumberg, N. Capitaine, T. Damour, T. Fukushima, B. Guinot, T.-Y. Huang, L. Lindegren, C. Ma, K. Nordtvedt, J. C. Ries, P. K. Seidelmann, D. Vokrouhlický, C. M. Will and C. Xu. *The IAU 2000 Resolutions for Astrometry, Celestial Mechanics, and Metrology in the Relativistic Framework: Explanatory Supplement.* Astronomical Journal, vol. 126, pages 2687–2706, December 2003. (Cited on pages 9, 12, 39, 57 and 68.)

[Stephani *et al.* 2009] H. Stephani, D. Kramer, M. MacCallum, C. Hoenselaers and E. Herlt. Exact solutions of einstein's field equations. Cambridge Monographs on Mathematical Physics. Cambridge University Press, 2009. (Cited on pages 34 and 40.)

[Synge 1960] J. L. Synge. Relativity: The general theory. North-Holland Publ. Co., Amsterdam, 1960. Russian translation: IL (Foreign Literature), Moscow, 1963. (Cited on pages 17, 22 and 52.)

[Teyssandier & Le Poncin-Lafitte 2006] P. Teyssandier and C. Le Poncin-Lafitte. *Angular distances in metric theories.* ArXiv General Relativity and Quantum Cosmology e-prints, November 2006. (Cited on page 55.)

[Teyssandier & Le Poncin-Lafitte 2008] P. Teyssandier and C. Le Poncin-Lafitte. *General post-Minkowskian expansion of time transfer functions.* Classical and Quantum Gravity, vol. 25, no. 14, page 145020, July 2008. (Cited on pages 17, 21, 23, 24, 26, 32 and 47.)

[Teyssandier 2009] P. Teyssandier. *Some recent developments in relativistic modeling of time and frequency transfers.* In M. Soffel, Lohrmann-Observatorium N. Capitaine (eds.) and Observatoire de Paris., editeurs, Proceedings of the "Journées 2008 Systèmes de référence spatio-temporels", 2009. (Cited on page 53.)

[Teyssandier 2012] P. Teyssandier. *Direction of light propagation to order G^2 in static, spherically symmetric spacetimes: a new derivation.* Classical and Quantum Gravity, vol. 29, no. 24, page 245010, December 2012. (Cited on pages 19, 27, 33, 39, 47, 60 and 100.)

[Thorne 1980] K. S. Thorne. *Multipole expansions of gravitational radiation.* Reviews of Modern Physics, vol. 52, pages 299–340, April 1980. (Cited on page 41.)

[Tommei *et al.* 2010] G. Tommei, A. Milani and D. Vokrouhlický. *Light-time computations for the BepiColombo Radio Science Experiment.* Celestial Mechanics and Dynamical Astronomy, vol. 107, pages 285–298, June 2010. (Cited on page 55.)

[Vecchiato *et al.* 2003] A. Vecchiato, M. G. Lattanzi, B. Bucciarelli, M. Crosta, F. de Felice and M. Gai. *Testing general relativity by micro-arcsecond global astrometry.* Astronomy & Astrophysics, vol. 399, pages 337–342, February 2003. (Cited on pages 69, 82 and 86.)

[Vecchiato *et al.* 2009] A. Vecchiato, M. Gai, M. G. Lattanzi, M. Crosta and A. Sozzetti. *Gamma astrometric measurement experiment (GAME) - Science case.* Advances in Space Research, vol. 44, pages 579–587, September 2009. (Cited on page 60.)

[Vecchiato *et al.* 2012] A. Vecchiato, U. Abbas, M. Bandieramonte, U. Becciani, L. Bianchi, B. Bucciarelli, D. Busonero, M. G. Lattanzi and R. Messineo. *The global sphere reconstruction for the Gaia mission in the Astrometric Verification Unit.* In Society of Photo-Optical Instrumentation Engineers (SPIE) Conference Series, volume 8451, September 2012. (Cited on pages 80, 82, 84 and 86.)

[Vincent *et al.* 2011] F. H. Vincent, T. Paumard, E. Gourgoulhon and G. Perrin. *GYOTO: a new general relativistic ray-tracing code.* Classical and Quantum Gravity, vol. 28, no. 22, page 225011, November 2011. (Cited on page 102.)

[Weinberg 1972] S. Weinberg. Gravitation and cosmology: Principles and applications of the general theory of relativity. July 1972. (Cited on pages 9 and 54.)

[Will 1993] C. M. Will. Theory and experiment in gravitational physics. March 1993. (Cited on page 12.)

[Will 2006] Clifford M. Will. *The Confrontation between General Relativity and Experiment.* Living Reviews in Relativity, vol. 9, no. 3, 2006. (Cited on page 9.)